2008

Sound reduction by a Helmholtz resonator

Myonghyon Han
Lehigh University

Han, Myonghyon

Sound Reduction by a Helmholtz Resonator

September 2008

SOUND REDUCTION

BY A HELMHOLTZ RESONATOR

by

Myonghyon Han

A Thesis
Presented to the Graduate and Research Committee
of Lehigh University
in Candidacy for the Degree of
Master of Science

In
The Department of Mechanical Engineering and Mechanics

Lehigh University

September, 2008

This thesis is accepted and approved in partial fulfillment of the requirements for the Master of Science.

07/03/08

Date

Thesis Advisor

Chairperson of Department

ACKNOWLEDGMENTS

I would like to express my sincere gratitude to my advisor, Prof. Donald Rockwell, for his knowledge, guidance and encouragement throughout present study. His efforts toward my academic progress have been invaluable. Also, I am very grateful to the Korean Army for its financial support.

I appreciate the assistance of the machine shop, particularly Mr. Richard Towne and Mr. James Bunderla for their craftsmanship. I am also very thankful to Mrs. JoAnn Casciano, Mrs. Geri Kneller for their kindness and administrative assistance. I extend many thanks to Yasushi Watanabe for his contribution on the initial development of the experimental set-up and wonderful discussions. I am also thankful to all my colleagues, Mr. Philip Breneman, Mr. Tunc Goruney, Mr. Turgut, Yilmaz, Egemen Tinar, Cem Alper Ozen,

I owe my heartfelt gratitude and thanks to my parents and my family, for their support and to my Korean best friends Wanggyu Im, Hwabok Wee, Kyunghwan Kim and Jinwoo Lee, who have been like brothers to me.

Finally, I am grateful to my beautiful lady, HyunJung Oh, for her encouragement, support, patience, and love.

TABLE OF CONTENTS

LIST OF FIGURES

NOMENCLATURE

A_C	Cross-sectional area of cavity duct
A_H	Cross-sectional area of mouth of Helmholtz resonator
A_{H0}	Cross-sectional area of volume of Helmholtz resonator
c	Sound speed
f_0	Frequency of spectral peak
f_1, f_2	Frequencies at the half-power points of spectral peak
f_S	Sampling rate
f_R	Resonant frequency
Δf	Frequency resolution
L'	Effective length
L_C	Length of cavity duct
L_H	Total length of Helmholtz resonator
L_{H0}	Actual length of Helmholtz resonator
L_{HM}	Length of mouth of Helmholtz resonator
L_{HN}	Length of neck of Helmholtz resonator
L_P	Length of cavity of plate
L_{P0}	Length of plate
n_a	Acoustic mode number
n_S	Number of samples per data set
R_H	Radius of Helmholtz resonator
T_H	Thickness of Helmholtz resonator
T_P	Thickness of plate

W_C	Width of cavity duct
W_{HM}	Width of mouth of Helmholtz resonator
W_P	Width of cavity of plate
W_{P0}	Width of plate
X_P	Volume length of Helmholtz resonator
λ	Wave length
ζ	Damping ratio

ABSTRACT

When subjected to external excitation, a Helmholtz resonator can show a strongly resonant response at a well-defined frequency. This resonant characteristic can be used to effectively attenuate the generation of sound, by attaching the resonator to a variety of geometrical configurations.

The first phase of the present investigation focuses on the effects of geometry on the resonant frequency of a Helmholtz resonator. The volume of the resonator is varied by adjustment of a piston, which forms the bottom, or end, surface of the resonator. Furthermore, the effect of cross-sectional area of the mouth (opening) of the resonator is investigated, via employment of different attachment plates at the resonator opening. For all of the foregoing modifications of the Helmholtz resonator, spectral analysis of pressure fluctuations within the resonator provides an indication of the frequency of Helmholtz resonance, and the corresponding amplitude of the spectral peak at the resonant state.

In the second part of the investigation, the Helmholtz resonator is employed to attenuate the oscillation characteristics of a deep cavity duct, i.e., a side branch. The Helmholtz resonator is attached to the side of the duct. As for the first part of this investigation, the consequence of variations of geometry and volume of the Helmholtz resonator are addressed. Substantial damping of the overall oscillation can be attained, as characterized by spectral analysis of the pressure fluctuations at critical locations in the system.

1. INTRODUCTION

Since ancient Greece, the Helmholtz resonator has been used to intensify and dampen sound fields. Knowledge of Helmholtz resonance and its theoretical description have been used over the years to design and analyze various systems. An advantage of the Helmholtz resonator is that it has the characteristic of strong sound attenuation, even though its geometry is relatively simple. When it is appropriately tuned, it can substantially reduce noise over the low frequency domain. Many researchers and engineers have been interested in, and employed, the Helmholtz resonator for a variety of applications, including a range of geometries, some of them as part of complex configurations.

1.1 Helmholtz Resonance

Hermann Ludwig Ferdinand von Helmholtz (August 31, 1821 – September 8, 1894) was born in Germany and had brilliant achievements as both a physician and a physicist. He created the device known as the Helmholtz resonator in the 1860s. Helmholtz resonance is widely known as the phenomenon of air resonance in the cavity or chamber that contains a gas. The highest amplitude sound is generated near and at the resonant frequency, which is determined by the volume and the neck dimensions of the Helmholtz resonator. A well-known configuration of such a resonator is the musical tone generated when air is blown across the top of an empty soda bottle.

In a Helmholtz resonator, the air in its neck behaves as a discrete mass, while the air in the cavity has the role of a spring. During oscillation, the gas within the volume of the resonator is alternately compressed and expanded at very low magnitudes. The inertia of the air in the neck of the resonator plays an important role.

1.2 Previous Related Investigation of Helmholtz Resonators

Adaptive-Passive Noise Control. The phenomenon of Helmholtz resonance has been utilized in adaptive-passive noise control. The resonant frequency is controlled by altering the dimension of the Helmholtz resonator, such as the length of the neck or the volume of the cavity of the resonator, or both of these. By using a means to adjust the parameters of the neck and chamber volume, it is possible to dampen noise over a frequency domain of interest. Various experiments have been carried out to determine the most effective methods of using adaptive Helmholtz resonators to control sound and, thereby, attenuation.

Koopman and Neise (1980, 1982) studied the use of adjustable resonators to dampen the tone produced by blade passage of centrifugal fans. The volume of the Helmholtz resonator was changed by use of a moveable Teflon piston. Their experimental results showed that the amplitude of the tone of the blade passage frequency could be decreased up to 29 dB without generating a negative side effect on the fan frequency. However, no definitive methods were suggested for achieving the optimal condition of sound reduction by variation of the cavity depth.

Little et al. (1994) investigated a fluidic Helmholtz resonator for use as an adaptive engine mount. Dimensions of the cross-sectional area of the neck of the Helmholtz resonator were modified to attenuate the noise. The various magnitudes of surface opening areas lead to a change in the inertance of the neck of the resonator. A creative electro-rheological fluid component was developed to continuously alter the cross-sectional area of the neck; this approach is different from the configuration of a widely utilized valve, which has a discontinuous characteristic. However, the algorithm for the controlling parameter that relates the opening of the surface area was not explained.

Lamancousa (1987) designed a changeable cavity of the Helmholtz resonator to substitute for expansion chamber mufflers in automobiles. Two types of modifiable arrangements of the cavity volume were considered. In the first device, the volume was continuously changed by increasing or decreasing the length of the cavity through a moveable piston inside the cavity. In the second type of device, separate volumes were employed; that is, the volume of the chamber was divided into several sub-volumes, which could be closed off. Using the approaches described in the foregoing, it was possible to attain either a continuous or discrete variation of volume of the resonator according to the revolution signal of the engine. In these devices, it was determined that insertion losses of more than 30 dB were achieved by manipulating the continuously changeable volume of the resonator. It should be noted that Krause et al. (1992, 1993) also experimentally investigated the effect of alterations of the volume and the neck of a Helmholtz resonator on attenuation of the source of noise in automotive tailpipes.

Matsuhisa et al. (1990, 1992) investigated the consequences of the variable volume of a resonator by using a removable piston inside the chamber. The resonator was attached to a duct in the manner of a side branch and the adjustment of the volume of the resonator was guided by comparison with the phase of the sound pressure in the duct, relative to that in the resonant cavity. The chamber of the resonator was controlled to maintain a constant phase difference of ninety degrees. Using this procedure, anti-resonance of the duct-resonator system was accomplished. In this experiment, three sensors were utilized to measure and compare the sound pressure in different positions. One microphone was used to measure the excitation frequency, one was employed to measure the pressure in the duct, and the remaining one measured the pressure in the cavity. It was found in this investigation that the use of an adjustable resonator produces reductions in sound pressure up to 30 dB for a speaker driven system and 20 dB for a fan-driven system.

McDonald et al (1992) performed tonal noise control by using a variable Helmholtz resonator, similar to that used in the experiments of Matsuhisa et al. (1990, 1992). The phase difference between the pressure and the resonator cavity in the duct system was employed to guide adjustment of the volume of the cavity and the length of resonator neck, in order to achieve sound reduction.

Selamet, Dickey and Novak (1995) showed that the individual dimensions of a Helmholtz resonator can play a great role in determination of the resonant frequency and the transmission loss characteristics. An increase of the ratio of the length scale of the volume to the diameter, ℓ/d, decreases the predominant resonant frequency. This phenomenon is similar to the result of using an effective length, which includes a correction length. Experiments show agreement with the analytical expression and numerical simulation.

DeBedout (1997) investigated an adaptive Helmholtz resonator, which optimized its performance according to changes in environmental conditions and excitation frequency. It was found that reduction in sound pressure up to 30 dB could be attained through a combination of a variable resonator and an appropriately controlled algorithm. The main advantages of this system are as follows. For the case of this adaptive-passive noise control device, the control algorithm is simple and the efficiency of the process is optimized. Furthermore, with the tunable Helmholtz resonator, it is possible to achieve optimal reductions of sound in response to changing environmental conditions and excitation frequency.

Tang (2003) investigated the effects of the taper and length of the resonator neck on the characteristics of a Helmholtz resonator. It was reported that an increase of the tapered length leads to improvement of sound reduction, and an increase of the cavity volume results in increased capacity for sound absorption of the Helmholtz resonator. These experiments showed that sound attenuation via the Helmholtz resonator of more than 50% could be achieved by changing the length of the tapered neck, compared to the untapered neck. The increase of the resonant frequency is proportional to the tapered length and is decreased by expanding the cavity volume at a fixed slope of the tapered section. In addition, this investigation showed that the resonant frequency is proportional to the slope of the tapered section at constant volume of the Helmholtz resonance chamber.

The previous studies of the Helmholtz resonator have provided fundamental knowledge for the present experiments. Taking into account these investigations, sound reduction via the selected Helmholtz resonator can be pursued. The resonant frequencies of the Helmholtz resonator are evaluated by experiments and an analytical method, while changing the geometrical dimensions of the Helmholtz resonator, including the neck cross-sectional area, the length of the neck, and the magnitude of the volume.

2. EXPERIMENTAL SYSTEM AND TECHNIQUES

2.1 OVERVIEW OF EXPERIMENTAL SYSTEM

All components of the experimental system were designed and manufactured in the Fluid Mechanics Laboratories at Lehigh University. The general experimental system can be separated into two main subsystems. The first subsystem is the actual Helmholtz resonator system with an open-closed cavity and the second one is the data acquisition and analysis program. The generated data from the first subsystem are delivered and analyzed by the second subsystem.

2.2 MAIN TEST SECTION

Helmholtz resonator. A simple schematic of the experimental set-up, combination of the Helmholtz resonator and cavity duct for sound reduction, is presented in Figure 2.1. The details of the Helmholtz resonator are shown in Figure 2.2a to 2.2b. It is made of Polyvinyl chloride, PVC and its cross-section is circular. The total length of Helmholtz resonator is denoted as L_H. This total length is equal to the sum of the actual length L_{H0} and the thickness of the neck and the end side. The total length L_H of Helmholtz resonator is 314.33 mm and the actual length, L_{H0}, which corresponds to the distance between neck and end side, is 288.92 mm. The radius R_H and the thickness T_H of Helmholtz resonator are 76.2 mm and 7.94 mm, respectively. The neck length L_{HN} is 12.7 mm and the cross-sectional area A_H of the neck is 1451.6 mm^2. The cross-sectional area has a width W_{HM} of 38.1 mm and length L_{HM} of 38.1 mm. The end of Helmholtz resonator is fabricated from PVC having a thickness of 9.53 mm. In order to measure sound pressure, a PCB pressure transducer is placed on the wall of Helmholtz resonator at a location 9.53 mm from the side of neck. Further details of the PCB transducer are described in the next section. A piston, ring, and a rod, the total length of which is 392.3 mm, are located inside the Helmholtz resonator and allow adjustment of the volume of the cavity.

Cavity duct. The dimensions of the cavity duct are given in Figure 2.3. It is made of an aluminum tube and the shape of its cross section is rectangular, as shown in figure 2.3. The total depth of the cavity duct is denoted as L_C. It has a value of 482.6 mm. The area of the opening of the duct is $A_C = 1290$ mm^2. This opening has a width W_C of 25.4 mm and length L_C of 50.8 mm. An aluminum endplate is used to cover and seal off the end of the cavity duct. Its thickness 12.7 mm, and it contains a PCB transducer to measure the sound pressure at the end of duct. Details of this transducer are given in the following section.

Plate. In the present experiments, three plates are utilized to investigate the resonant frequency of the Helmholtz resonator. The geometry of the plate is defined in Figure 2.4a to 2.4c. Each plate has a rectangular shape with a width W_{P0} of 63.5 mm, length L_{P0} of 63.5 mm and thickness T_P of 3.18 mm. These plates are made of aluminum with a rectangular hole at the center. The width W_P of the cavity has values of 3.18 mm, 6.35 mm and 9.53 mm for a fixed length L_P of 38.1 mm.

2.3 ACQUISITION AND PROCESSING OF PRESSURE DATA

Pressure transducers. PCB transducers (Model No. U103A02) were employed to measure the sound pressure. These transducers have a defined sensitivity in units of mv/psi or mv/kpa. The acquired data from the transducers were transferred to a PCB Piezotronics multi-channel sensor signal conditioner, Model 48A. The acquired signal from each transducer is independently amplified and filtered. The same value of gain is used for all sound pressure measurements. This gain control plays an important role in preventing voltage signals of the sound pressure from exceeding the restricted voltage input level of the A/D (analog/digital) board.

Acquisition of pressure signals. The modified sound pressure signals were transmitted to ports on a National Instruments board (Model PCI-MI0-16E-4) with 12- bit resolution. When the board receives voltage pressure signals from the sensor signal conditioner, the board can acquire data at the rate of 250KS/s, where K = 10^3 and S stands for the number of samples. In these experiments, eight channels are utilized. Six are connected to the air transducers and two remain unconnected. The actual sampling rate for each channel, which is decreased by the number of used channels in a board, is equal to 31.25 KS/s. Two aspects should be considered in order to decide whether this sampling rate is acceptable. First of all, the sampling rate should be at least two times greater than the maximum frequency of interest. In the time domain, a minimum of five samples is theoretically needed, but a minimum of ten samples is actually adequate. Considering the foregoing, it is desirable for the acquisition system to employ a sampling rate at least ten times greater than the maximum frequency in this experiment, which is equal to 2×10^4 Hz. This value is approximately a factor of two smaller than the transmission rate of 31.25 KS/s per channel. Also, it is important to understand that one A/D (analog digital converter) is utilized, in order to translate an analog voltage signal into a digital one. Transmission and acquisition of eight voltage signals is achieved by employing a multiplexing process. The scan interval corresponds to the inverse of the maximum data acquisition rate per channel, which is approximately equal to 32 microseconds. The physical meaning of this is the procedure is the required time for one cycle of data acquisition from transducer No. 1 to the last transducer.

Processing of pressure signals. A Pentium 2-350 MHz computer and Labview software were employed to acquire data from the transducers. Also a Pentium 4 CPU 2.80 GHz computer and Matlab were employed to analyze the data. The main parameters for spectra of pressure utilizing the Fast Fourier Transform (FFT) must be properly denoted, in order to achieve optimal resolution in the frequency domain, as well as minimization of the size of the acquired data. Two parameters should be considered, in order to decide on the optimal resolution and the sampling rate. The first one is the number of samples acquired per data set, which is related to the resolution. The second one is the sampling rate. The sampling rate must be at least two times greater than the maximum frequency in the present experiments. Therefore, the required sampling rate has various values, depending on the maximum frequency for each experiment. The frequency resolution (Δf) corresponds to the sampling rate (f_S) divided by the number of samples per data set (n_S). After the sampling rate is determined, based on the maximum frequency, the resolution and the number of samples are evaluated by the formula $n_S = f_S / \Delta f$. In these experiments, $\Delta f = 1$ is considered to be the frequency resolution and the lowest and highest frequency are equal to 1 and 1000 Hz, respectively. The sampling rate was selected as 4096 samples per second, which is approximately two times larger than the value of 2000 Hz calculated by the Nyquist criterion, when the maximum frequency of interest in the present research is equal to 1000 Hz. Therefore, the number of samples per data set (n_S) results in $4096 = 2^{12}$ samples per data set.

Q-factor. The Q factor is defined as $Q = f_0 / (f_1 - f_2)$, in which f_0 is the frequency of the tone, and f_1 and f_2 are the frequencies at the half-power points of the spectral peak. Also, the Q factor has the following relationship with ζ: $Q = 1/2\zeta$. This relationship can be used as a convenient way of determining the damping ratio ζ.

3. PRESSURE RESPONSE CHARACTERISTICS

In this chapter, an outline of experimental parameters, methods of data presentation and characteristics of sound pressure in a Helmholtz resonator due to pure tone excitation will be described.

3.1 Summary of range of geometric parameters

Figure 3.1 shows an overview of combinations of width W_H of the Helmholtz resonator, neck length L_{HN} and depth X_P of the adjustable volume in Helmholtz resonator. These cases are marked by the character **O**. For each of these cases, a pure tone is used to excite the Helmholtz resonator over a wide range of frequency, in order to excite the predominant sound acoustic modes.

In the next section, the first set of experiments is described; they involve spectra of the pressure fluctuation at a fixed cross-sectional area of the cavity duct, which has an area $A_C = 1290$ mm^2, a width W of 25.4 mm, and a length L of 50.8 mm, at a constant value of cavity length $L_C = 482.6$ mm. These experiments were performed to find the resonant frequency of the cavity duct, as well as to compare the resonant frequency obtained by experiments with theory.

The second set of experiments is separated into two parts. The first part includes various values of chamber volume of the resonator as function of length X_P, from 25.4 mm to 177.8 mm, while maintaining a fixed cross-sectional area, $A_{H0} = 1452$ mm^2 and neck length, $L_{HN} = 12.7$ mm. The second part contains variations of the chamber volume as function of length X_P, from 25.4 mm to 177.8 mm, while changing the area of the opening from 121 mm^2 to 363 mm^2. The purpose of these experiments is not only to provide a resonant frequency of the Helmholtz resonator, but also to compare experimental and theoretical values of resonant frequency.

Finally, a combined experiment involving both the cavity duct and the Helmholtz resonator are implemented over the length X_P = 25.4 mm to 177.8 mm at a given value of cavity length L_C = 486.2mm. The major purpose of these experiments is to investigate the sound reduction in Helmholtz resonator.

3.2 METHOD OF PRESENTATION OF DATA

The results of the experiments are given in the form of spectra of the pressure fluctuation, which is measured at the end of the deep cavity and the side wall of Helmholtz resonator. For a given experiment, approximately 70 spectra were acquired. Acoustic modes and amplitudes of the sound pressure over the frequency domain are expressed by two-dimensional plots of pressure spectra. These two-dimensional plots are shown on linear scales. The amplitudes of sound pressure are expressed in units of Pascals (N/m^2).

3.3 RESONANCE OF CAVITY DUCT

In this section, the resonant frequency is obtained through excitation by a pure tone. The area A_C of cavity opening is 1290 mm^2 and the depth L_C of the cavity duct is 486.2 mm. A detailed schematic of the cavity duct is shown in Figure 2.3. The range of the pure tone is 1 to 1000 Hz. Figure 3.2 shows representative spectra of the pressure fluctuation. The first sound acoustic mode occurs at 160 Hz, and corresponds to the maximum amplitude.

3.4 EFFECT OF GEOMETRICAL PARAMETERS OF RESONATOR ON RESONANT RESPONSE

The effect of variations of the cross-sectional area A of the Helmholtz resonator are given in Figures 3.3 though 3.6, while changing the cavity volume, as a function of X_P from 25.4 mm to 178 mm. Also, a pure tone is employed over the frequency range 1 to 1000 Hz, in order to excite the Helmholtz resonator.

As shown in Figure 3.7, the resonant frequencies of the free Helmholtz resonator are obtained for the case where no plate is attached to the opening (mouth). The area A_H of the opening and the length L_{HN} of neck are 1452 mm^2 and 12.7 mm, respectively. By adjusting the cavity volume, various resonant frequencies corresponding to volume variations are acquired in Figures 3.8a though 3.8d. A linear scale is used for pressure amplitude. The first acoustic mode is shown at $f = 450$ Hz, with the length $X_P = 25.4$ mm. However, as the volume expands, decrease of the resonant frequency occurs. The first acoustic mode for the maximum value of volume is at $f = 175$ Hz.

In Figures 3.9 to 3.14, the cross-sectional area A_H of the Helmholtz resonator is varied by using three plates. Each has a different open area. These plates have values of width W_P from 3.18 mm to 9.53 mm, for a fixed length $L_P = 38.1$ mm and thickness $T_P =$ 3.18 mm. Detailed schematics of each plate are shown in Figure 2.4a to 2.4c.

Figure 3.9 gives spectra of the pressure fluctuation inside the Helmholtz resonator, due to pure tone excitation at successive values of frequency, at a value of width $W_H = 3.18$ mm. The effects of different values the length X_P of the volume of the Helmholtz resonator is shown in Figures 3.10a through 3.10d. The first acoustic mode appears at $f = 247$ Hz, with the length $X_P = 25.4$ mm. The frequency of this first mode decreases as the length X_P increases. The foregoing of the first acoustic mode at maximum volume is $f = 100$ Hz.

Figure 3.11 indicates the spectra of the pressure fluctuation inside the Helmholtz resonator, with the plate having a width $W_H = 6.35$ mm; it is attached to the Helmholtz resonator. The separate plots represent different values of the length X_P in Figures 3.12a through 3.12d. The first acoustic mode appears at $f = 288$ Hz, at a value of length $X_P = 25.4$ mm. The first acoustic mode decreases as the length X_P increases, and the first acoustic mode at the maximum value of volume occurs at $f = 115$ Hz. The frequency of this first acoustic mode tends to increase with larger values of width W_H.

The response associated with the largest plate, having a value of width $W_H = 9.53$ mm, is represented in Figures 3.13. These plots are expressed as a function of the length X_P in Figures 3.14a through 3.14d. The first acoustic mode appears at $f = 312$ Hz, at a value of length $X_P = 25.4$ mm. The first acoustic mode is at $f = 124$ Hz, when the length X_P reaches its maximum value. The data for this plate follows the two aforementioned trends.

Figures 3.15 to 3.21 show the resonant frequency for the combination of the Helmholtz resonator and a deep cavity duct. The detailed geometry is given in Figure 2.2 to 2.3. The range of first mode resonant frequency is from $f = 339$ Hz to 293 Hz. The results indicate that the presence of the Helmholtz resonator leads to sound reduction, when the pressure magnitude of the present arrangement is compared with that of cavity duct given in Figure 3.2. That is, the pressure amplitude with the Helmholtz resonator is approximately minimum 20 percent of the pressure amplitude without the Helmholtz resonator, for the first acoustic mode.

4. BACK GROUND LEVEL OF RESONANCE

In the following section, the process of calculations of resonant frequency for the cavity duct and Helmholtz resonator will be described. This process is helpful to predict resonant frequencies and to explain the organized acoustic peaks of sound pressure fluctuation. Fast Fourier Transform, FFT is employed to order to analyze data for the purpose of evaluating resonant frequencies in present process. Also, the effects of parameters in the cavity duct and Helmholtz resonator are described, including the changes of neck length, cross sectional area and cavity volume of Helmholtz resonator.

4.1 DEVELOPMENT OF RESONANT FREQEUNCY

Resonance occurs when an oscillation attains maximum amplitude at given frequency, called the natural, or resonant, frequency. In the present experiments, two different analytical methods are used in order to evaluate the resonant frequency of a combination of cavity duct and Helmholtz resonator. First of all, for the case of the cavity duct side branch, the resonant frequency f_R can be denoted as a function of the acoustic mode number n_a , speed of sound c, and cavity depth L_c. The expression of the resonant frequency f_R is

$$f_R = \frac{c \cdot n_a}{4 \cdot L_c} \tag{4.1}$$

where the sound speed is c = 343.5 m/s and the room temperature is 20℃. The detailed processes of evaluation for resonant frequency are described in Appendix A. Figures 4.1 through 4.4 present comparisons of experimental and theoretical values of resonant frequency. Also, Figure 4.5 indicates the difference between experimental values and analytical values according to the first acoustic mode, while adjusting the volume of resonator.

A Helmholtz resonator consists of a neck and a cavity volume. The volume of air in the neck is analogous to a mass on a spring and the body volume of Helmholtz resonator is analogous to a spring of defined spring constant. The resonant frequency is:

$$f_R = \frac{c}{2\pi}\sqrt{\frac{S}{L'V}} \tag{4.2}$$

The length L′ is the effective length, and is not equal to the actual length L. The effective length L′ should be utilized in order to enhance accuracy, when the resonant frequency in Helmholtz resonator is evaluated. The additional length is employed at each end of the neck, because the acoustic length of the neck is longer than the physical length of neck. This additional length is affected by two factors. First of all, the effective length L′ depends on whether both ends are flanged or unflanged. An added length, which is equal to 0.85R, is added to the actual length L, when the end that terminates within the cavity volume has a flange. Also, the extra length, which has a value of 0.6R, is added to an original length L, when the end that opens into the atmosphere, has no flange. So the effective length L′ is L′ = L +0.85R + 0.6R, where the radius R is related to cross-sectional area of the neck. For the present experiment, an equivalent, circular opening should be calculated in order to evaluate the radius R, because the shape of cross-sectional area of the neck is rectangular.

4.2 EFFECT OF THE MOUTH AREA OF HELMHOLTZ RESONATOR

The resonant frequencies of the Helmholtz mode and the corresponding amplitudes are presented in Figures 3.3 through 3.6. Each plot is expressed as a function of frequency *f*. Three different plates with various areas are used, in order to change the cross-sectional area of the neck, but the volume of chamber is fixed. The area of the opening of each plate is modified by varying the width W from 3.18 mm to 9.53 mm at a fixed length L and thickness T. In these experiments, for all plates, the resonant frequencies increase with an increase of the cross-sectional area of the plate, when the Helmholtz resonator has a constant volume and length of neck. These phenomena demonstrate fully the influence of the cross-sectional area of the neck, as a shown formula (4.2) above.

4.3 EFFECT OF THE VOLUME OF HELMHOLTZ RESONATOR

In Figure 3.7, the cross-sectional area of the neck is equal to 1452 mm^2, and the volume of the Helmholtz resonator is adjusted from 481,769 mm^3 to 3,261,769 mm^3 by moving the position of a piston inside the resonator, which is indicated as the length X_P of volume. Also, the resonant frequency is expressed as a function of frequency *f* for each volume. The results of these experiments satisfy the formula of the resonant frequency, given in equation (4.2). This plot shows that the resonant frequency is reduced with an increase of the cavity volume, when the cross-sectional area and the length of neck have a constant value. The air in the cavity volume of a resonator has the properties of a spring, which has a defined force constant or spring constant. The adjustment of the dimensions that determine the volume of the resonator correspond to modification of the spring constant. In other words, a small cavity volume is analogous to a spring with high spring constant. In these experiments, therefore, the resonant frequencies are inverse proportional to the volume of the Helmholtz resonator, and the increase of the volume results in a decrease of the resonant frequency.

5. Discussion of Sound Reduction

For theoretical design of a Helmholtz resonator, it is important to determine specific frequency band of interest, in order to achieve optimal sound reduction. In the present experiments, the oscillations associated with the resonant frequencies of a deep cavity duct are selected for attenuation via a Helmholtz resonator.

5.1 EXPERIMENTAL RESULTS OF SOUND REDUCTION

In the present experiments, a Helmholtz resonator is attached to an open-closed cavity duct in order to reduce the sound pressure generated within in cavity duct. The cross-sectional area A_C of the cavity duct is A_C = 1290.32 mm^2, and its length L_C is L_C = 482.6 mm. The details of this geometry are shown in Figure 2.2. The Helmholtz resonator used in the present research has a length L_H of 314.33 mm and radius R_H of 76.2 mm, and the detailed geometry is described in Figures 2.2a and 2.2b. Two air transducers are utilized for measurement of sound pressure. One is attached to the end plate of cavity duct, and the other one is connected to Helmholtz resonator. The results of sound reduction from use of the Helmholtz resonator could be presented by comparing the data from two air transducers attached to the end plate and the resonator. Figure 3.2 presents the resonant frequencies of a cavity duct excited by pure tone without a Helmholtz resonator. The first mode of the resonant frequency appears at f = 160 Hz with its amplitude of 420 N/m^2, which is selected for the purpose of reduction of sound pressure. Considering equation (4.2), the resonant frequency has a close relationship with the neck length, the cross-sectional area and the resonator volume. For the first phase, the effects of variation of the cross-sectional area and the length of the neck are investigated. The cross-sectional area A_H is determined as $A_H = 241.94$ mm^2, and the identical area is formed on the wall of cavity duct. The neck length L_N becomes equal to the thickness of the cavity wall, and the thickness of 3.18 mm is used as neck length. The theoretical volume of the resonator is 1,776,510 mm^3 for the reduction of sound pressure at the selected resonant frequencies, while considering its effective neck length and cross-sectional area. The volume calculated by equation (4.2) is the same as the value when volume length X_P of Helmholtz resonator is 96.27 mm.

Figures 3.15 through 3.21 show experimental results from the system for which the Helmholtz resonator is employed. Each plot clearly demonstrates sound reduction via the Helmholtz resonator. Figure 3.15 indicates that the cavity duct and the Helmholtz resonator have the amplitudes of 11.19 N/m^2 at $f = 342$ and 5.00 N/m^2 at $f = 338$ Hz, respectively. The amplitude of the sound pressure drops by 97 percent, when the Helmholtz resonator is employed in the system. In Figure 3.16, a 90 percent reduction in sound pressure is shown, and the amplitudes of the cavity duct and Helmholtz resonator are 41.50 N/m^2 and 9.44 N/m^2 at the same frequency $f = 315$ Hz, respectively. The amplitude with the Helmholtz resonator falls off to 86 percent of the amplitude without the Helmholtz resonator in Figure 3.17, and the cavity duct and Helmholtz resonator have the amplitude of 56.67 N/m^2 at $f = 303$ and 9.47 N/m^2 at $f = 302$ Hz, respectively. Figure 3.18 shows that the cavity duct and Helmholtz resonator have the amplitudes of 71.75 N/m^2 and 8.28 N/m^2 at the same frequency $f = 338$ Hz. The amplitude of sound pressure drops by an 83 percent. An 82 percent reduction in sound pressure is shown in Figure 3.19, and the amplitudes of the cavity duct and Helmholtz resonator are 76.06 N/m^2 at $f = 293$ Hz and 6.85 N/m^2 at $f = 293$ Hz, respectively. Figure 3.20 presents a 81 percent decline in the sound pressure, and the cavity duct and Helmholtz resonator have the amplitude of 80.96 N/m^2 at f = 289 and 5.91 N/m^2 at f = 289 Hz, respectively. The amplitude with the Helmholtz resonator falls off to 80 percent of the amplitude without the Helmholtz resonator in Figure 3.21, and the cavity duct and Helmholtz resonator have amplitudes of 85.18 N/m^2 at f = 288 and 4.90 N/m^2 at f = 287 Hz.

It is observed that when the Helmholtz resonator is employed in the system, there is a shift of the acoustic mode to higher frequency, as the volume of Helmholtz resonator is continuously increased. Three methods are used in order to describe the phase shift. The first is classical one-dimensional acoustic theory. The Helmholtz resonator transmission loss is defined as

$$TL = 10 \cdot \log_{10} \left| 1 + \frac{A_H}{A_c} \cdot \left[\frac{1 + \phi + (\phi - 1) \cdot e^{-2ikL_{HN}}}{1 + \phi - (\phi - 1) \cdot e^{-2ikL_{HN}}} \right] \right|^2 ,$$

$$\phi = \frac{A_{H0}}{A_H} \cdot \left(\frac{e^{-2ikL_{HN}} - 1}{e^{-2ikL_{HN}} + 1} \right) \tag{5.1}$$

Where A_H is the cross-sectional area of the mouth of the Helmholtz resonator, L_{HN} is the neck length of Helmholtz resonator, A_{H0} is the cross-sectional area of the volume and $K = \frac{2\pi}{\lambda}$ is the wave number, λ is the wave length, and A_C is the cross-sectional area of the cavity duct. The simulated resonant frequencies of the Helmholtz resonator attached to the cavity duct are shown in Figure 5.1. However, calculated results are not equal to the experimental results, when the frequencies calculated by equation (5.1) are compared with the experimental results for the first acoustic mode.

For the second part of the study, starting from 76.2 mm, the volume length X_P is increased by 2 mm in each experiment in order to satisfy the theoretical volume of

1,776,510 mm^3, which corresponds to the volume length X_P of 95.74 mm and effective length L′ of 15.9 mm. In the thirteen experiment, the length of the volume reaches 101.6 mm. However, significant effects are not shown in Figure 5.2a to 5.21.

Finally, the effect of length of the neck of resonator is considered. The range of neck length is calculated to find the appropriate volume of the Helmholtz resonator. Figure 5.3 shows the required volume, while considering the actual length of the neck. In the present experiment, the actual length of neck L_N is selected as L_N =12.7 mm, and the theoretical volume is 2,224,072 mm^3, which corresponds to the volume length X_P of 121.14 mm. The resonant mode is generated at f = 268 Hz, with an amplitude of 91.69 N/m^2. This result indicates that there is a shift of the acoustic mode to lower frequency, and the resonant frequency does not occur at the same resonant frequency of cavity duct.

Therefore, it is concluded that an additional type of resonance, where involves the combination of a Helmholtz resonator and a cavity duct, can occur, and this resonance is associated with a phase shift.

CONCLUSIONS

The goals of the present investigation were, first of all, to investigate the resonance characteristics of an isolated Helmholtz resonator, then to attenuate the oscillations in a deep cavity duct, i.e., a side branch, via attachment of the resonator to the wall of the duct.

The volume of the Helmholtz resonator, as well as the geometrical details of its neck and its opening (mouth), influence its resonance characteristics, as determined by spectral analysis of pressure fluctuations within the resonator. These variations can lead to a substantial increase or decrease of the resonant frequency. Furthermore, the theoretically predicted resonant frequencies are compared with those measured experimentally. In doing so, the role of end corrections at the opening (mouth) of the resonator is addressed.

When the resonator is attached to the wall of the deep cavity duct, i.e., side branch, the oscillation of the entire deep duct- Helmholtz resonator system can be substantially attenuated. The manner in which variations of volume of the resonator influence the degree of attenuation of the various spectral components is characterized. An unexpected observation is a shift of the resonant acoustic mode of the attenuated system to a higher value of frequency, relative to that in the unattenuated system. This aspect deserves further investigation.

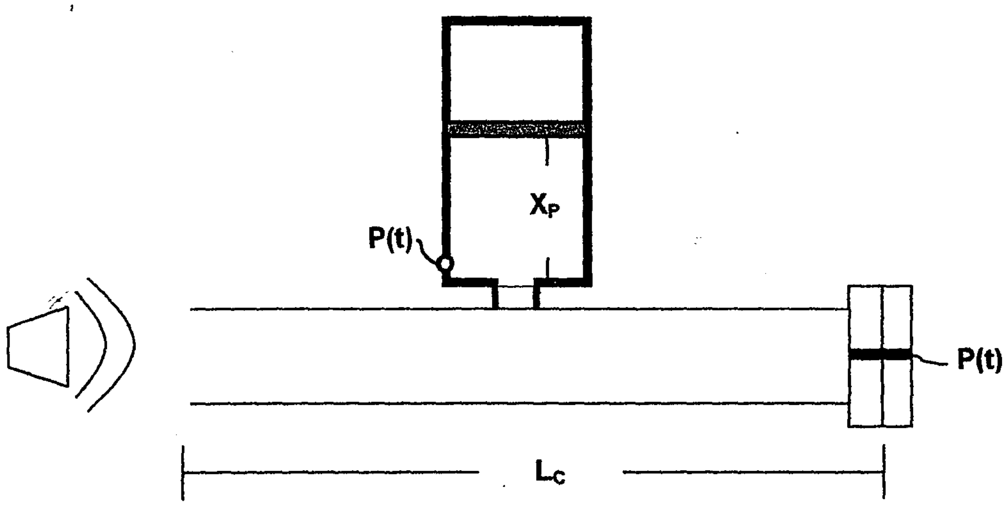

Figure 2.1: Schematic of the Helmholtz resonator and cavity duct.

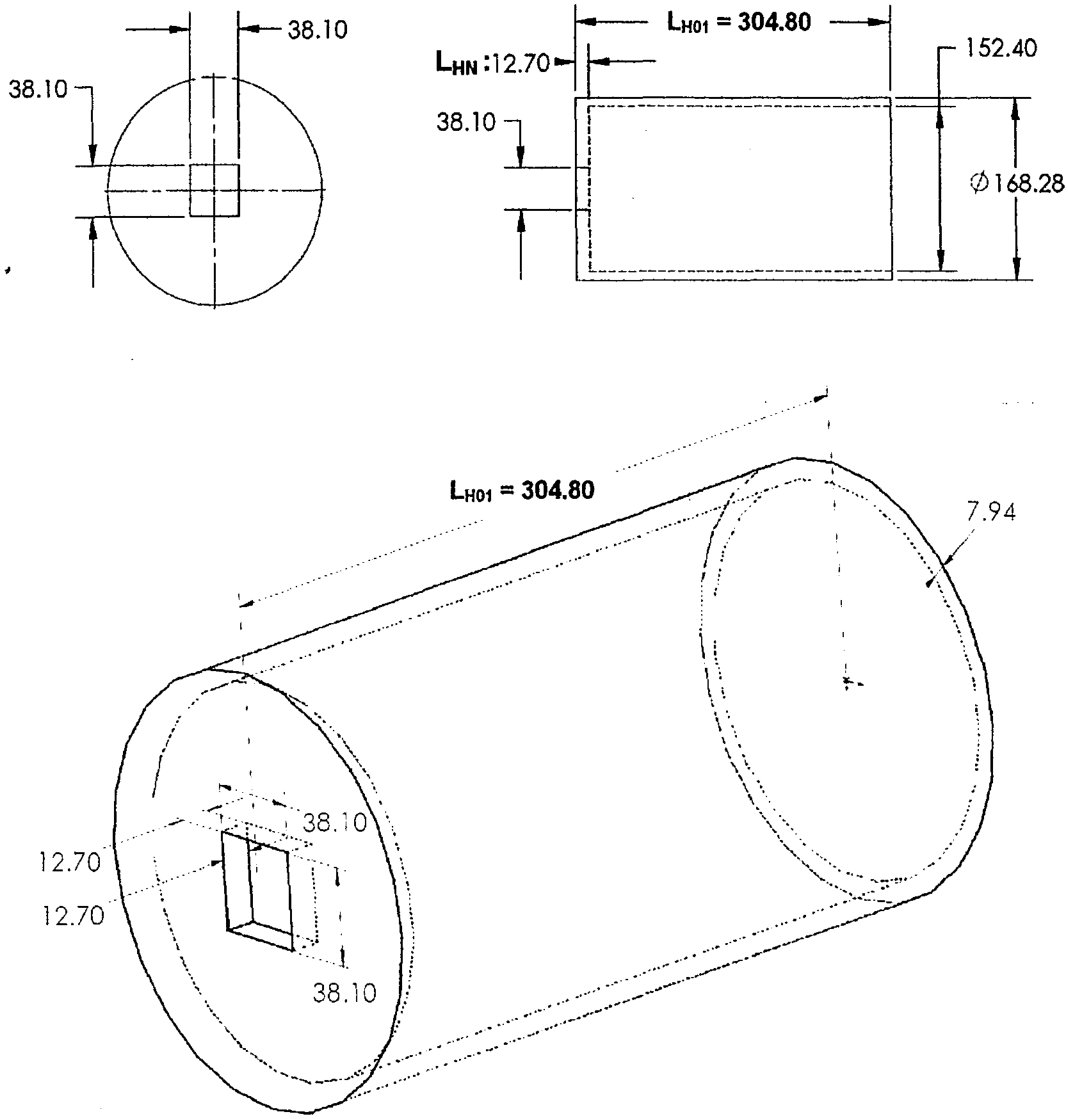

$L_H = L_{H01} + L_{H02}$

Figure 2.2a: Detailed schematic of the Helmholtz resonator corresponding to the body. The unit of length is mm.

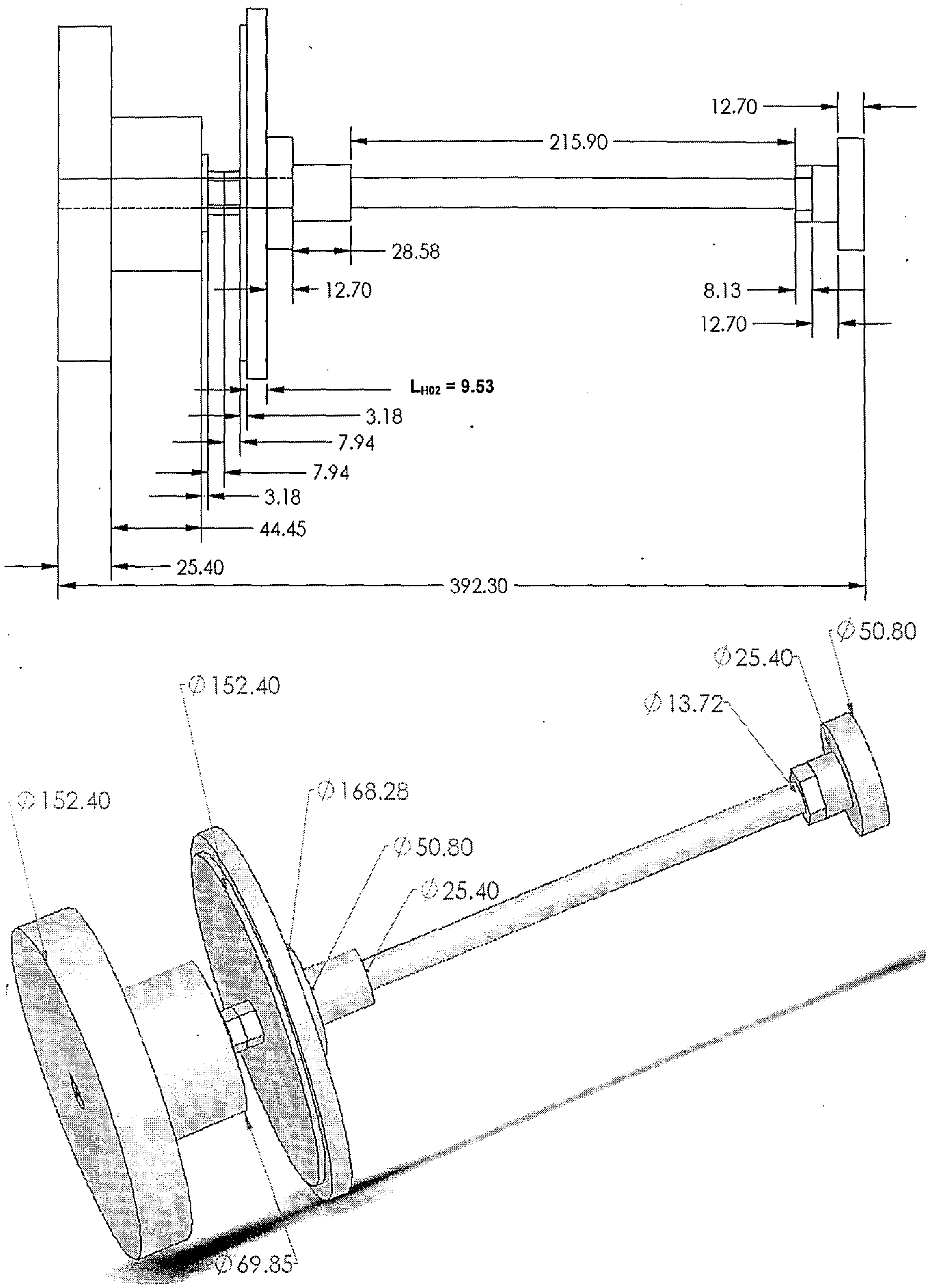

Figure 2.2b: Detailed schematic of the Helmholtz resonator involving a ring and a rod. The unit of length is mm.

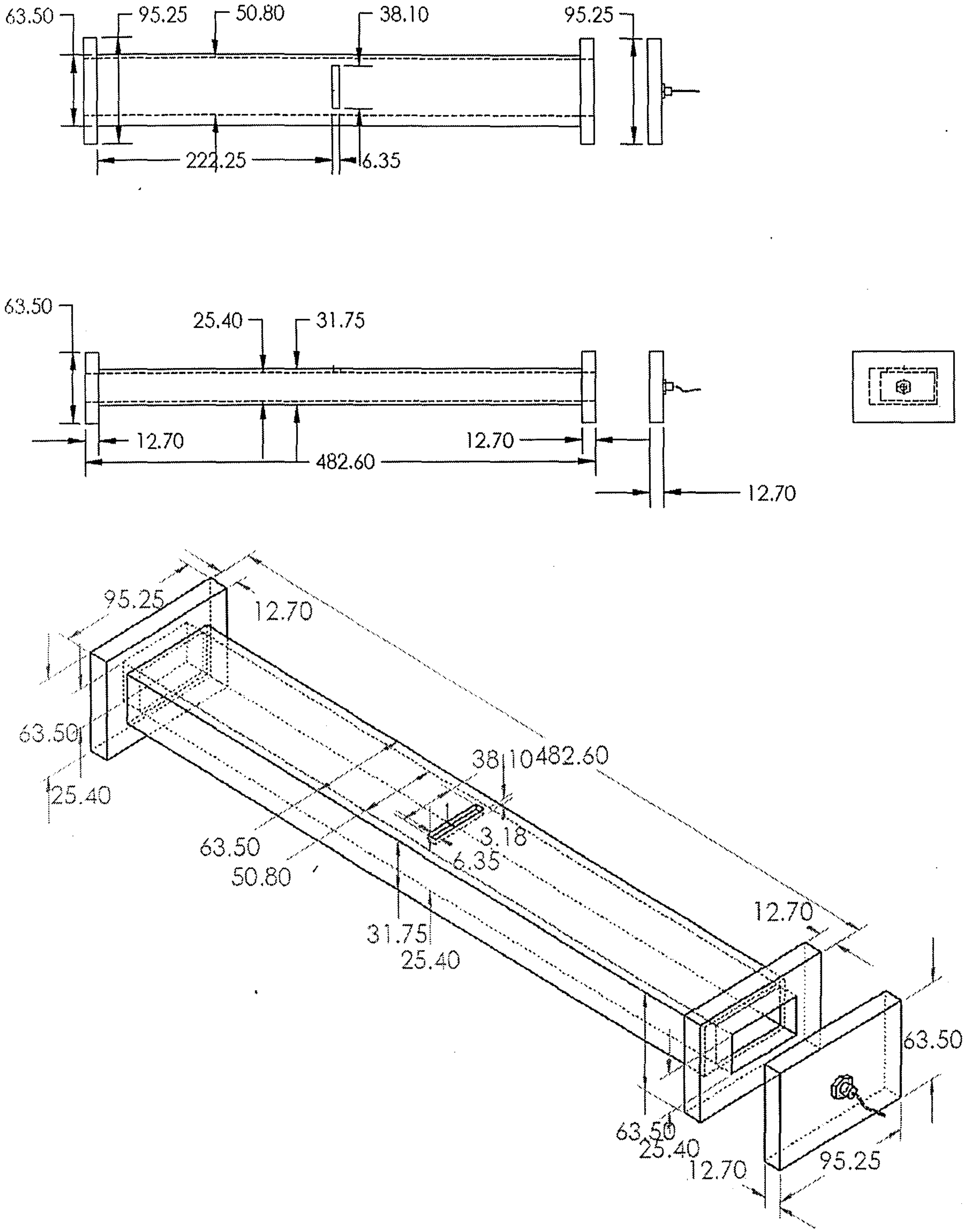

Figure 2.3: Detailed schematic of cavity duct. The unit of length is mm.

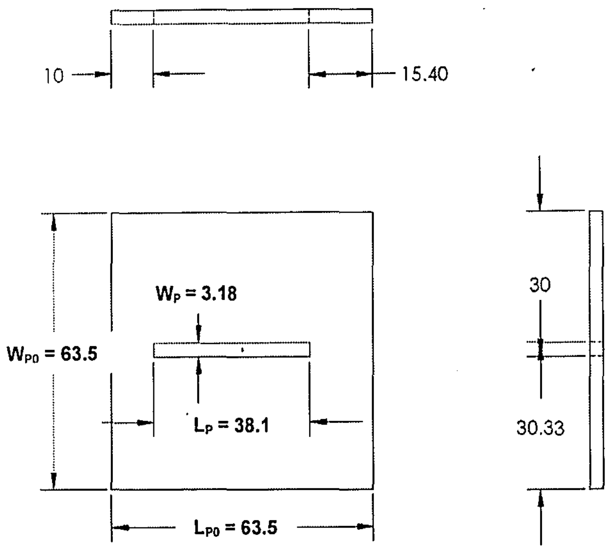

Figure 2.4a: Detailed schematic of plate with width of 3.18 mm. The unit of length is mm.

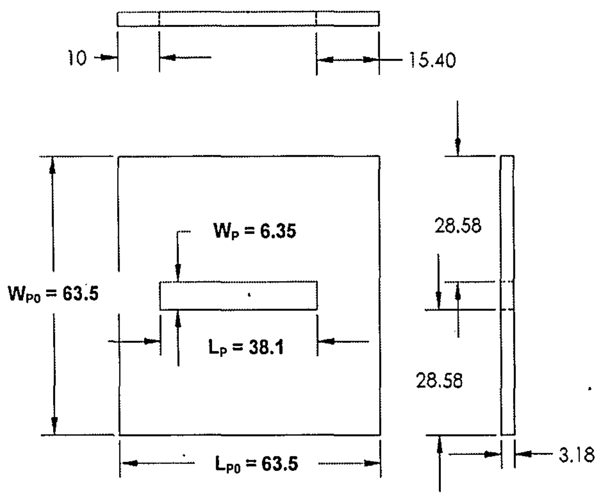

Figure 2.4b: Detailed schematic of plate with width of 6.35 mm. The unit of length is mm.

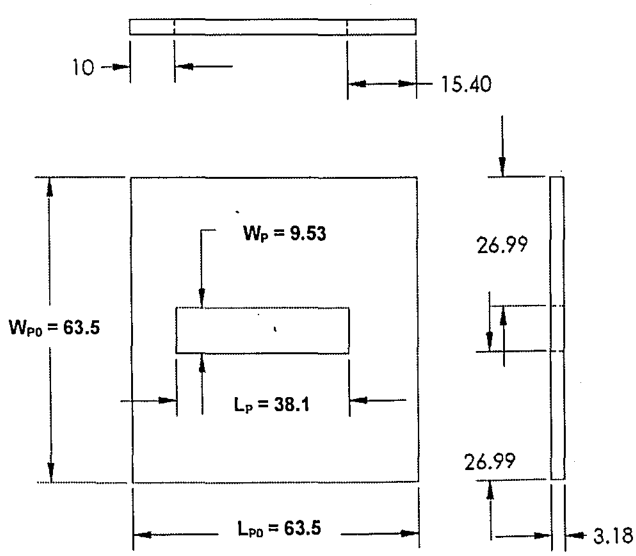

Figure 2.4c: Detailed schematic of plate with width of 9.53 mm. The unit of length is mm.

Thickness Of Neck (T)	Xp / Area(A)	1	2	3	4	5	6	7	Length Of Duct (L_C)
12.7 mm	1452 mm^2	O	O	O	O	O	O	O	-
3.18 mm	121 mm^2	O	O	O	O	O	O	O	-
	242 mm^2	O	O	O	O	O	O	O	O (486.2mm)
	362 mm^2	O	O	O	O	O	O	O	-

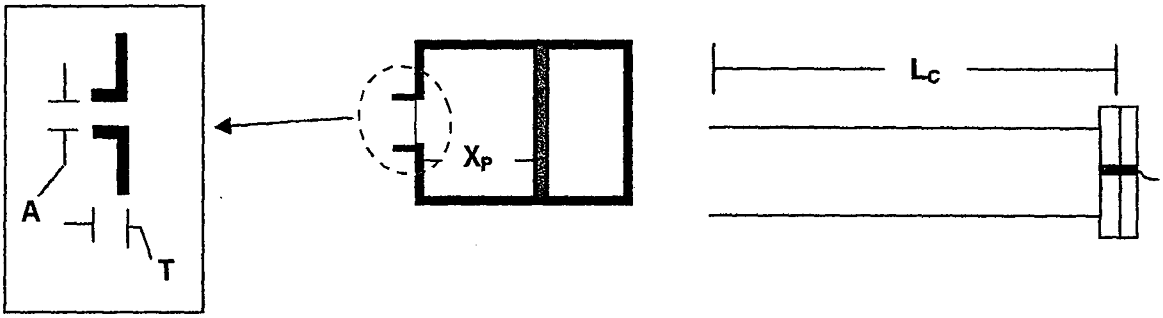

Figure 3.1: Overview of present experiments in term of the parameters of the experimental set-up.

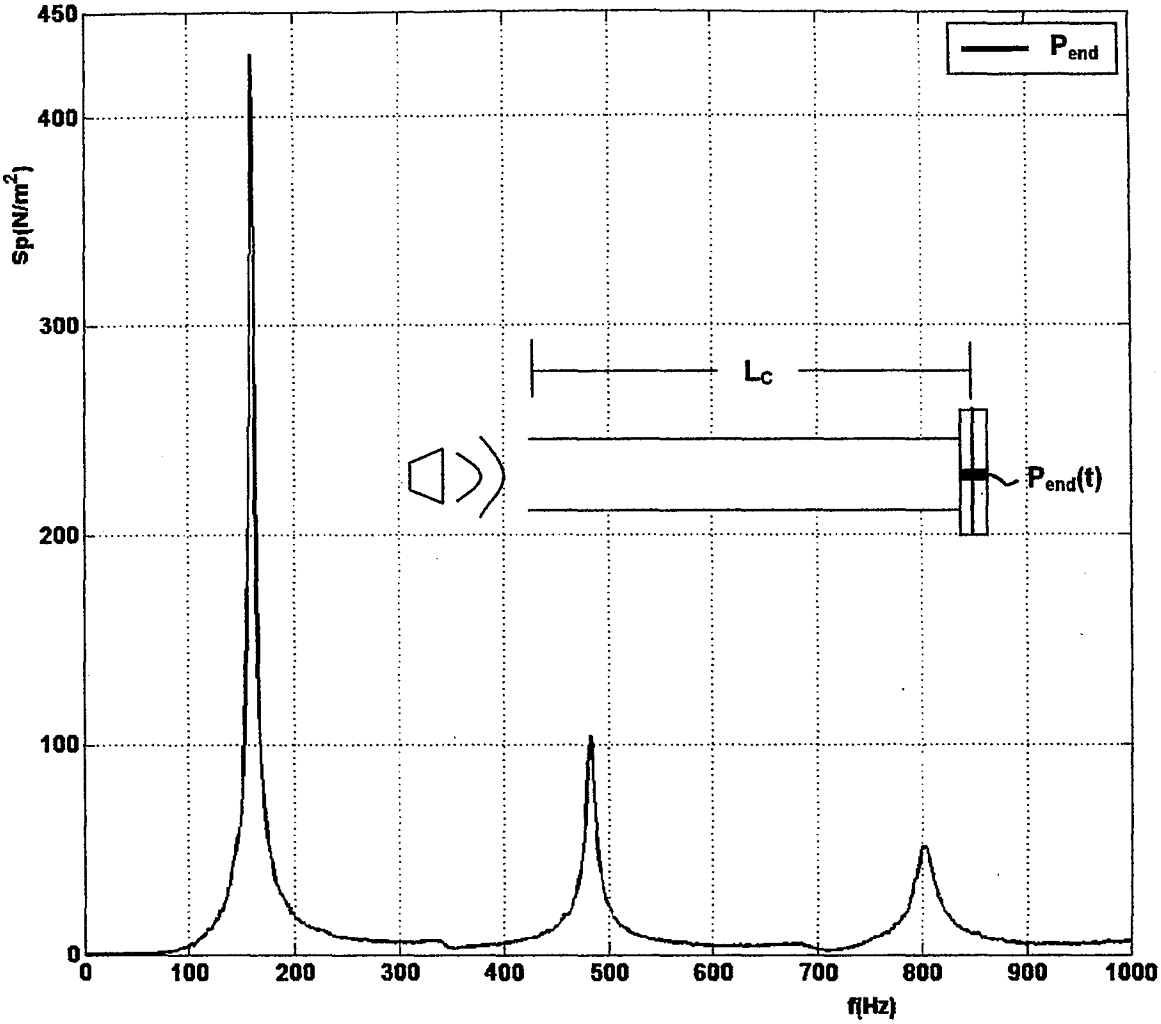

Figure 3.2: Natural frequency of open-closed cavity excited by pure tone at successive values of frequency. Frequency range is 1 to 1000 Hz. Length L_C of cavity is 482.6mm.

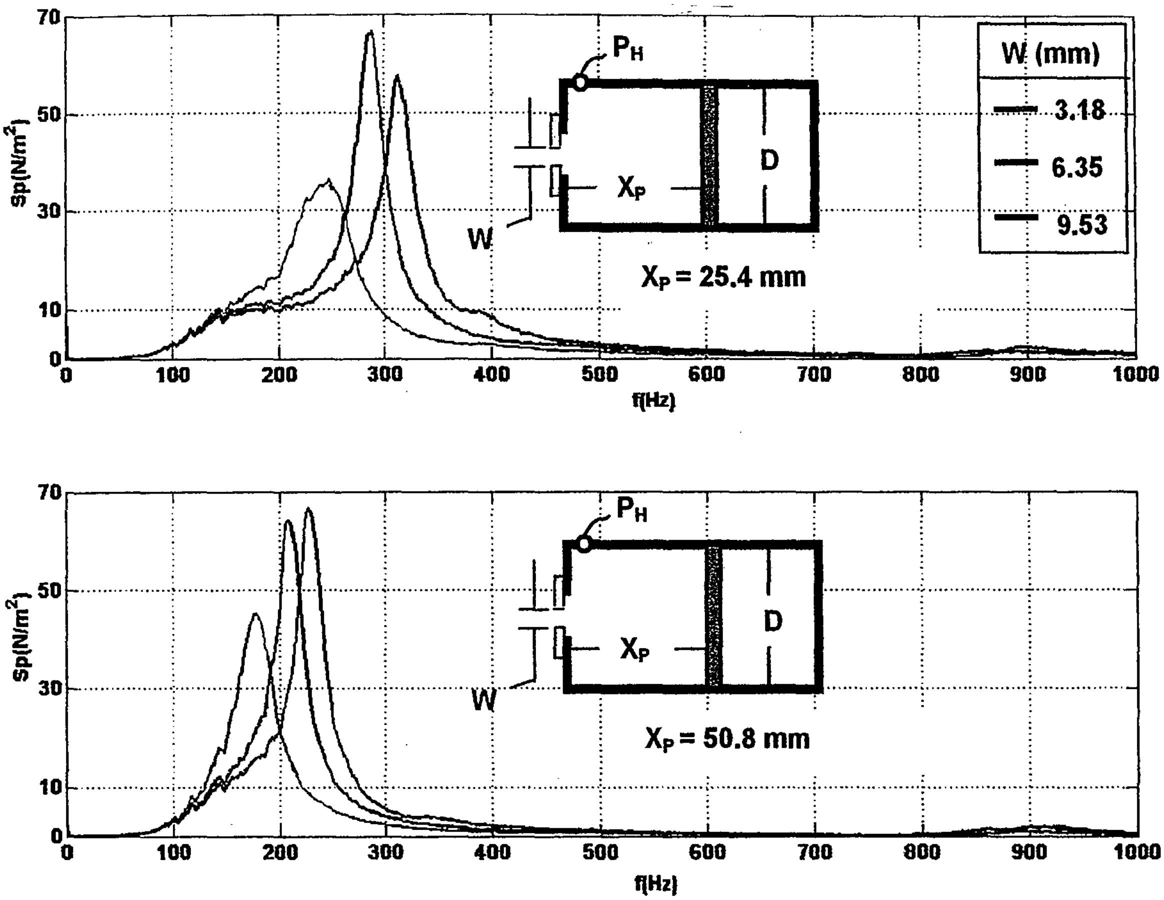

Figure 3.3: Spectra of pressure fluctuations inside the Helmholtz resonator due to pure tone excitation at successive values of frequency, as a function of length X_P and width W for fixed value of mouth length L = 38.1 mm.

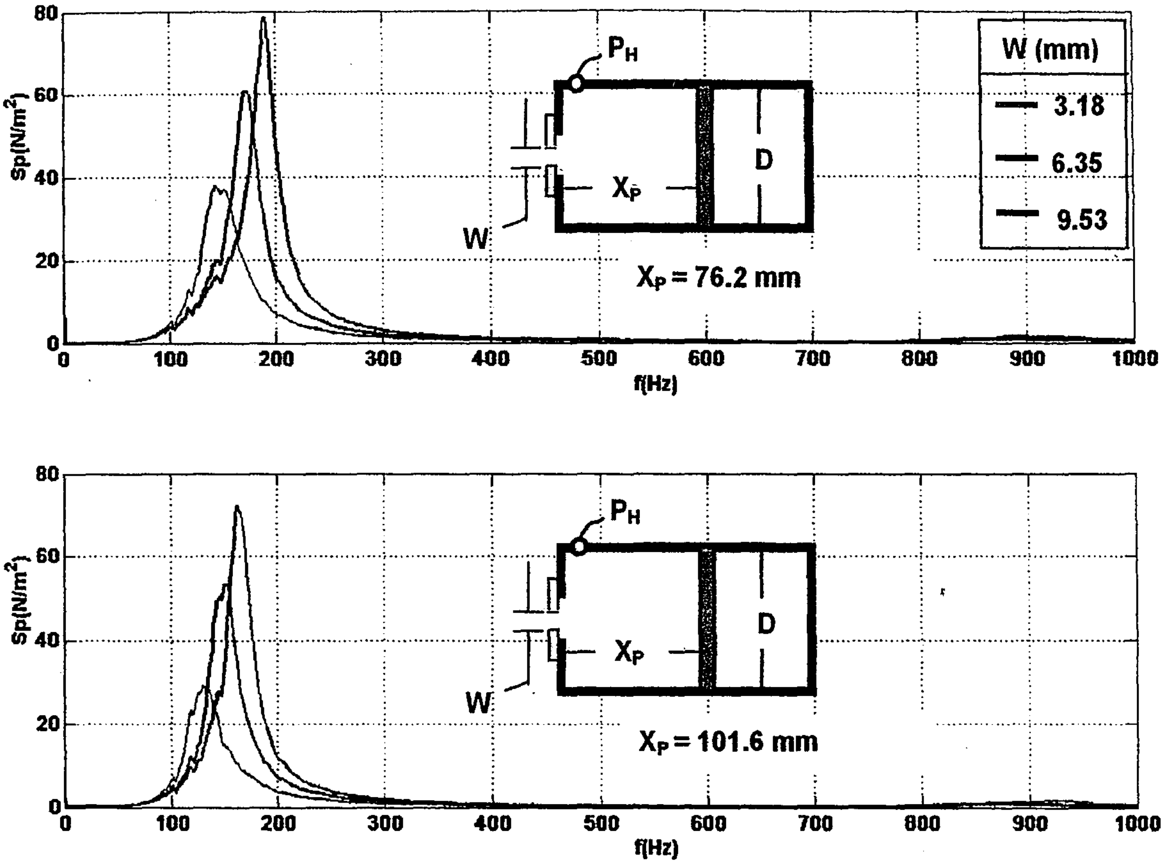

Figure 3.4: Spectra of pressure fluctuations inside the Helmholtz resonator due to pure tone excitation at successive values of frequency, as a function of length X_P and width W for fixed value of mouth length L = 38.1 mm.

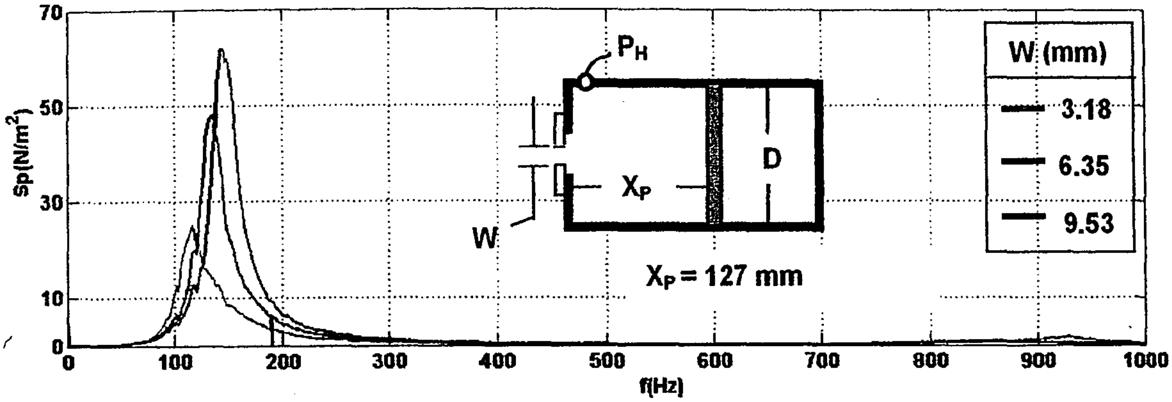

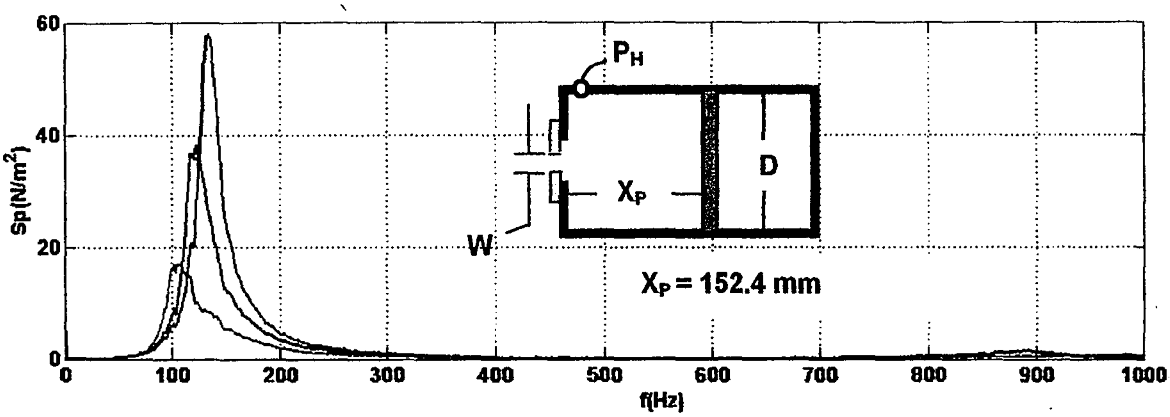

Figure 3.5: Spectra of pressure fluctuations inside the Helmholtz resonator due to pure tone excitation at successive values of frequency, as a function of length X_P and width W for fixed value of mouth length L = 38.1 mm.

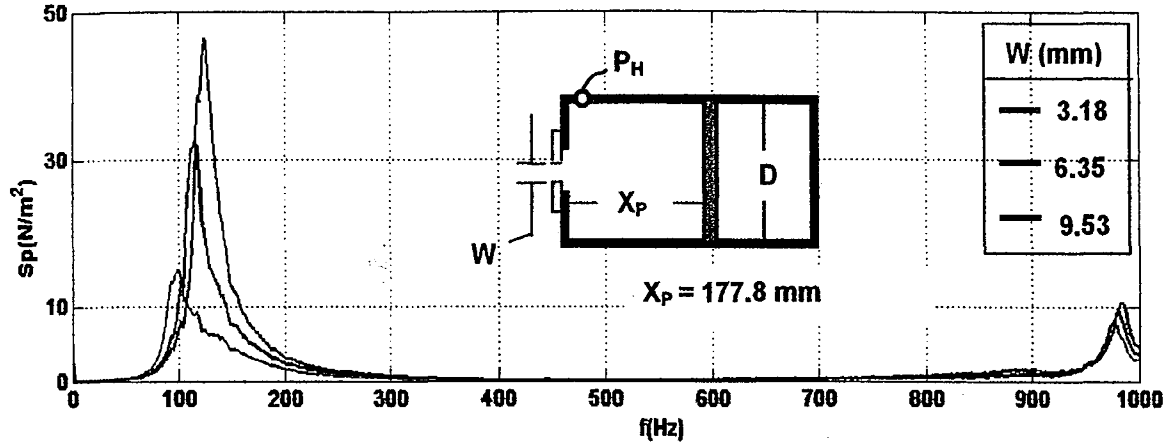

Figure 3.6: Spectra of pressure fluctuations inside the Helmholtz resonator due to pure tone excitation at successive values of frequency, as a function of length X_P and width W for fixed value of mouth length L = 38.1 mm.

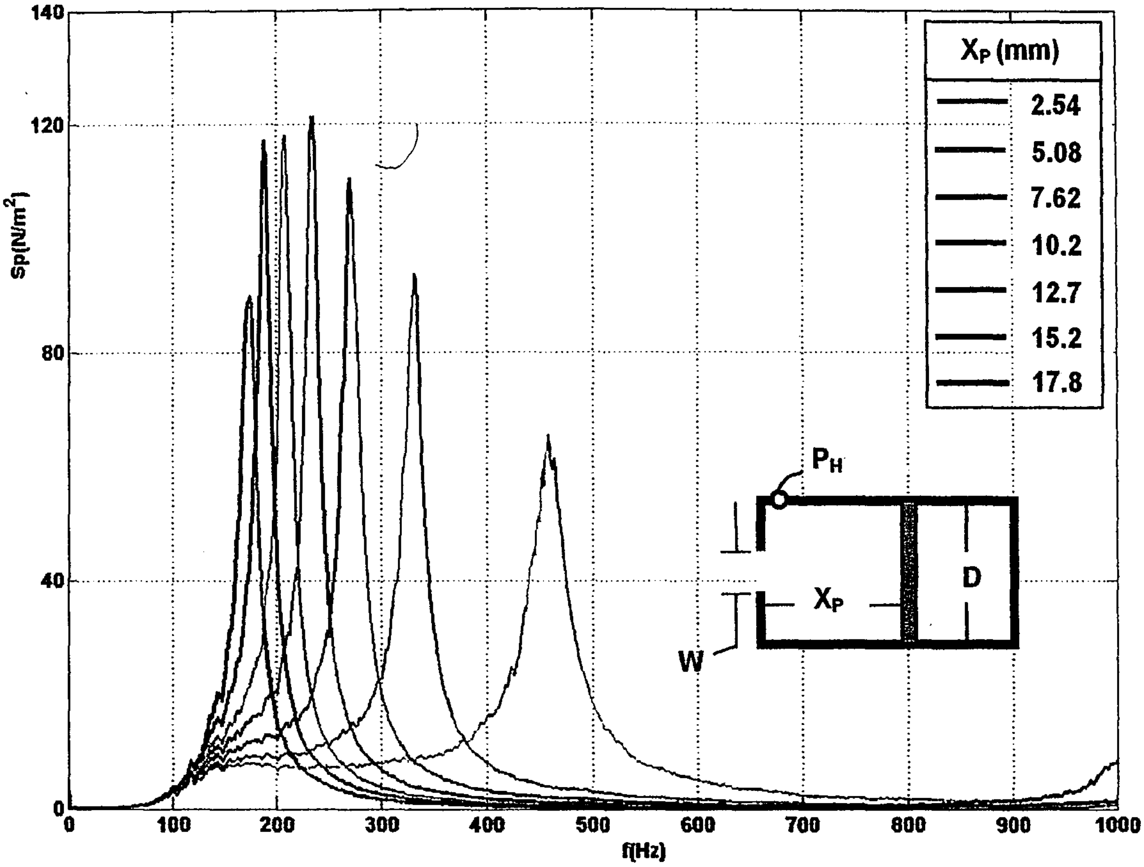

Figure 3.7: Spectra of pressure fluctuations inside the Helmholtz resonator due to pure tone excitation at successive values of frequency. Area of mouth of resonator is A = 1452 mm^2. Diameter of resonator is D = 152.4 mm. Detailed schematic is given in Figure 2.2 and 2.4.

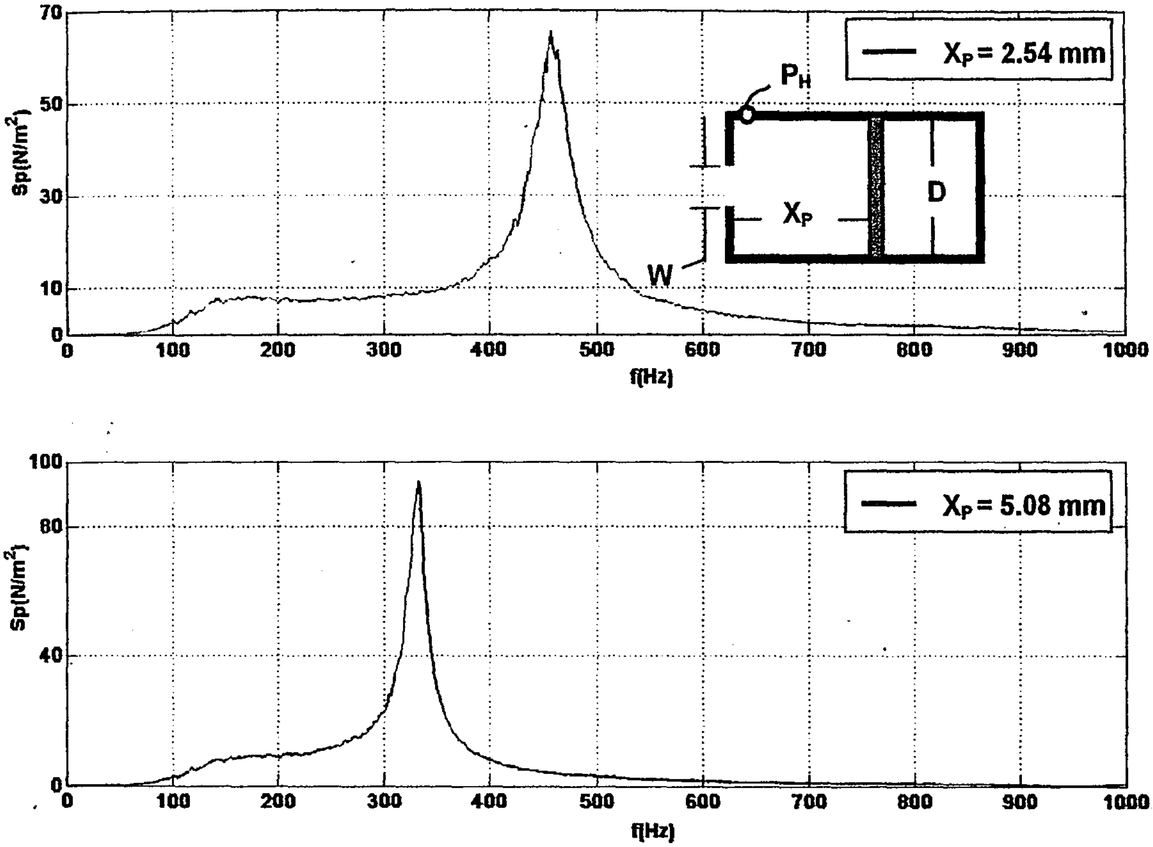

Figure 3.8a: Response spectrum of Helmholtz resonator as a function of length X_P for fixed value of mouth width W = 38.1 mm and length L = 38.1 mm.

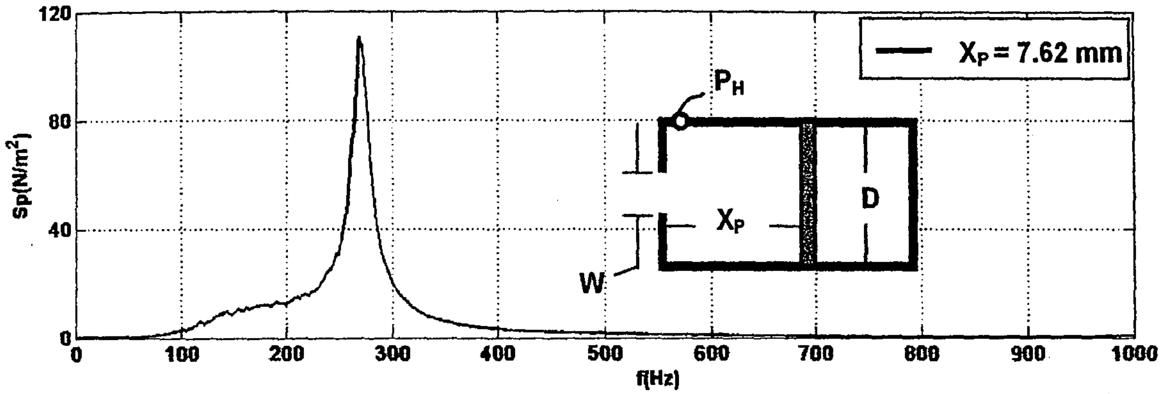

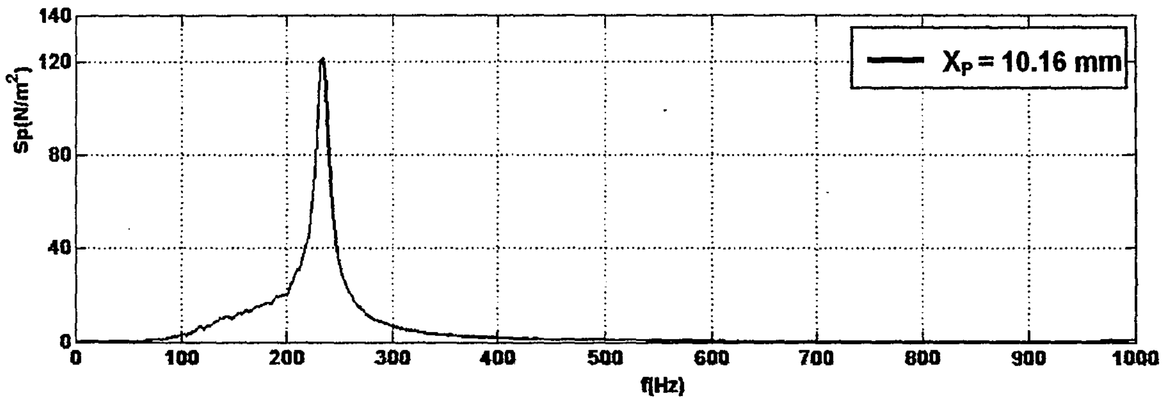

Figure 3.8b: Response spectrum of Helmholtz resonator as a function of length X_P for fixed value of mouth width W = 38.1 mm and length L = 38.1 mm.

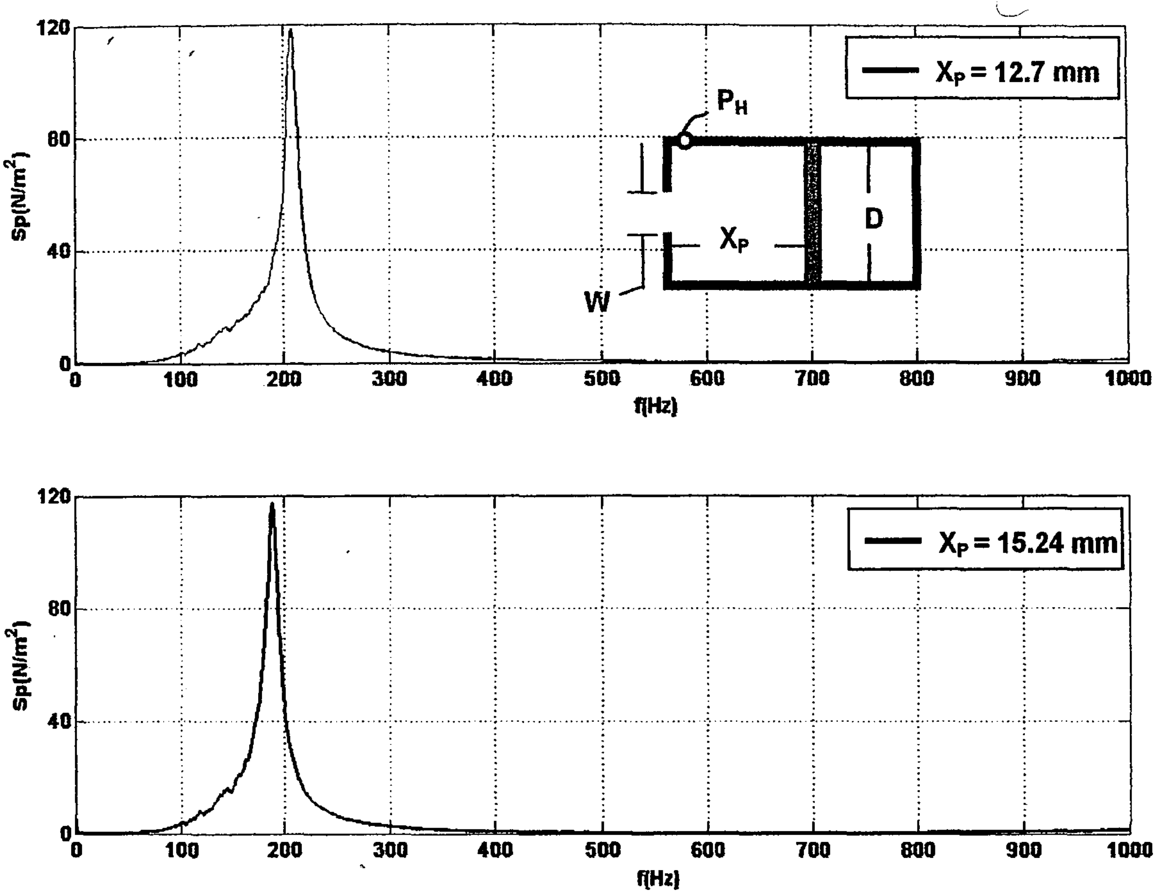

Figure 3.8c: Response spectrum of Helmholtz resonator as a function of length X_P for fixed value of mouth width W = 38.1 mm and length L = 38.1 mm.

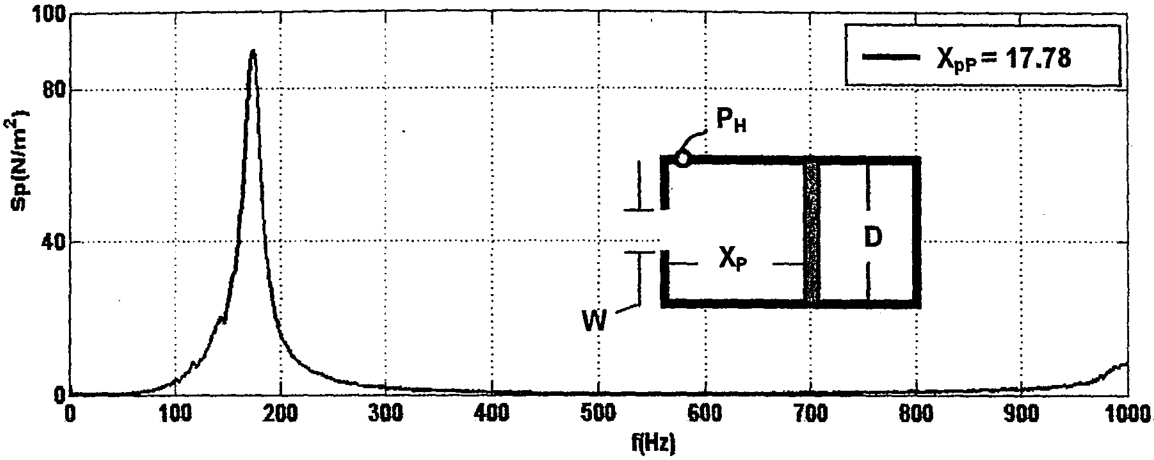

Figure 3.8d: Response spectrum of Helmholtz resonator as a function of length X_P for fixed value of mouth width W = 38.1 mm and length L = 38.1 mm.

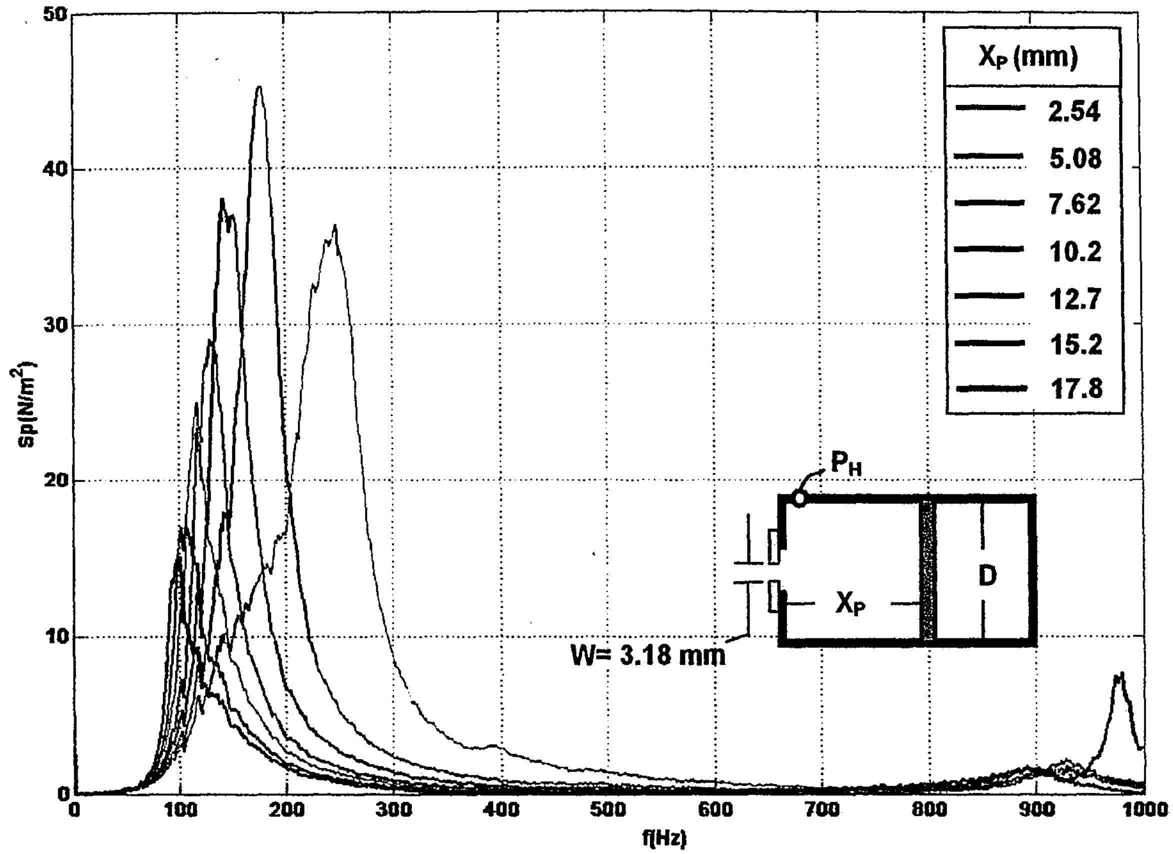

Figure 3.9: Spectra of pressure fluctuations inside the Helmholtz resonator due to pure tone excitation at successive values of frequency. Area of mouth of resonator is A = 120.97 mm^2. Diameter of resonator is D = 152.4 mm. Detailed schematic is given in Figure 2.2 and 2.4.

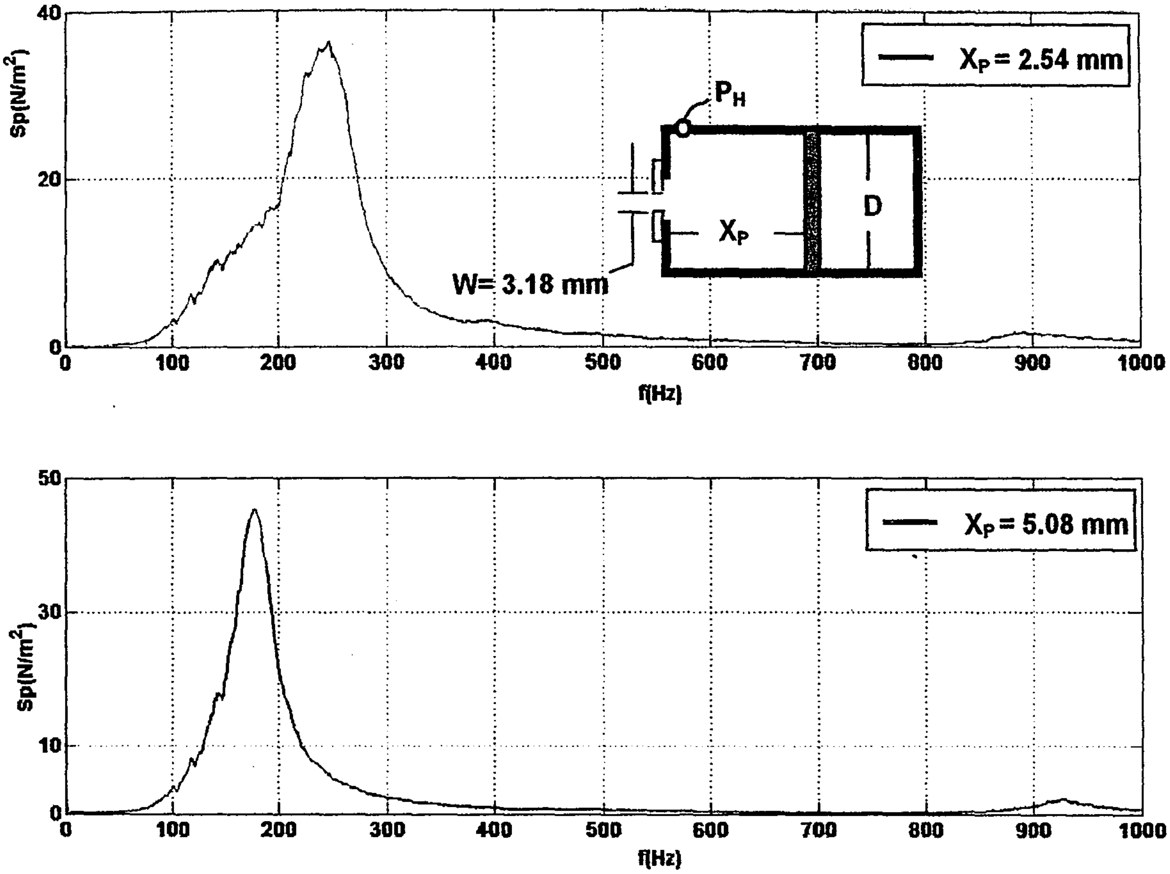

Figure 3.10a: Response spectrum of Helmholtz resonator as a function of length X_P for fixed value of mouth width W = 3.18 mm and length L = 38.1 mm.

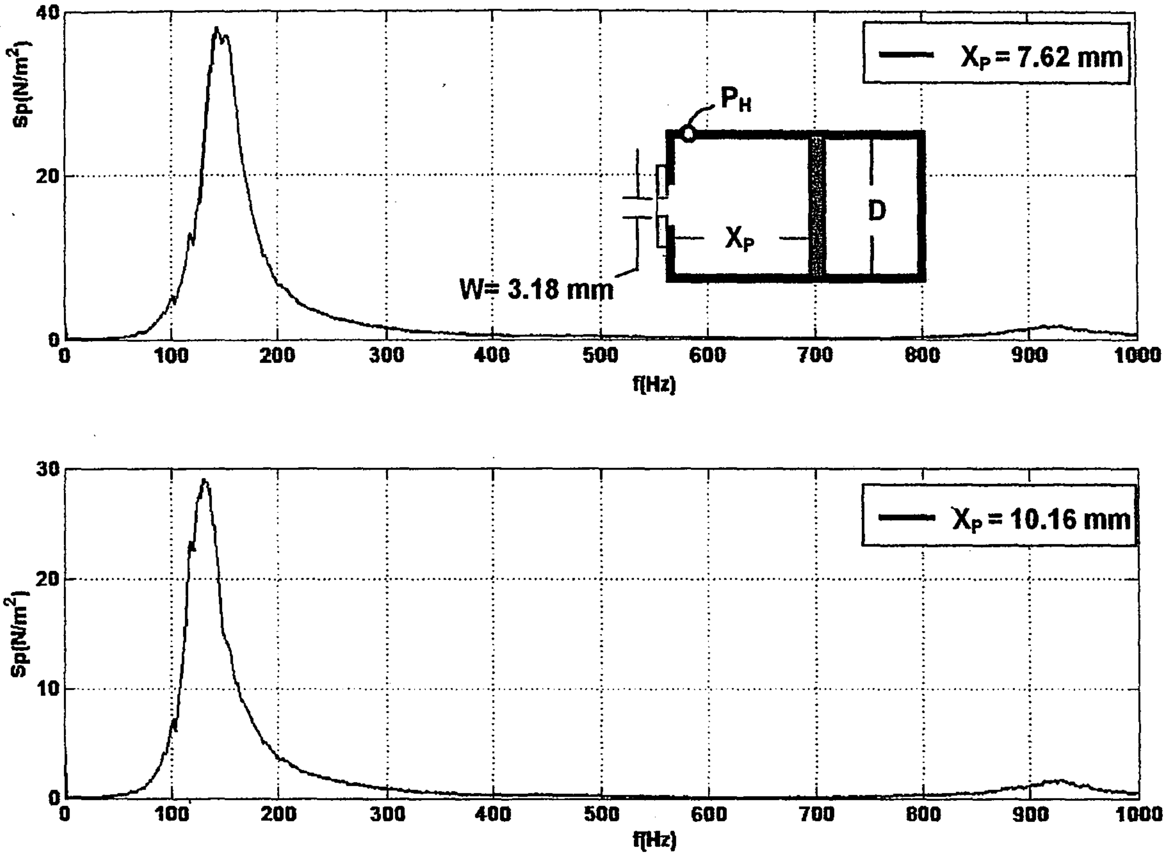

Figure 3.10b: Response spectrum of Helmholtz resonator as a function of length X_P for fixed value of mouth width W = 3.18 mm and length L = 38.1 mm.

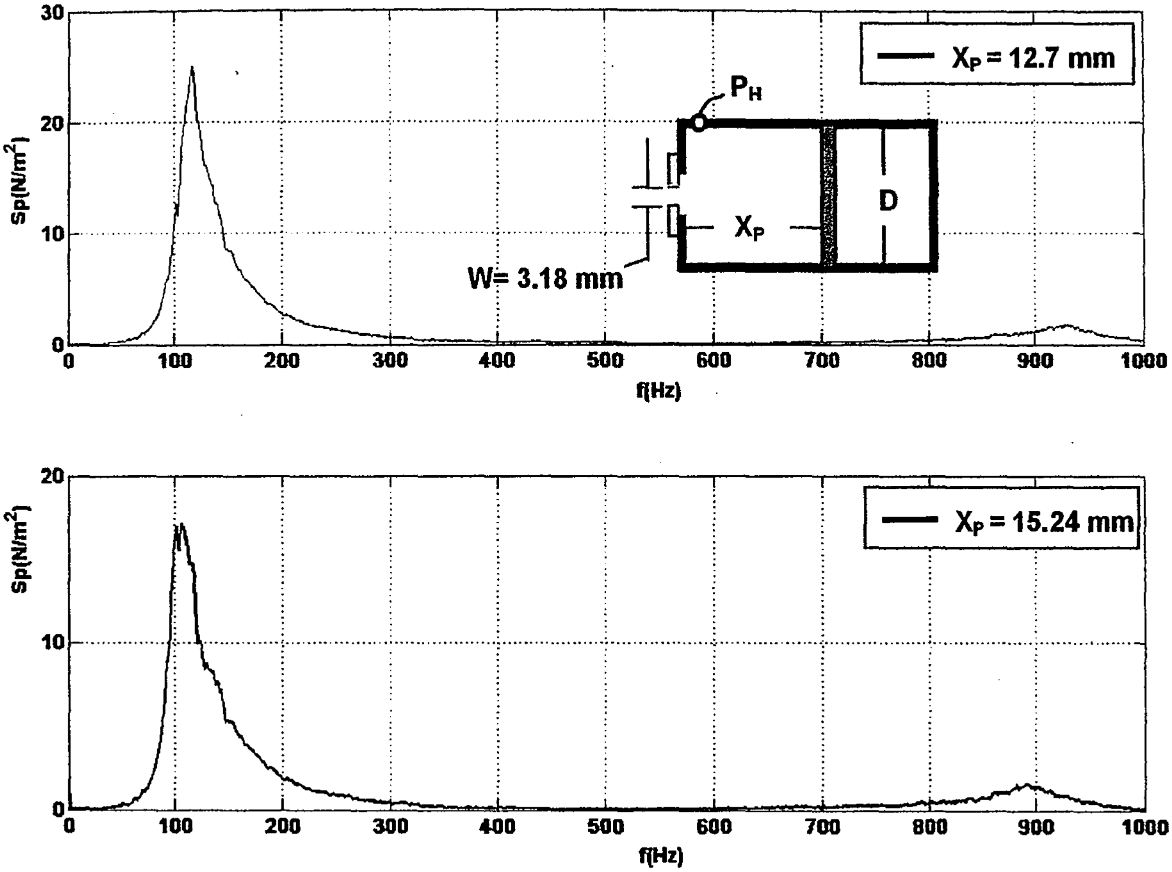

Figure 3.10c: Response spectrum of Helmholtz resonator as a function of length X_P for fixed value of mouth width W = 3.18 mm and length L = 38.1 mm.

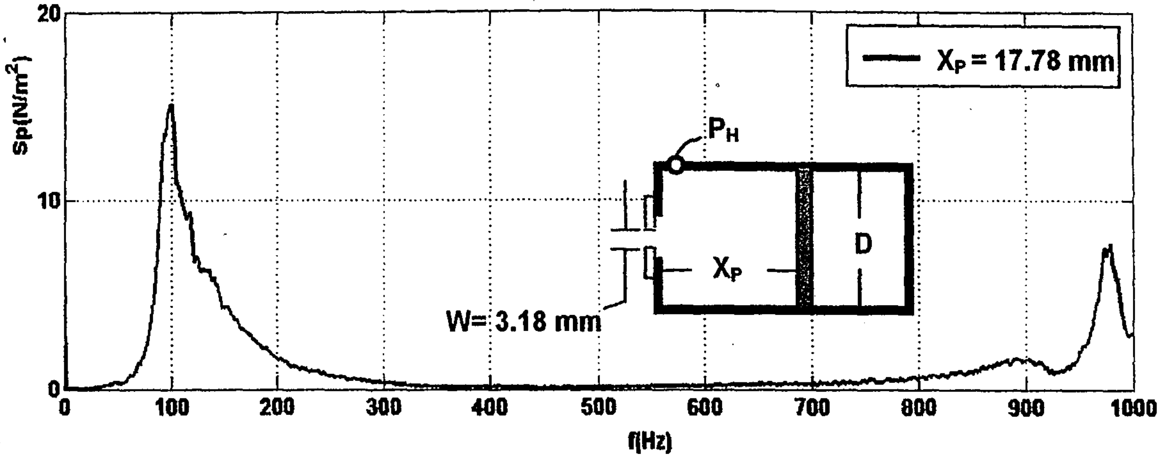

Figure 3.10d: Response spectrum of Helmholtz resonator as a function of length X_P for fixed value of mouth width W = 3.18 mm and length L = 38.1 mm.

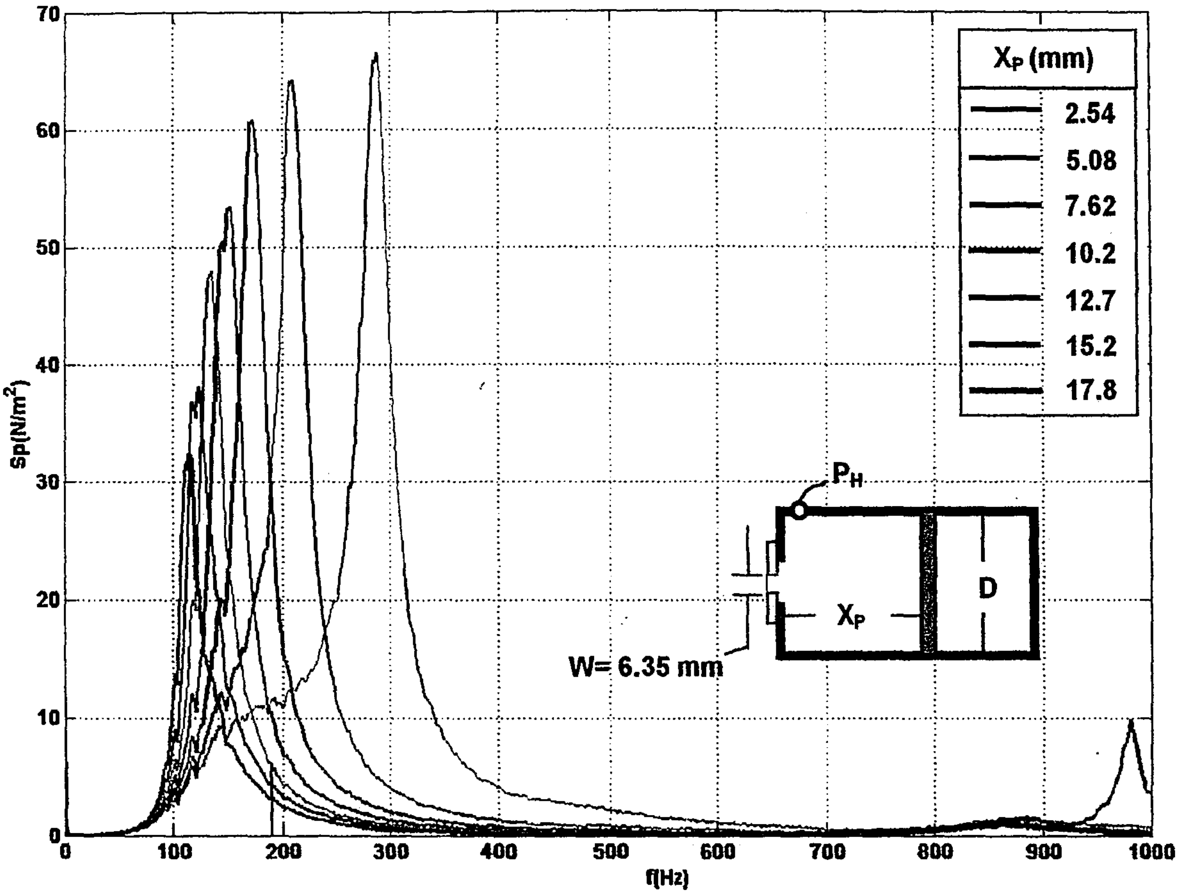

Figure 3.11: Spectra of pressure fluctuations inside the Helmholtz resonator due to pure tone excitation at successive values of frequency. Area of mouth of resonator is $A = 241.94\ mm^2$. Diameter of resonator is D = 152.4 mm. Detailed schematic is given in Figure 2.2 and 2.4.

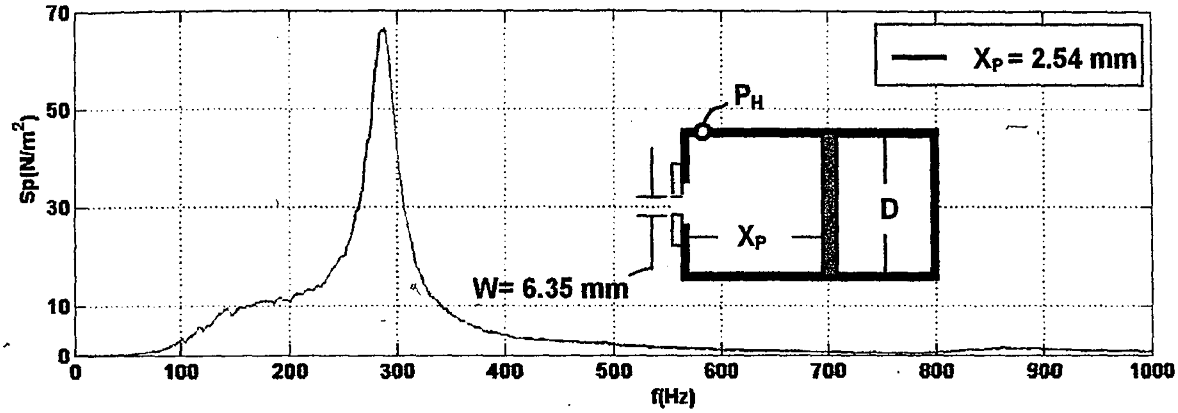

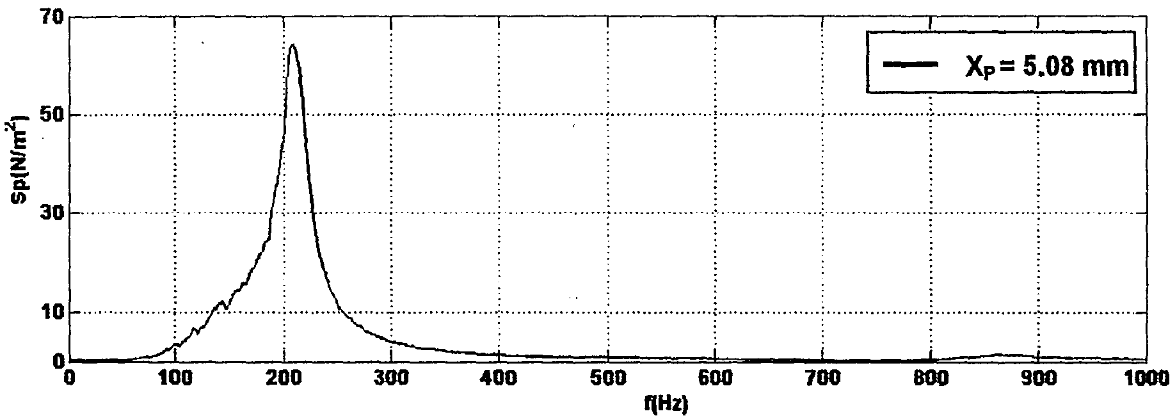

Figure 3.12a: Response spectrum of Helmholtz resonator as a function of length X_P for fixed value of mouth width W = 6.35 mm and length L = 38.1 mm.

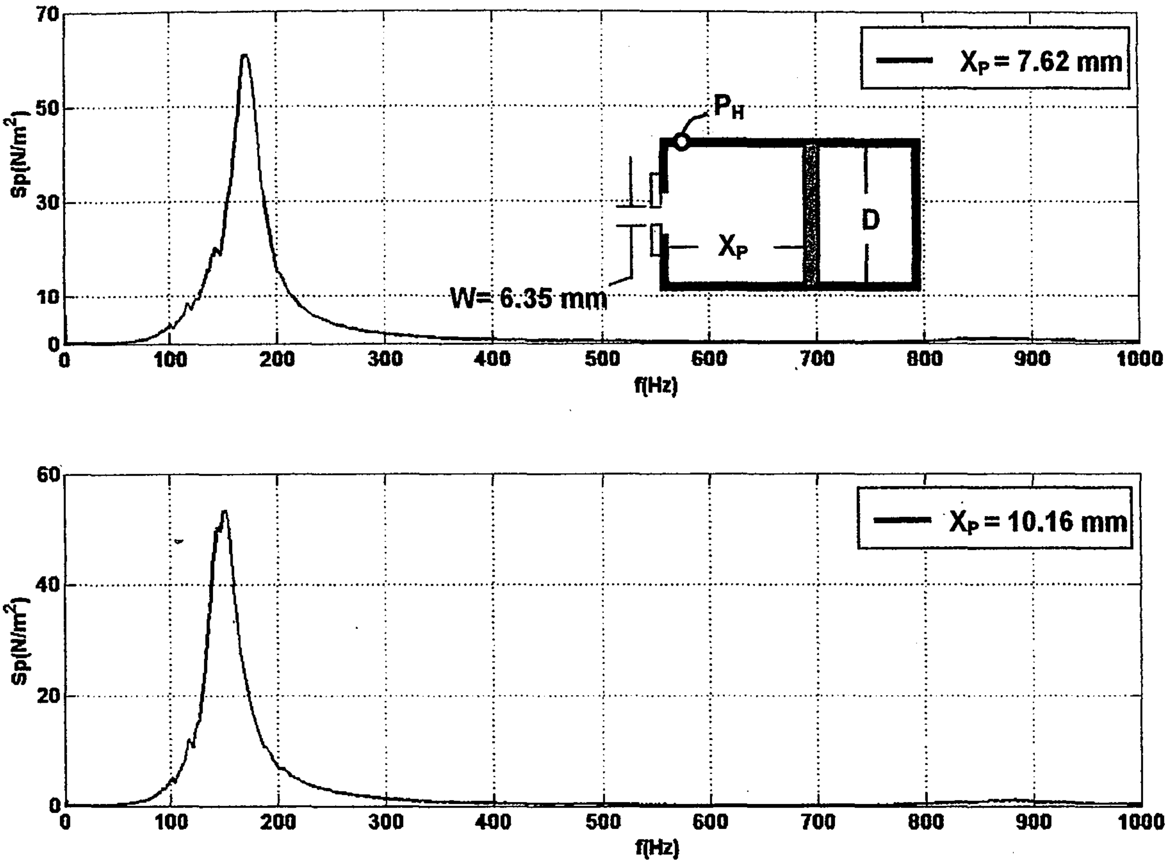

Figure 3.12b: Response spectrum of Helmholtz resonator as a function of length X_P for fixed value of mouth width W = 6.35 mm and length L = 38.1 mm.

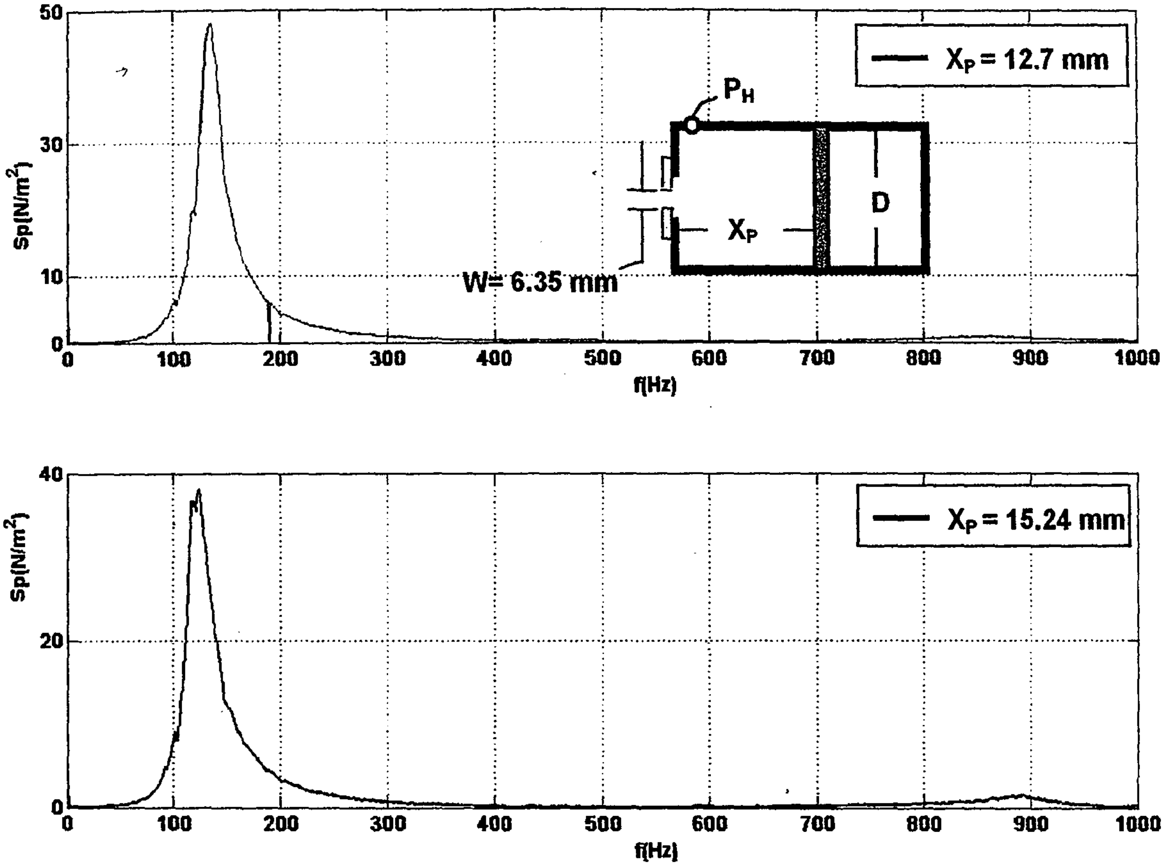

Figure 3.12c: Response spectrum of Helmholtz resonator as a function of length X_P for fixed value of mouth width W = 6.35 mm and length L = 38.1 mm.

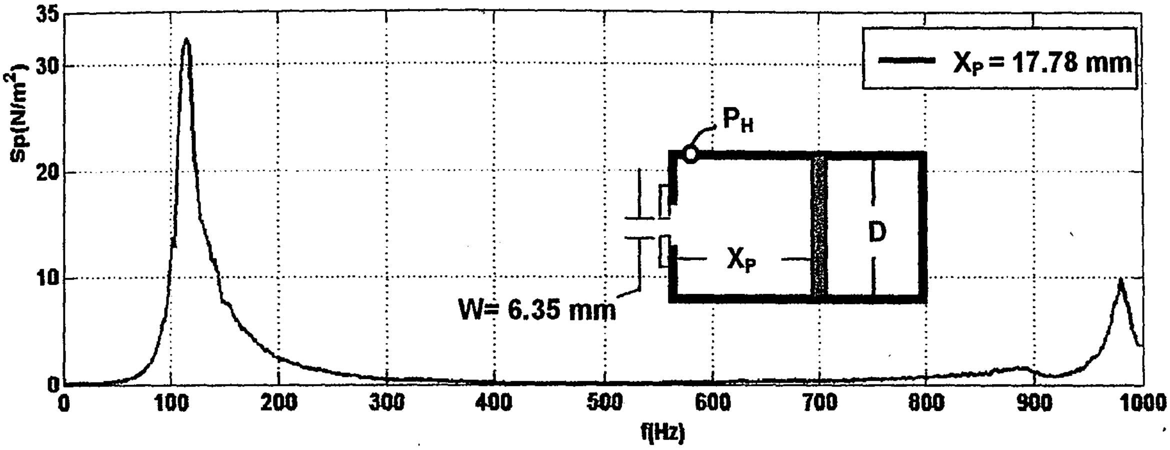

Figure 3.12d: Response spectrum of Helmholtz resonator as a function of length X_P for fixed value of mouth width W = 6.35 mm and length L = 38.1 mm.

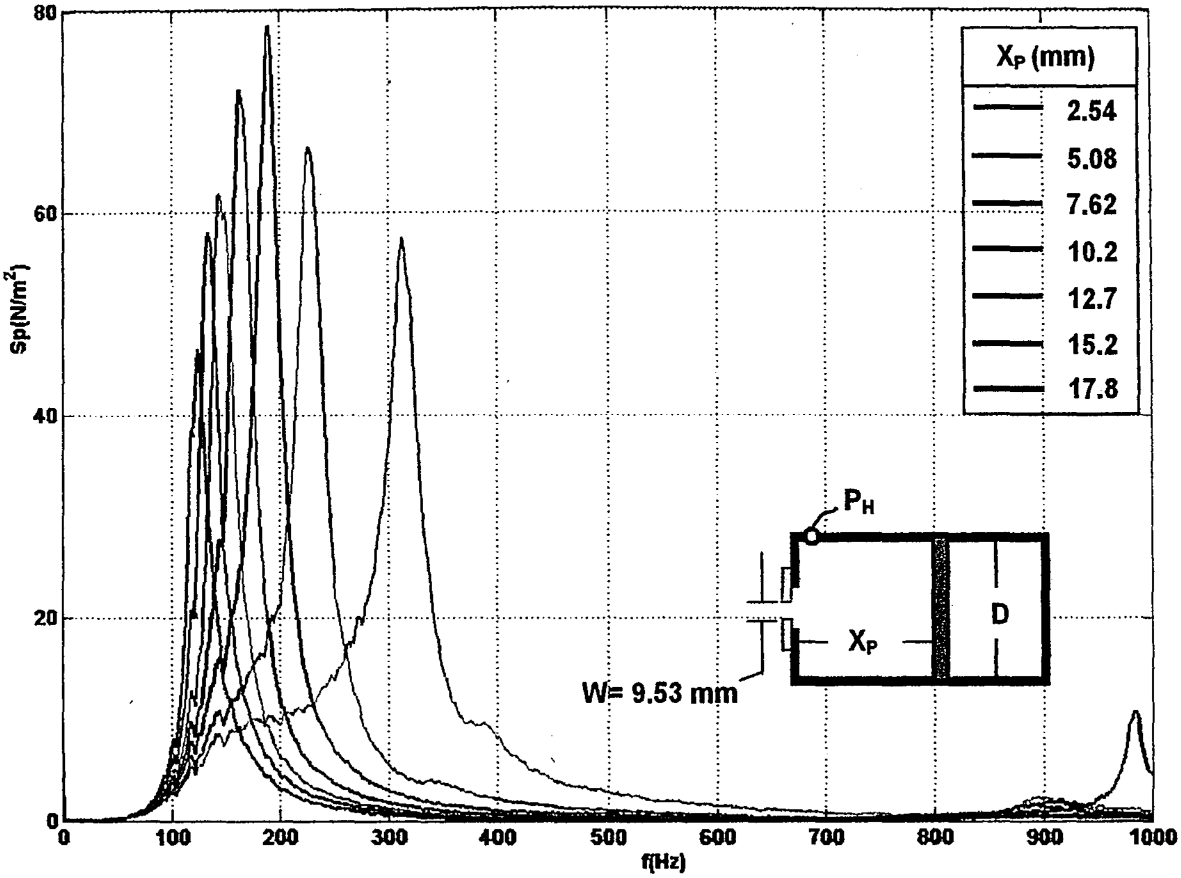

Figure 3.13: Spectra of pressure fluctuations inside the Helmholtz resonator due to pure tone excitation at successive values of frequency. Area of mouth of resonator is A = 362.90 mm^2. Diameter of resonator is D = 152.4 mm. Detailed schematic is given in Figure 2.2 and 2.4.

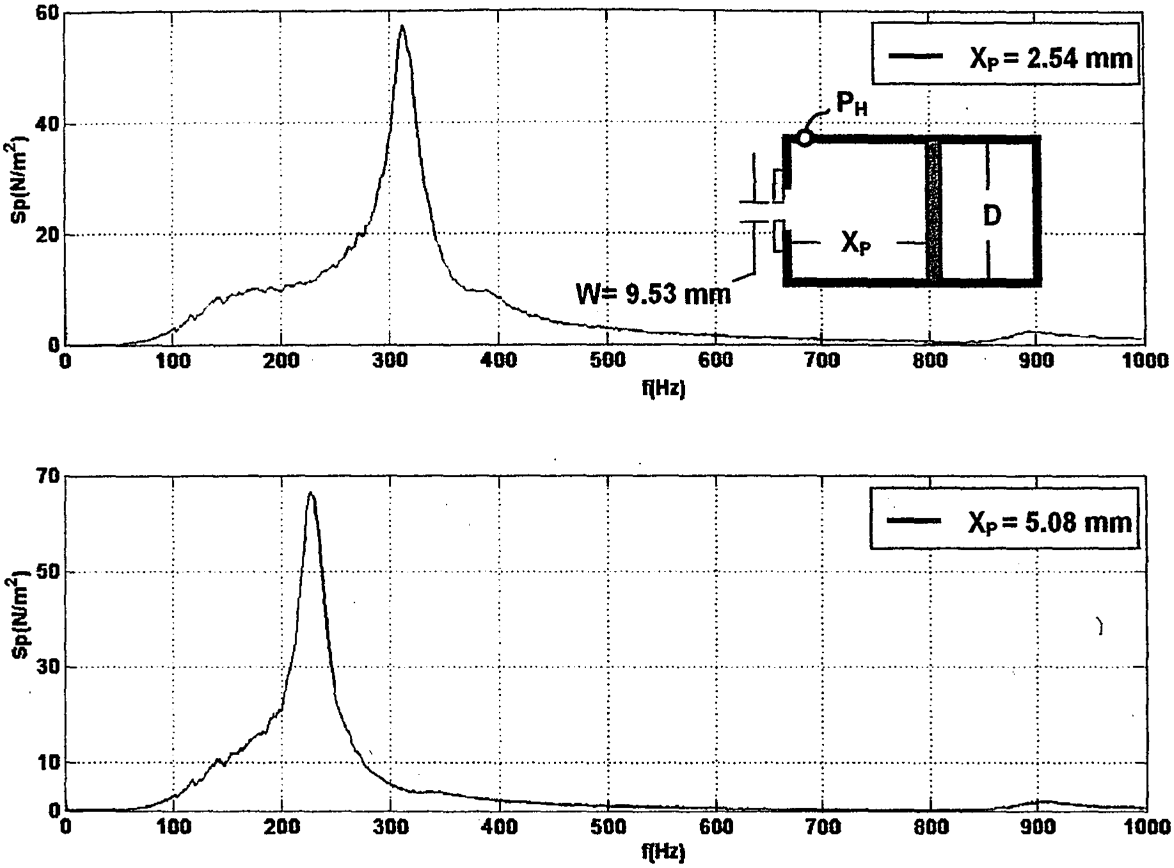

Figure 3.14a: Response spectrum of Helmholtz resonator as a function of length X_P for fixed value of mouth width W = 9.53 mm and length L = 38.1 mm.

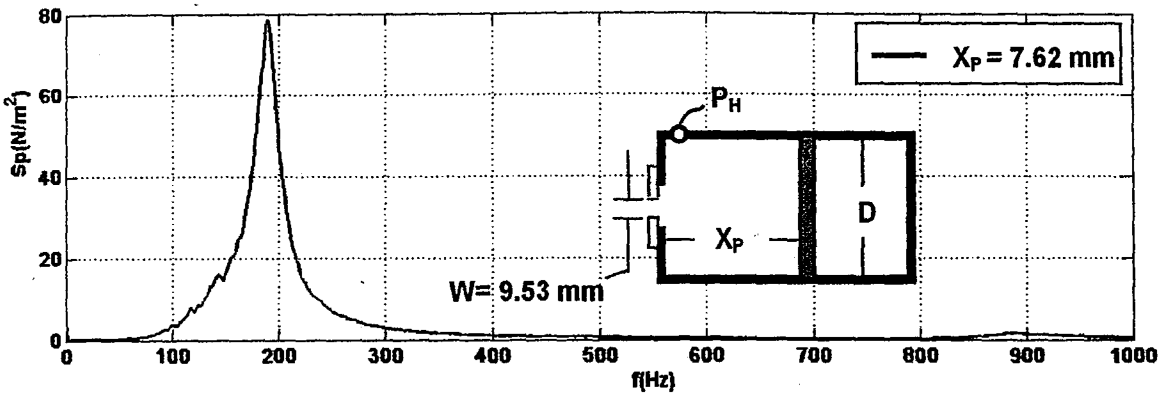

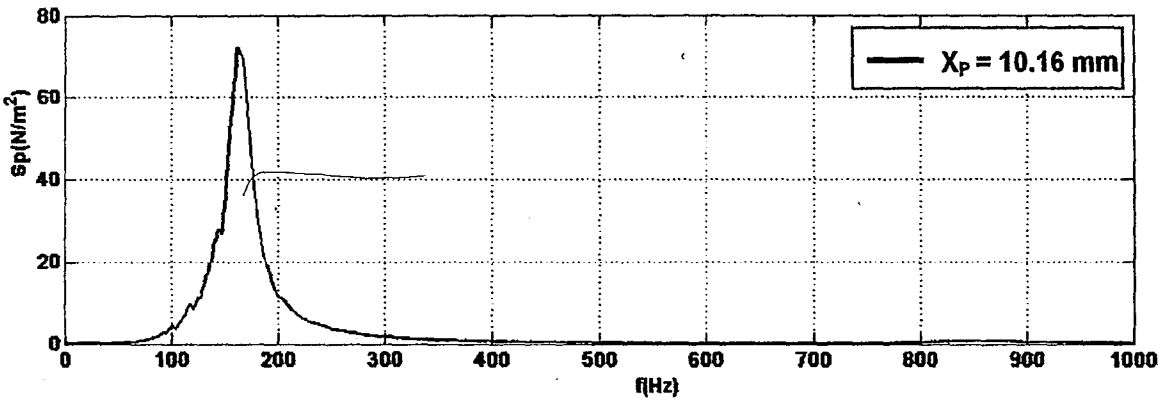

Figure 3.14b: Response spectrum of Helmholtz resonator as a function of length X_P for fixed value of mouth width W = 9.53 mm and length L = 38.1 mm.

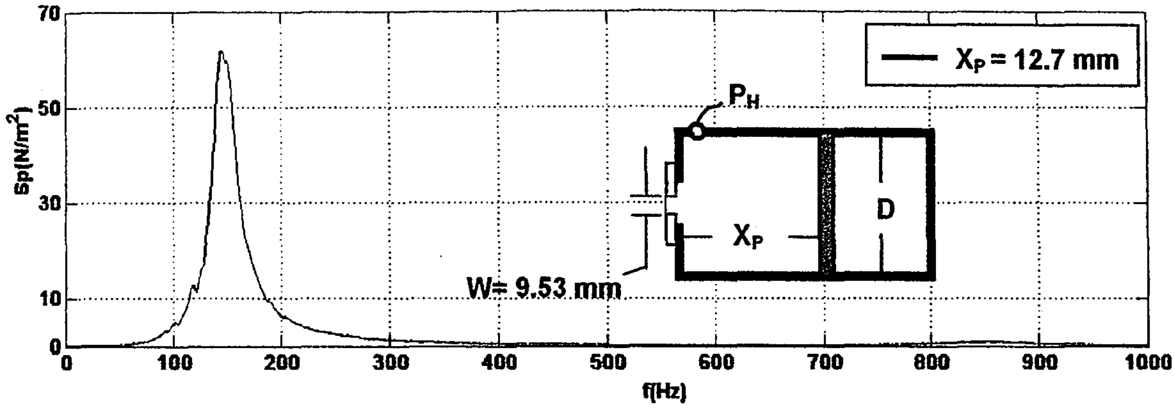

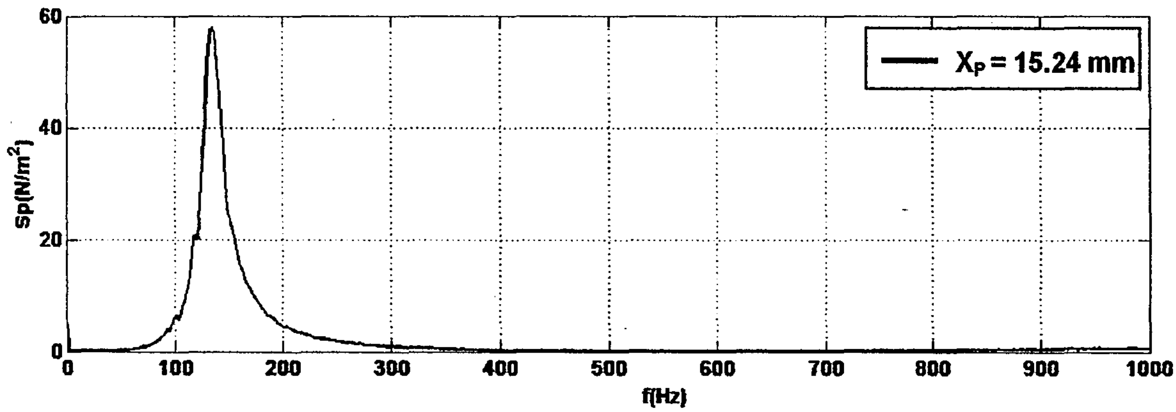

Figure 3.14c: Response spectrum of Helmholtz resonator as a function of length X_P for fixed value of mouth width W = 9.53 mm and length L = 38.1 mm.

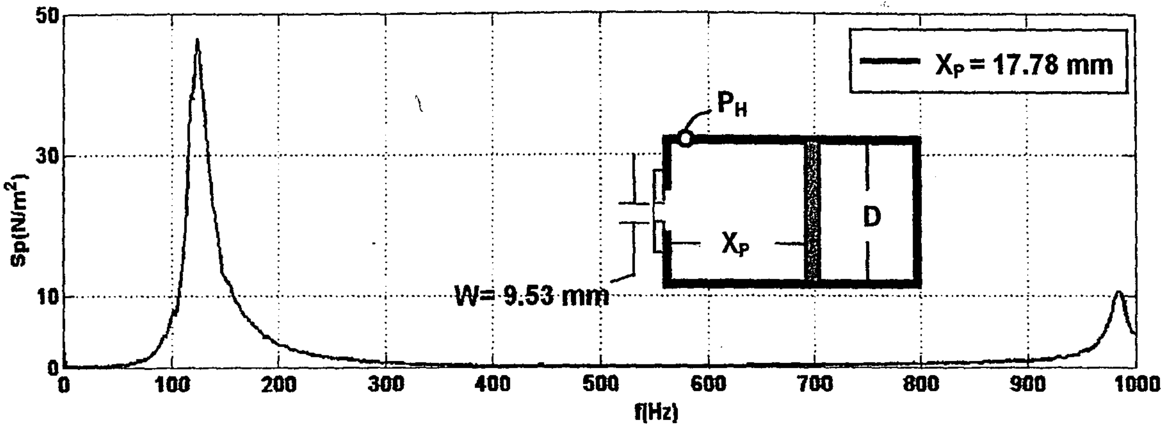

Figure 3.14d: Response spectrum of Helmholtz resonator as a function of length X_P for fixed value of mouth width W = 9.53 mm and length L = 38.1 mm.

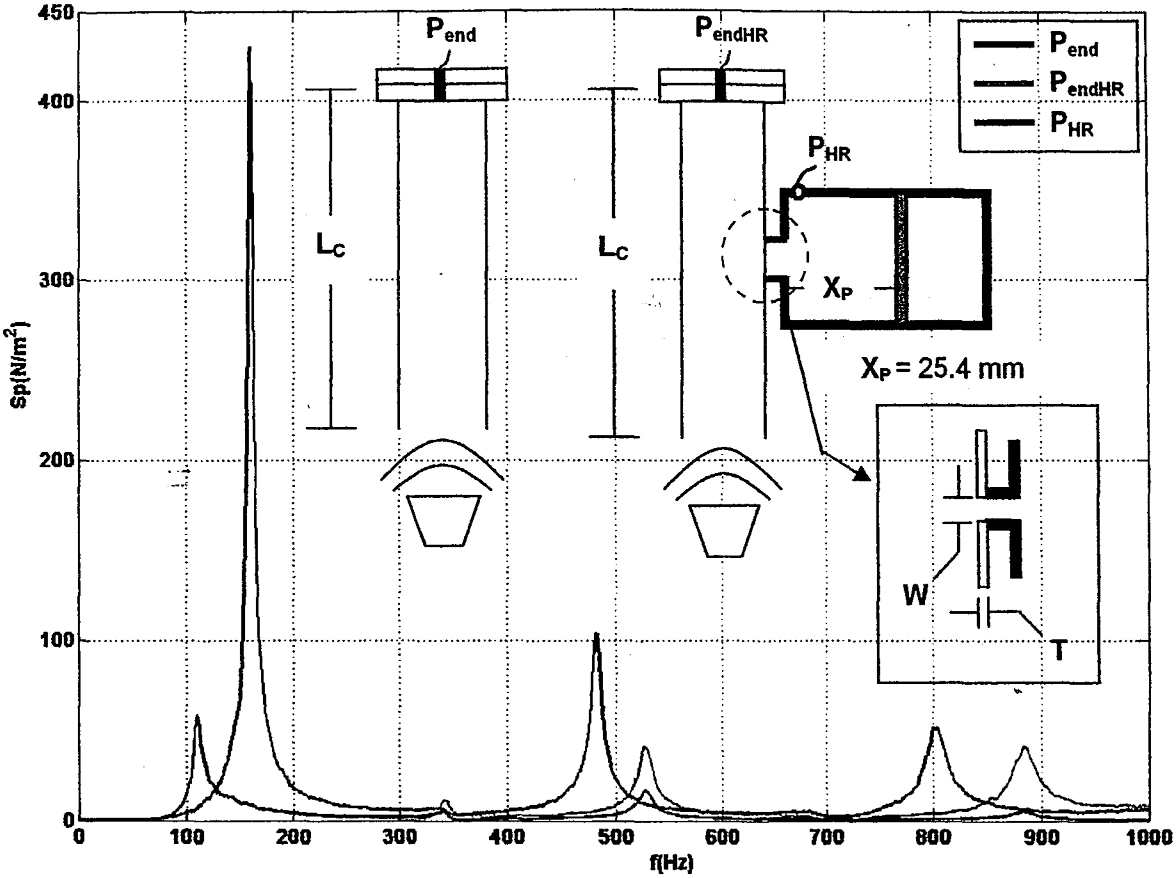

Figure 3.15: Spectra of pressure fluctuations inside duct with and without the Helmholtz resonator due to pure tone excitation as a function of length X_P. The mouth area of Helmholtz resonator on duct is A = 242 mm^2 and the thickness T of cavity wall is 3.28 mm.

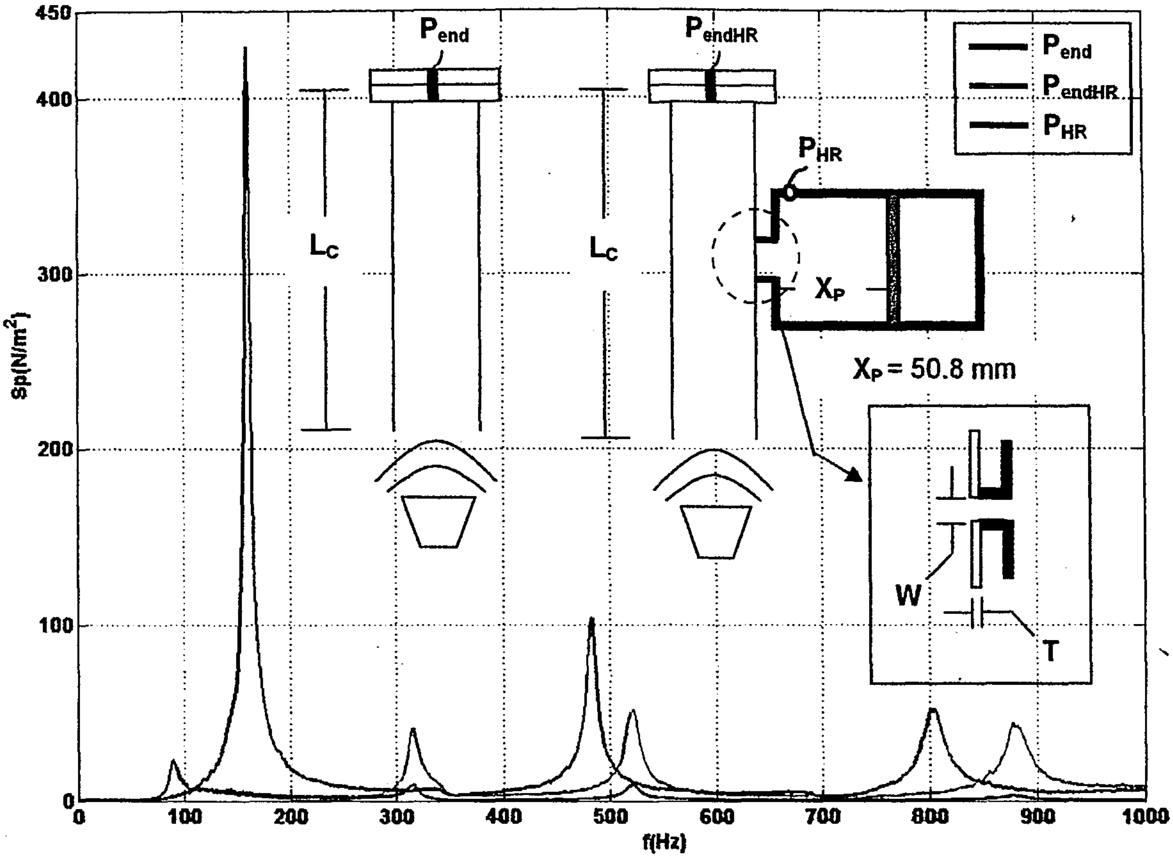

Figure 3.16: Spectra of pressure fluctuations inside duct with and without the Helmholtz resonator due to pure tone excitation as a function of length X_P. The mouth area of Helmholtz resonator on duct is A = 242 mm^2 and the thickness T of cavity wall is 3.28 mm.

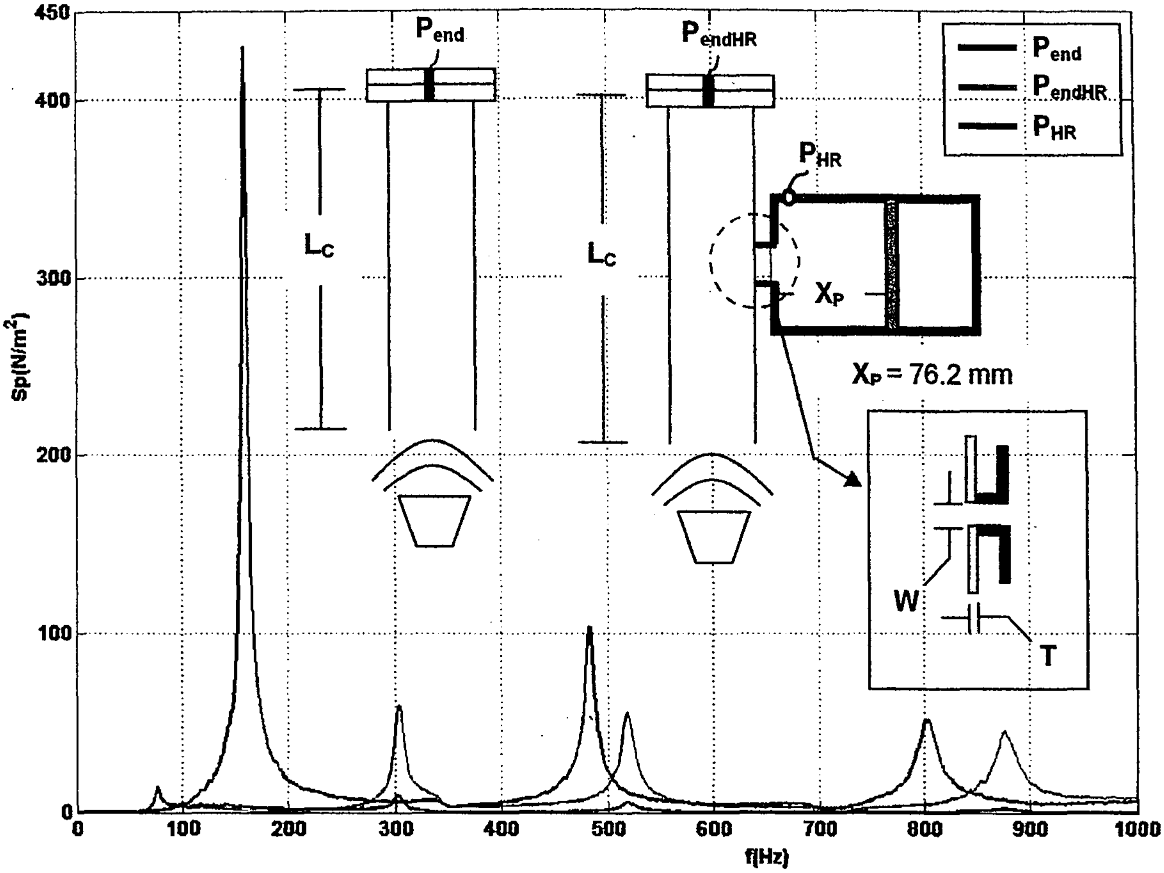

Figure 3.17: Spectra of pressure fluctuations inside duct with and without the Helmholtz resonator due to pure tone excitation as a function of length X_P. The mouth area of Helmholtz resonator on duct is A = 242 mm^2 and the thickness T of cavity wall is 3.28 mm.

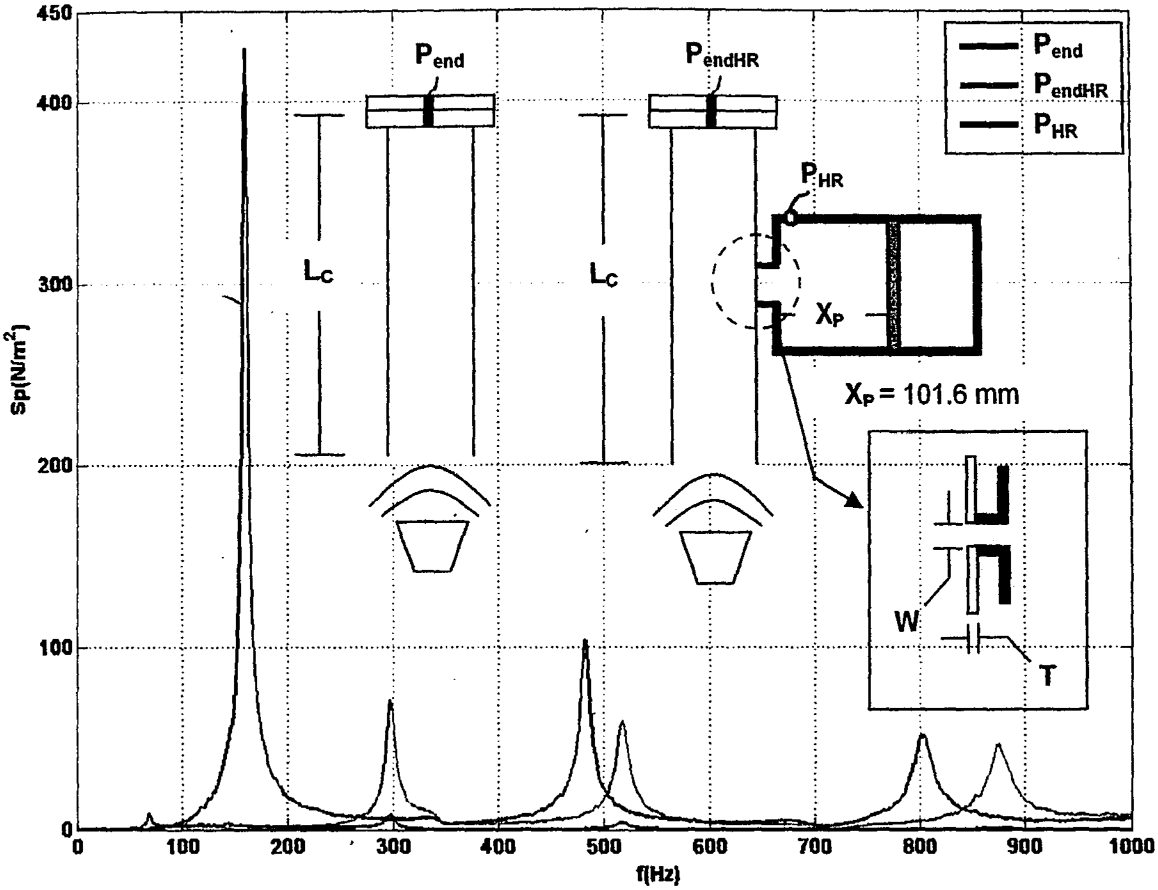

Figure 3.18: Spectra of pressure fluctuations inside duct with and without the Helmholtz resonator due to pure tone excitation as a function of length X_P. The mouth area of Helmholtz resonator on duct is A = 242 mm^2 and the thickness T of cavity wall is 3.28 mm.

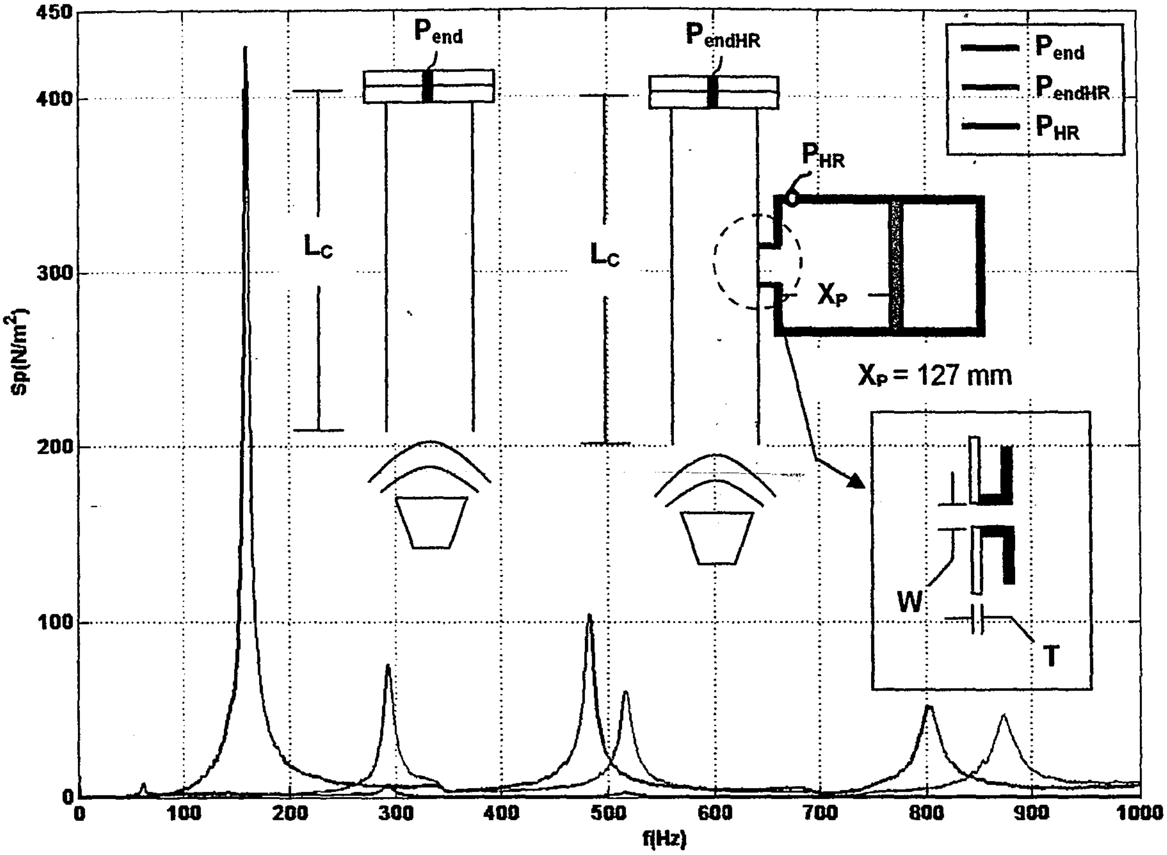

Figure 3.19: Spectra of pressure fluctuations inside duct with and without the Helmholtz resonator due to pure tone excitation as a function of length X_P. The mouth area of Helmholtz resonator on duct is A = 242 mm^2 and the thickness T of cavity wall is 3.28 mm.

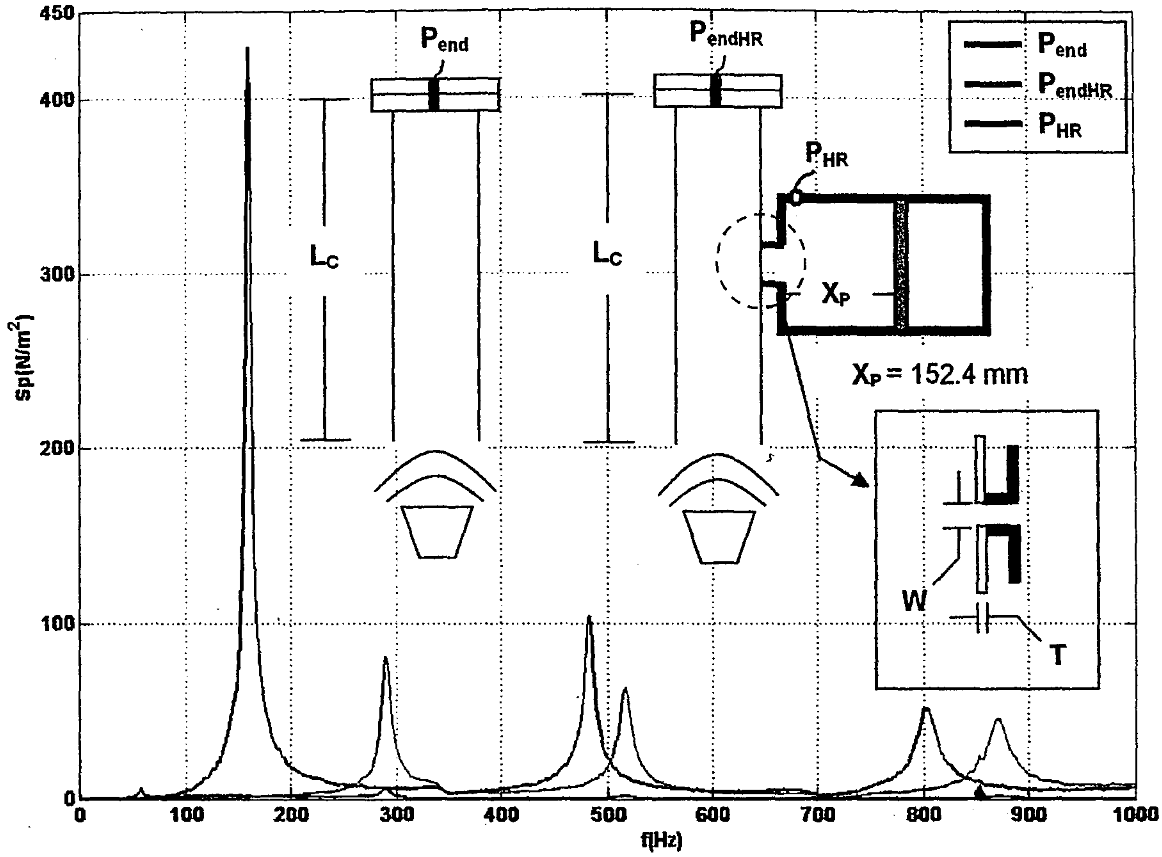

Figure 3.20: Spectra of pressure fluctuations inside duct with and without the Helmholtz resonator due to pure tone excitation as a function of length X_P. The mouth area of Helmholtz resonator on duct is A = 242 mm^2 and the thickness T of cavity wall is 3.28 mm.

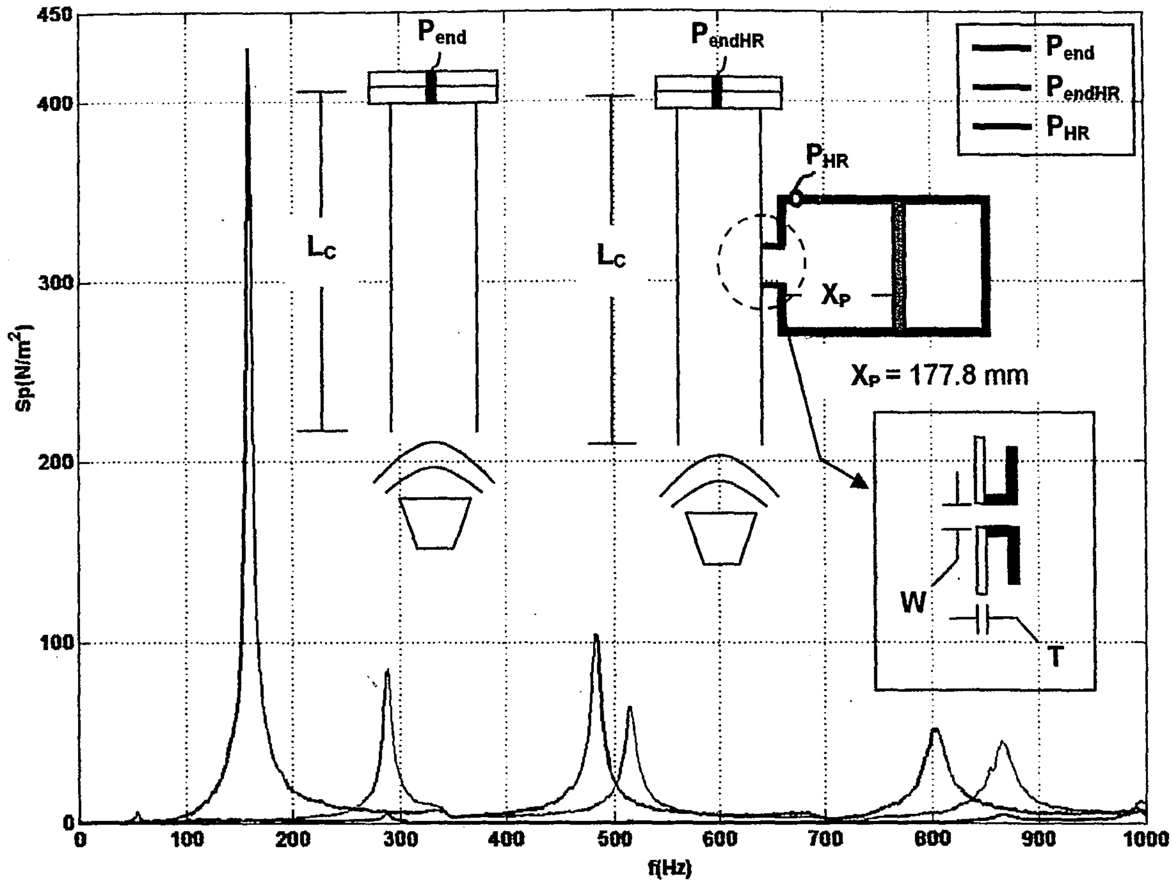

Figure 3.21: Spectra of pressure fluctuations inside duct with and without the Helmholtz resonator due to pure tone excitation as a function of length X_P. The mouth area of Helmholtz resonator on duct is A = 242 mm^2 and the thickness T of cavity wall is 3.28 mm.

			Acoustic Mode		
			1	2	3
Cavity Duct		f(Hz)	160	482	800
		N/m^2	430	104	52
Cavity Duct With Helmholtz Resonator	X_p = 25.4 mm	f(Hz)	342	527	873
		N/m^2	11.19	41.22	41.92
		SR(%)	2.6	39.6	80.6
	X_p = 50.8 mm	f(Hz)	315	522	872
		N/m^2	41.5	51.58	42.84
		SR(%)	9.7	49.6	82.4
	X_p = 76.2 mm	f(Hz)	303	519	871
		N/m^2	59.67	55.71	42.55
		SR(%)	13.9	53.6	81.8
	X_p = 101.6 mm	f(Hz)	297	518	869
		N/m^2	71.75	59.51	42.08
		SR(%)	16.7	57.2	80.9
	X_p = 127.0 mm	f(Hz)	293	516	865
		N/m^2	76.07	60.56	42.02
		SR(%)	17.7	58.2	80.8
	X_p=152.4 mm	f(Hz)	289	516	864
		N/m^2	80.96	63.75	43.63
		SR(%)	18.8	61.3	83.9
	X_p = 177.8 mm	f(Hz)	288	515	862
		N/m^2	85.18	64.29	43.98
		SR(%)	19.8	61.8	84.6

SR(= Sound Reduction): (Helmholtz resonator / Cavity duct)×100

Figure 3.22: The results from experiments of combination of the Helmholtz resonator and cavity duct.

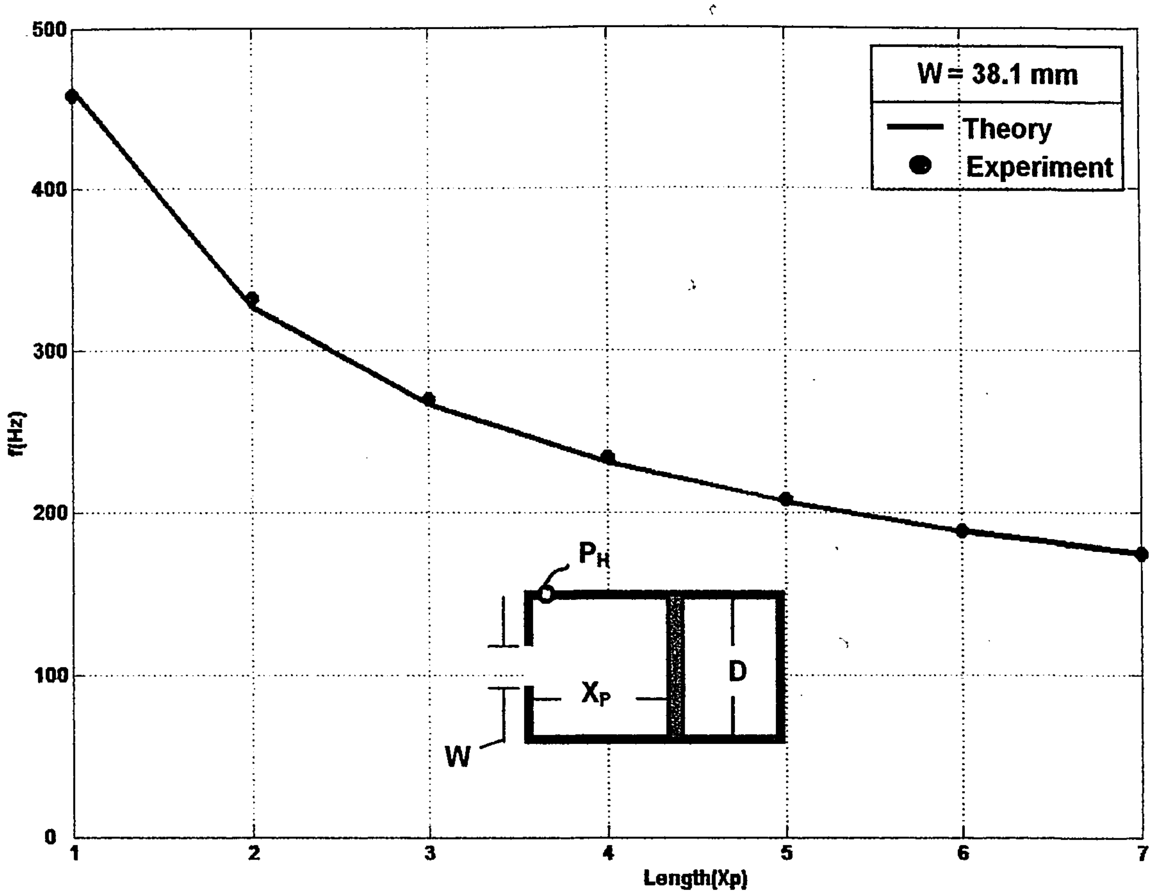

Figure 4.1: Natural frequency of Helmholtz resonator. Area of mouth of resonator is A = 1452 mm^2. Diameter of resonator is D = 152.4 mm.

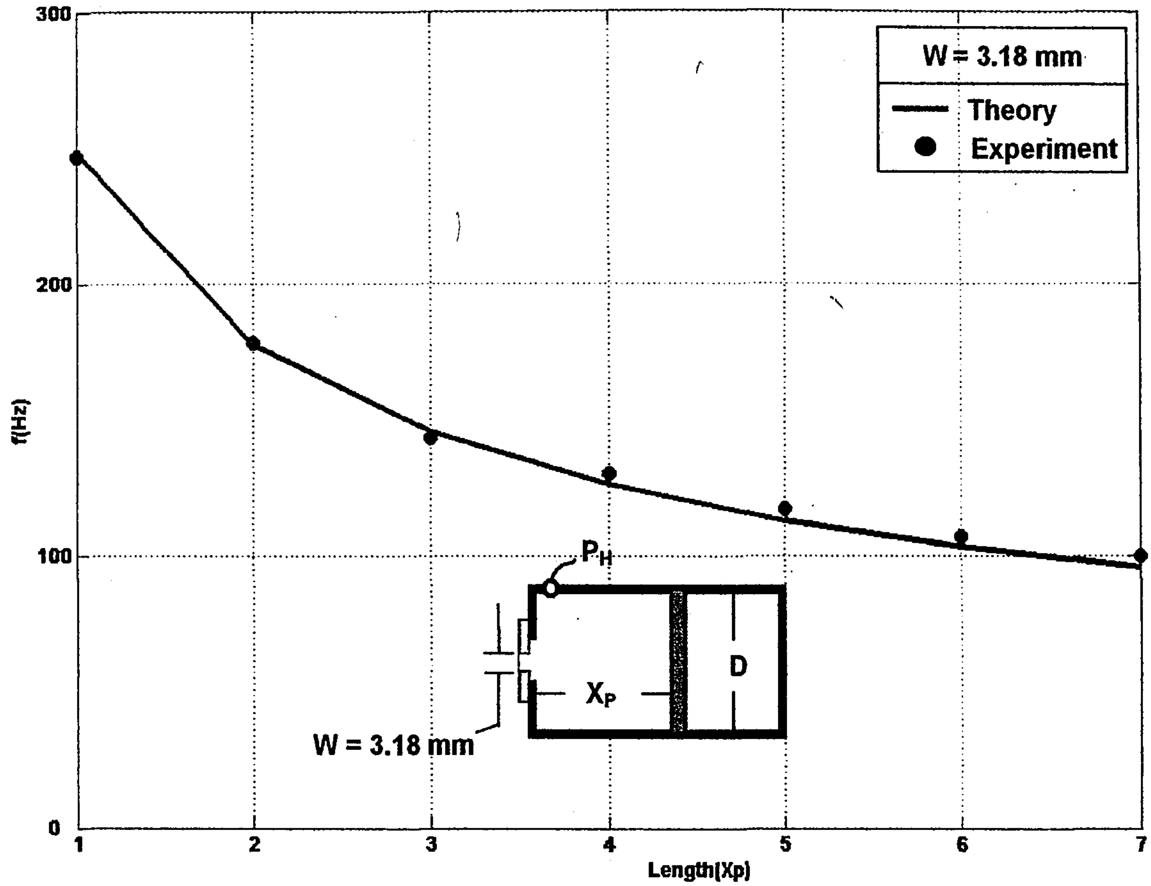

Figure 4.2: Natural frequency of Helmholtz resonator with plate. Area of mouth of plate is A = 120.97 mm^2. Diameter of resonator is D = 152.4 mm.

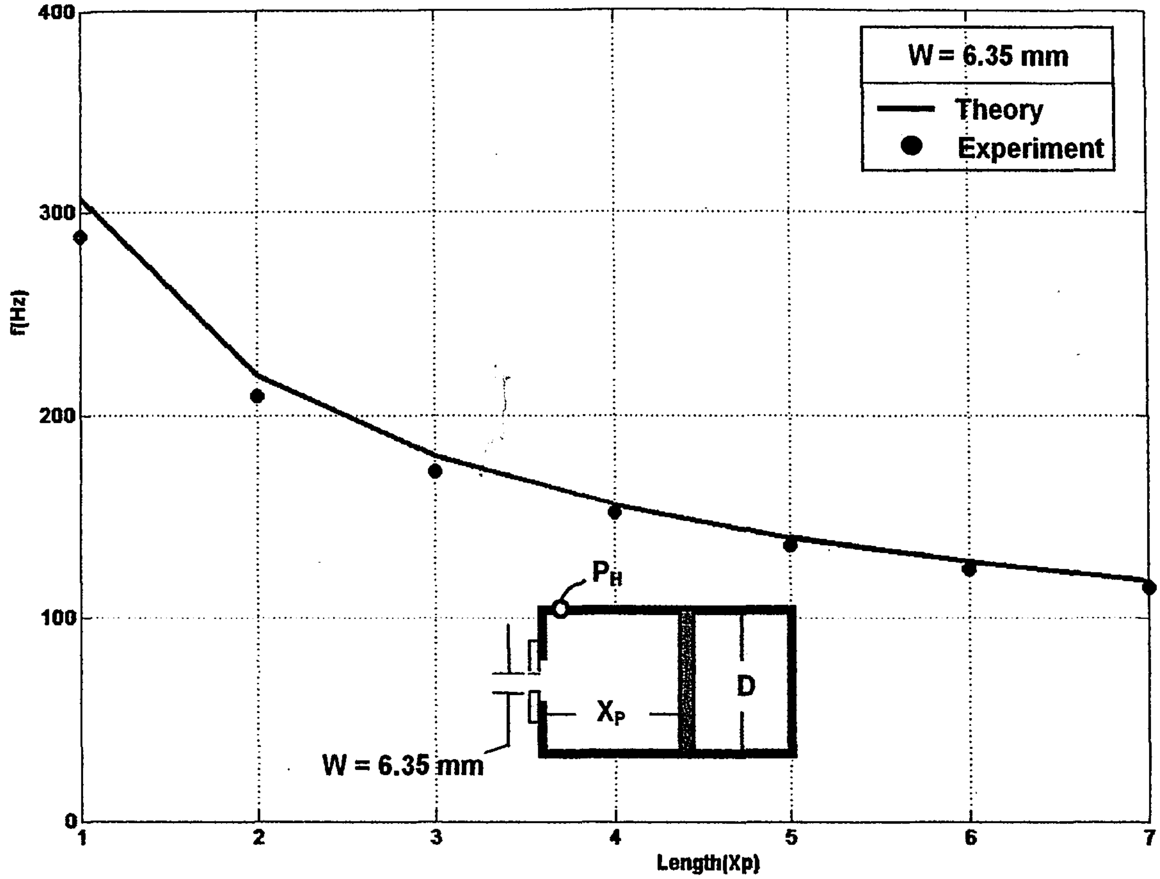

Figure 4.3: Natural frequency of Helmholtz resonator with plate. Area of mouth of plate is A = 241.94 mm^2. Diameter of resonator is D = 152.4 mm.

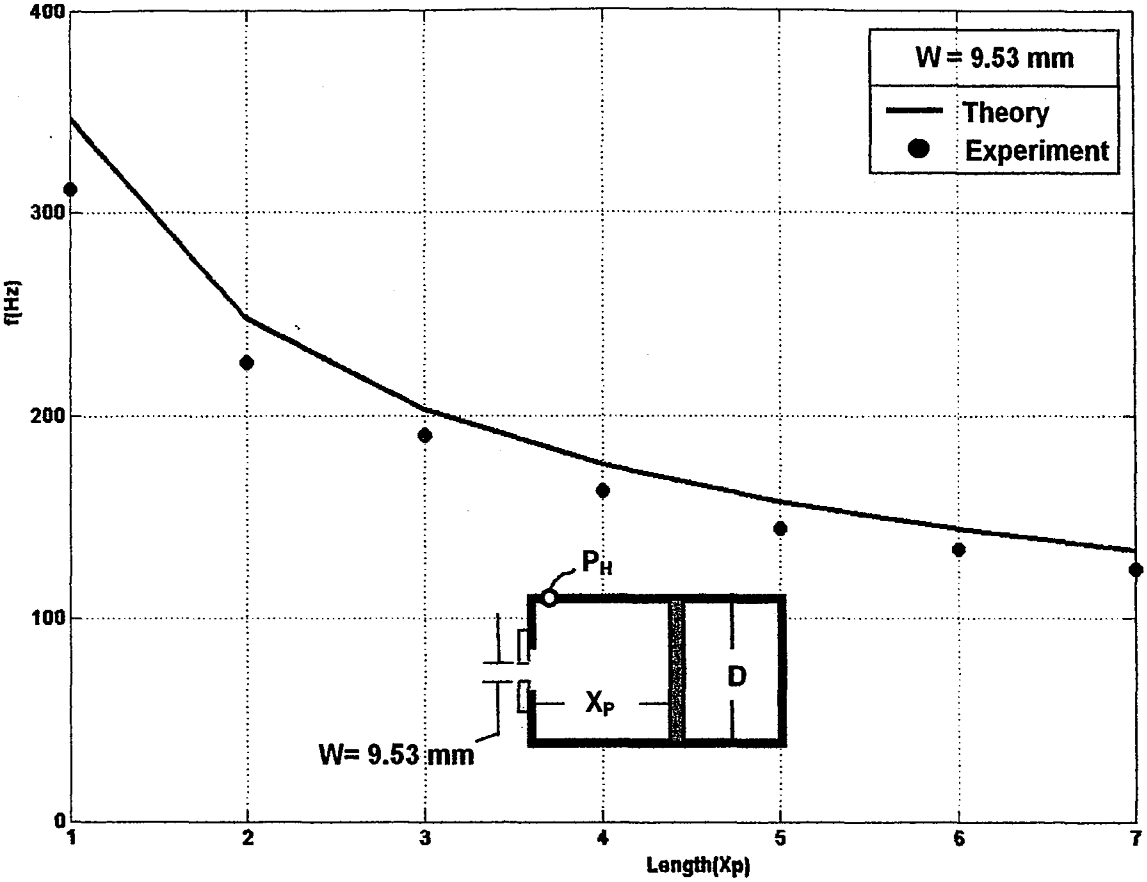

Figure 4.4: Natural frequency of Helmholtz resonator with plate. Area of mouth of plate is A = 362.90 mm^2. Diameter of resonator is D = 152.4 mm.

Volume Length (x_P)	Helmholtz Resonator			Helmholtz Resonator with Plate 1		
	Theory	Experiment	Error (%)	Theory	Experiment	Error (%)
25.4 mm	462	458	0.9	248	247	0.4
50.8 mm	327	332	-1.5	177	178	-0.6
76.2 mm	267	270	-1.1	145	143	1.4
101.6 mm	231	234	-1.3	126	130	-3.2
127.0 mm	207	208	-0.5	113	117	-3.5
152.4 mm	189	189	0.0	103	107	-3.9
177.8 mm	175	175	0.0	95	100	-5.3

Volume Length (x_P)	Helmholtz Resonator with Plate 2			Helmholtz Resonator with Plate 3		
	Theory	Experiment	Error (%)	Theory	Experiment	Error (%)
25.4 mm	307	288	6.2	346	312	9.8
50.8 mm	219	209	4.6	247	226	8.5
76.2 mm	180	172	4.4	203	190	6.4
101.6 mm	156	152	2.6	176	163	7.4
127.0 mm	140	136	2.9	157	144	8.3
152.4 mm	127	124	2.4	144	134	6.9
177.8 mm	118	115	2.5	133	124	6.8

Plate 1: width = 3.18 mm, Plate 2: width = 6.35 mm, Plate 3: width = 9.53mm

Figure 4.5: The comparison of values between theory and experiment

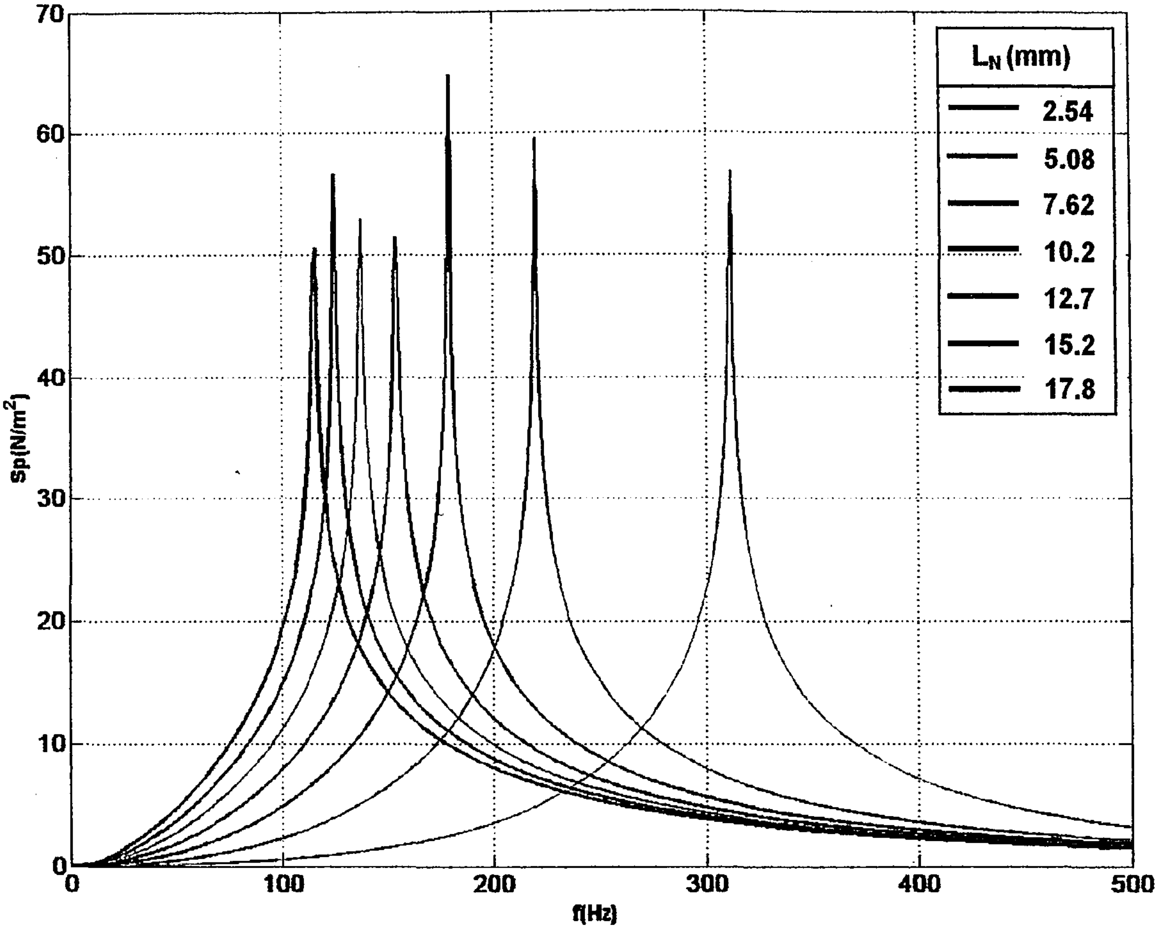

Figure 5.1: Spectra of transmission loss calculated by Equation (5.1),

$$TL = 10 \cdot \log_{10} \left| 1 + \frac{A_H}{A_c} \cdot \left[\frac{1+\phi+(\phi-1)\cdot e^{-2ikL_N}}{1+\phi-(\phi-1)\cdot e^{-2ikL_N}} \right] \right|^2, \ \phi = \frac{A_V}{A_H} \cdot \left(\frac{e^{-2ikL_N}-1}{e^{-2ikL_N}+1} \right)$$

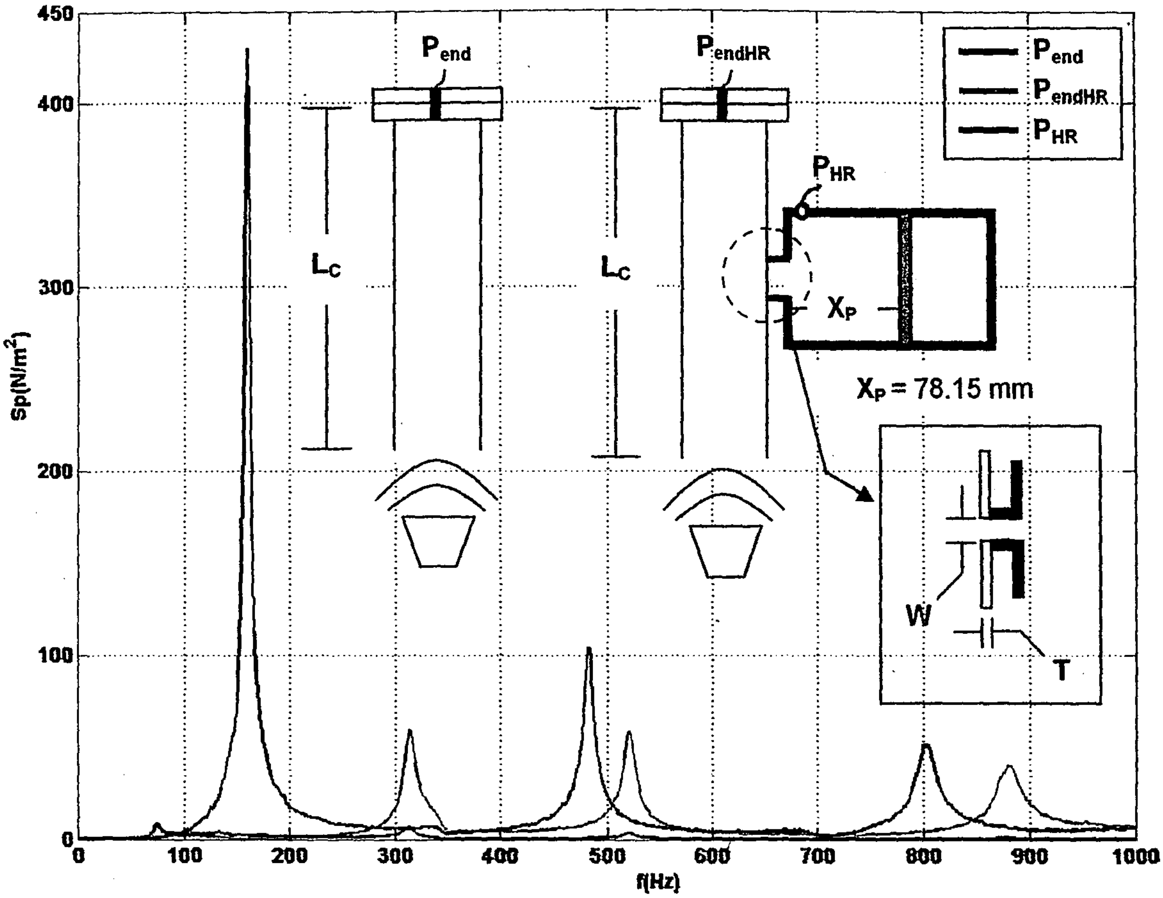

Figure 5.2a: Spectra of pressure fluctuations inside duct with and without the Helmholtz resonator due to pure tone excitation as a function of length X_P. The mouth area of Helmholtz resonator on duct is A = 242 mm^2 and the thickness T of cavity wall is 3.18 mm. The length of volume is X_P = 78.15 mm and the volume of the resonator is 1,444,076 mm^3.

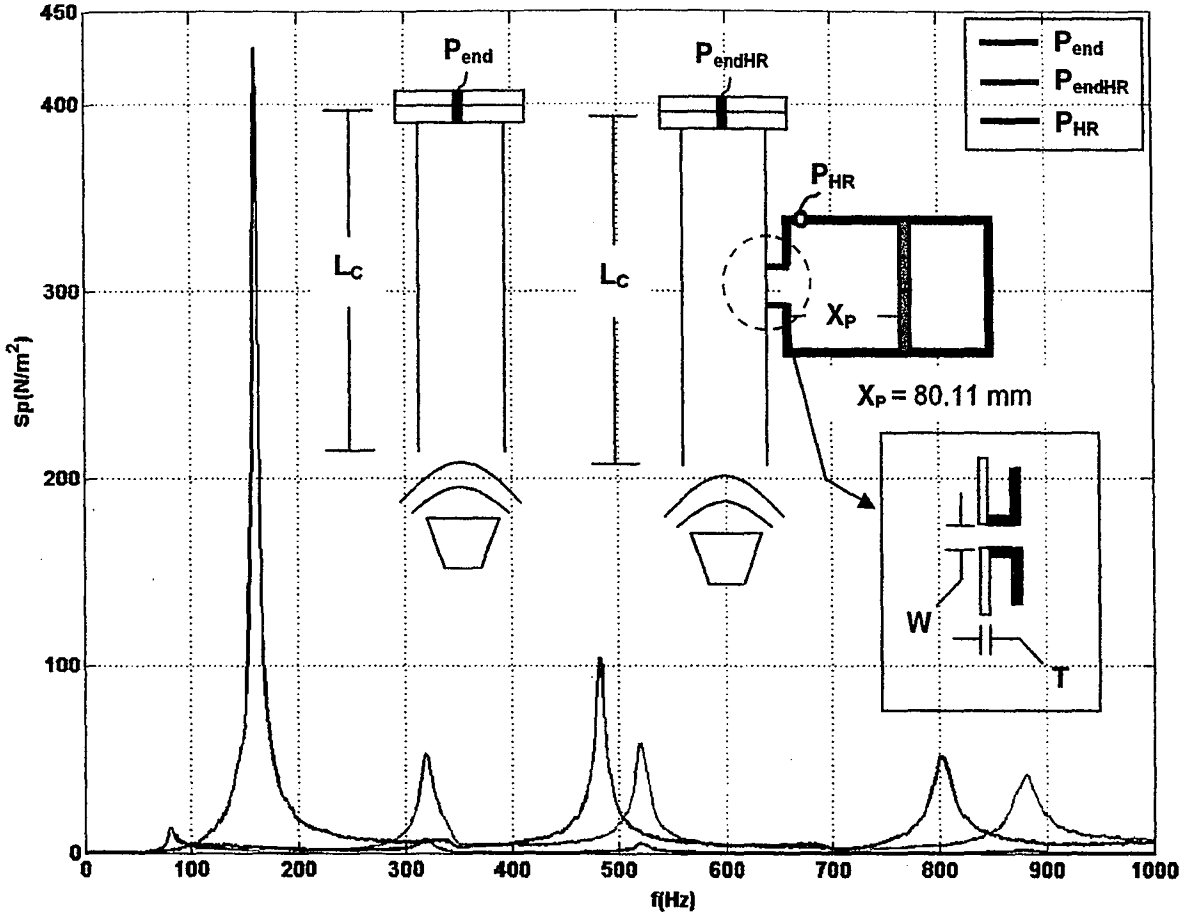

Figure 5.2b: Spectra of pressure fluctuations inside duct with and without the Helmholtz resonator due to pure tone excitation as a function of length X_P. The mouth area of Helmholtz resonator on duct is A = 242 mm^2 and the thickness T of cavity wall is 3.18 mm. The length of volume is X_P = 80.11 mm and the volume of the resonator is 1,479,717 mm^3.

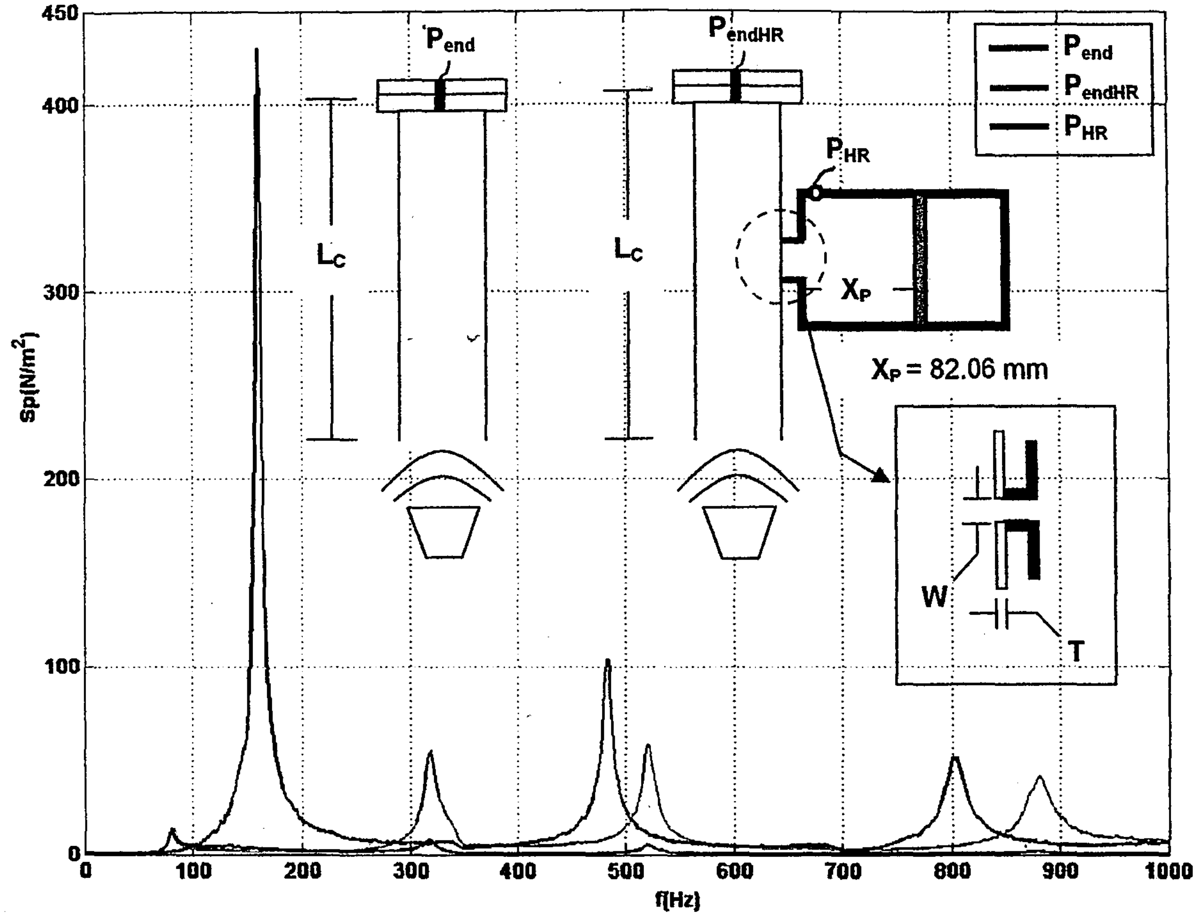

Figure 5.2c: Spectra of pressure fluctuations inside duct with and without the Helmholtz resonator due to pure tone excitation as a function of length X_P. The mouth area of Helmholtz resonator on duct is A = 242 mm^2 and the thickness T of cavity wall is 3.18 mm. The length of volume is X_P = 82.06 mm and the volume of the resonator is 1,515,358 mm^3.

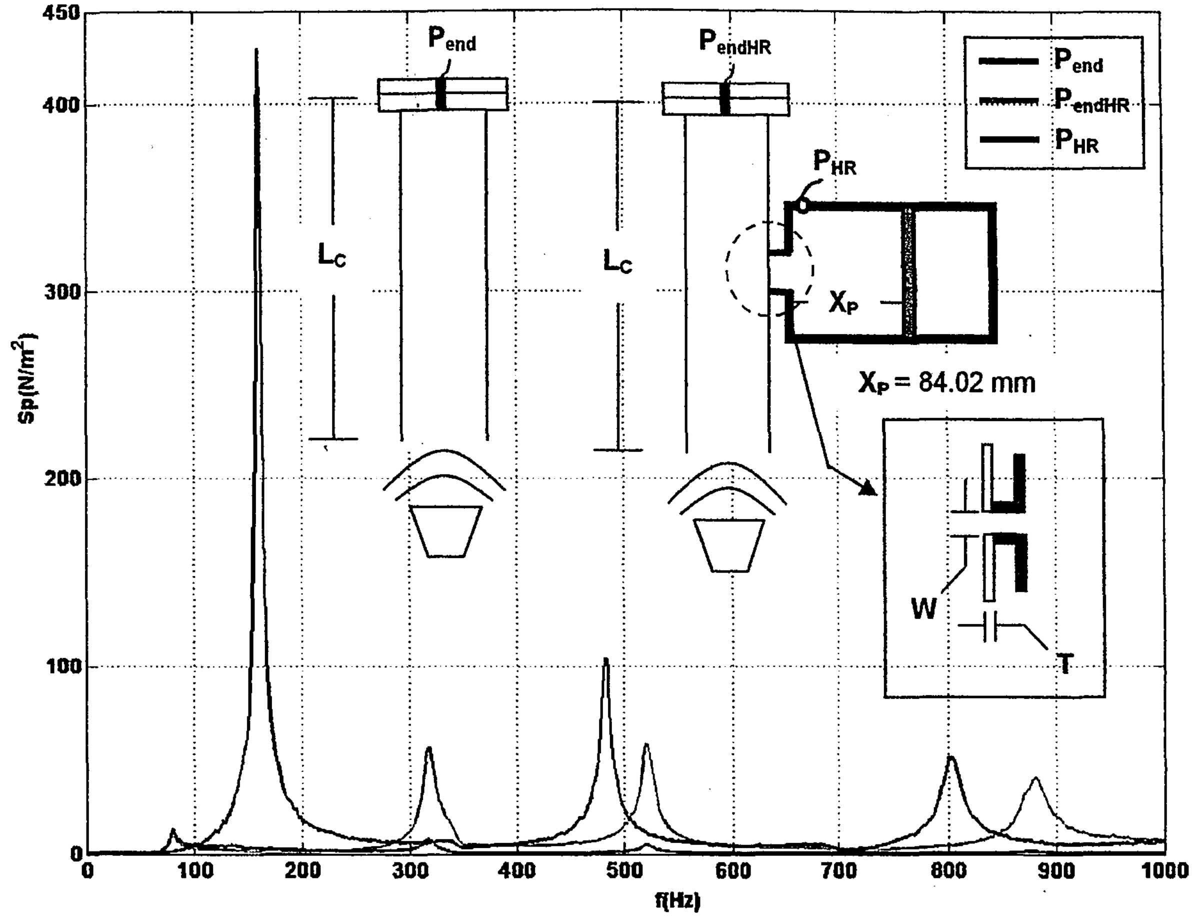

Figure 5.2d: Spectra of pressure fluctuations inside duct with and without the Helmholtz resonator due to pure tone excitation as a function of length X_P. The mouth area of Helmholtz resonator on duct is A = 242 mm^2 and the thickness T of cavity wall is 3.18 mm. The length of volume is X_P = 84.02 mm and the volume of the resonator is 1,551,000 mm^3.

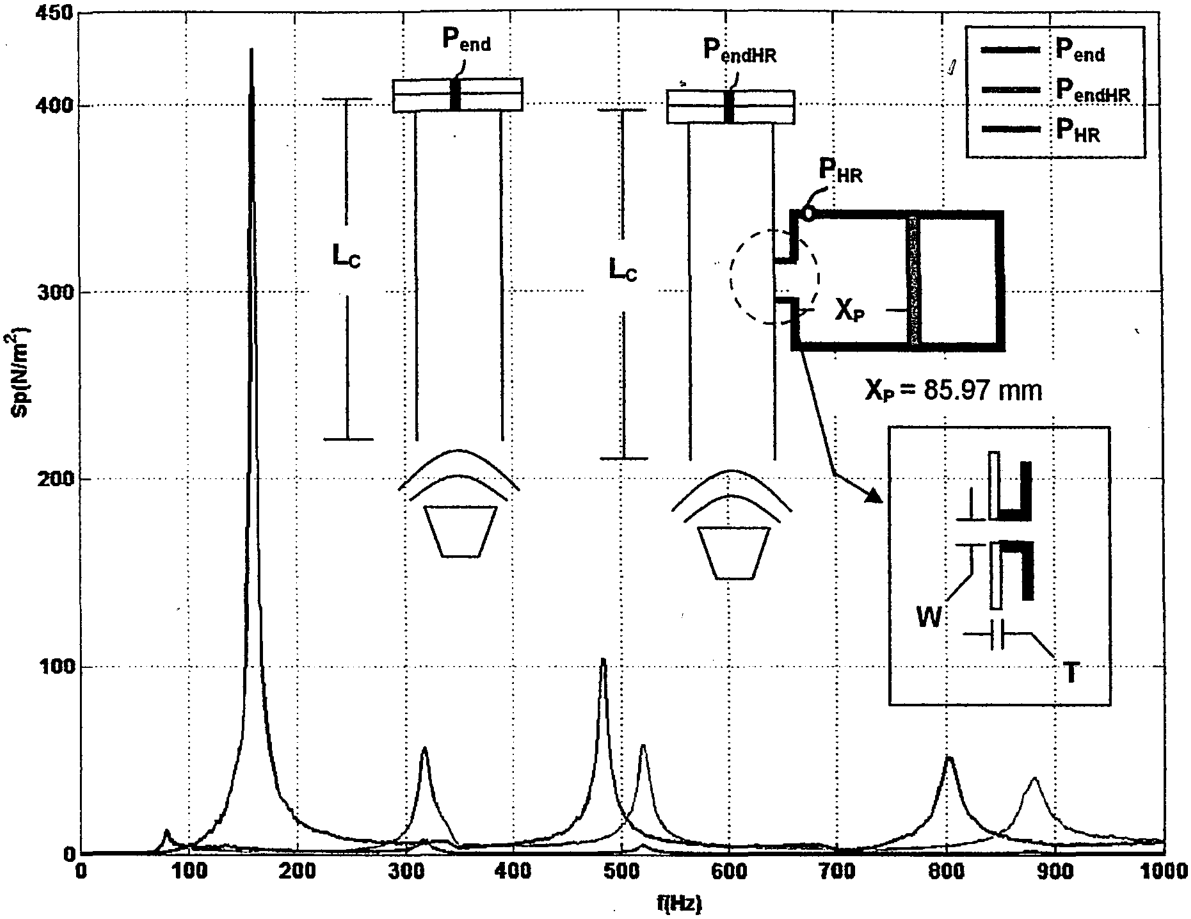

Figure 5.2e: Spectra of pressure fluctuations inside duct with and without the Helmholtz resonator due to pure tone excitation as a function of length X_P. The mouth area of Helmholtz resonator on duct is A = 242 mm^2 and the thickness T of cavity wall is 3.18 mm. The length of volume is X_P = 85.97 mm and the volume of the resonator is 1,586,641 mm^3.

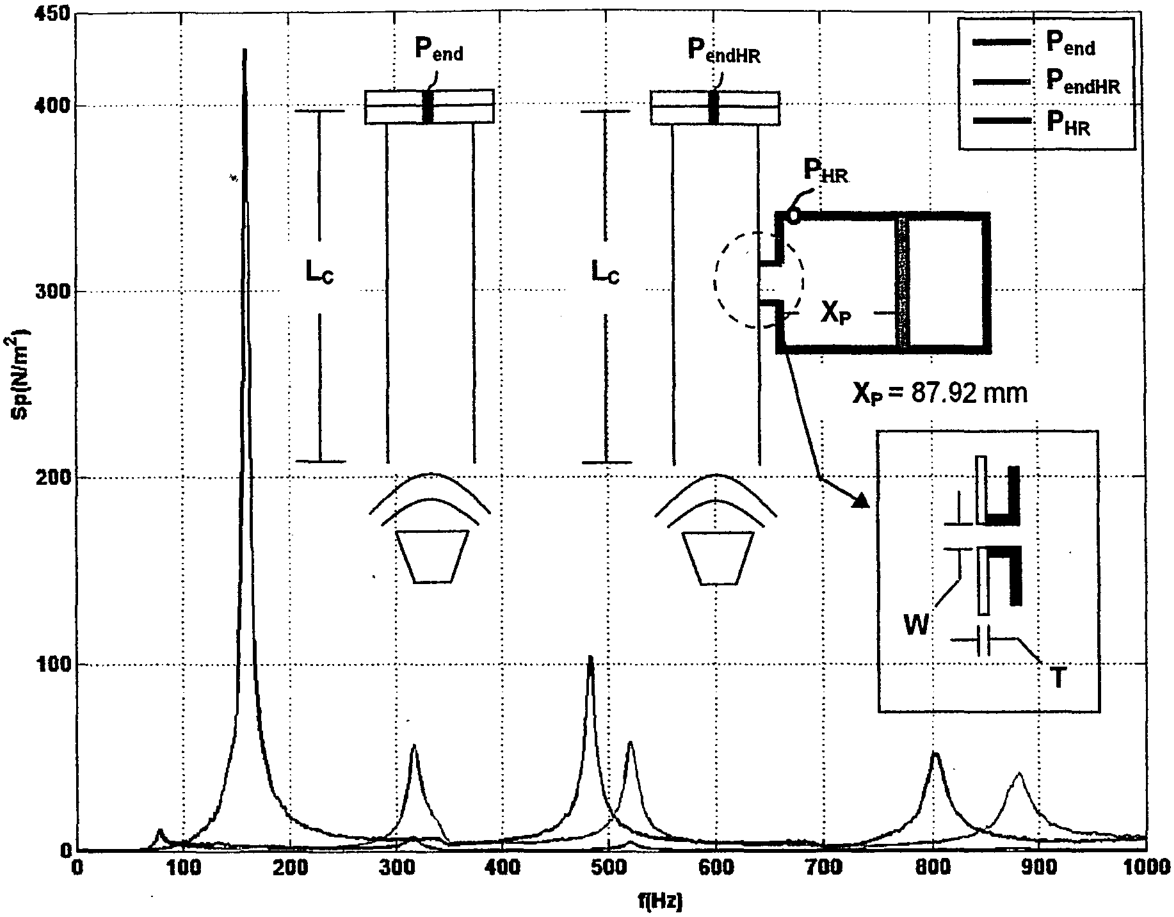

Figure 5.2f: Spectra of pressure fluctuations inside duct with and without the Helmholtz resonator due to pure tone excitation as a function of length X_P. The mouth area of Helmholtz resonator on duct is A = 242 mm^2 and the thickness T of cavity wall is 3.18 mm. The length of volume is X_P = 87.92 mm and the volume of the resonator is 1,622,282 mm^3.

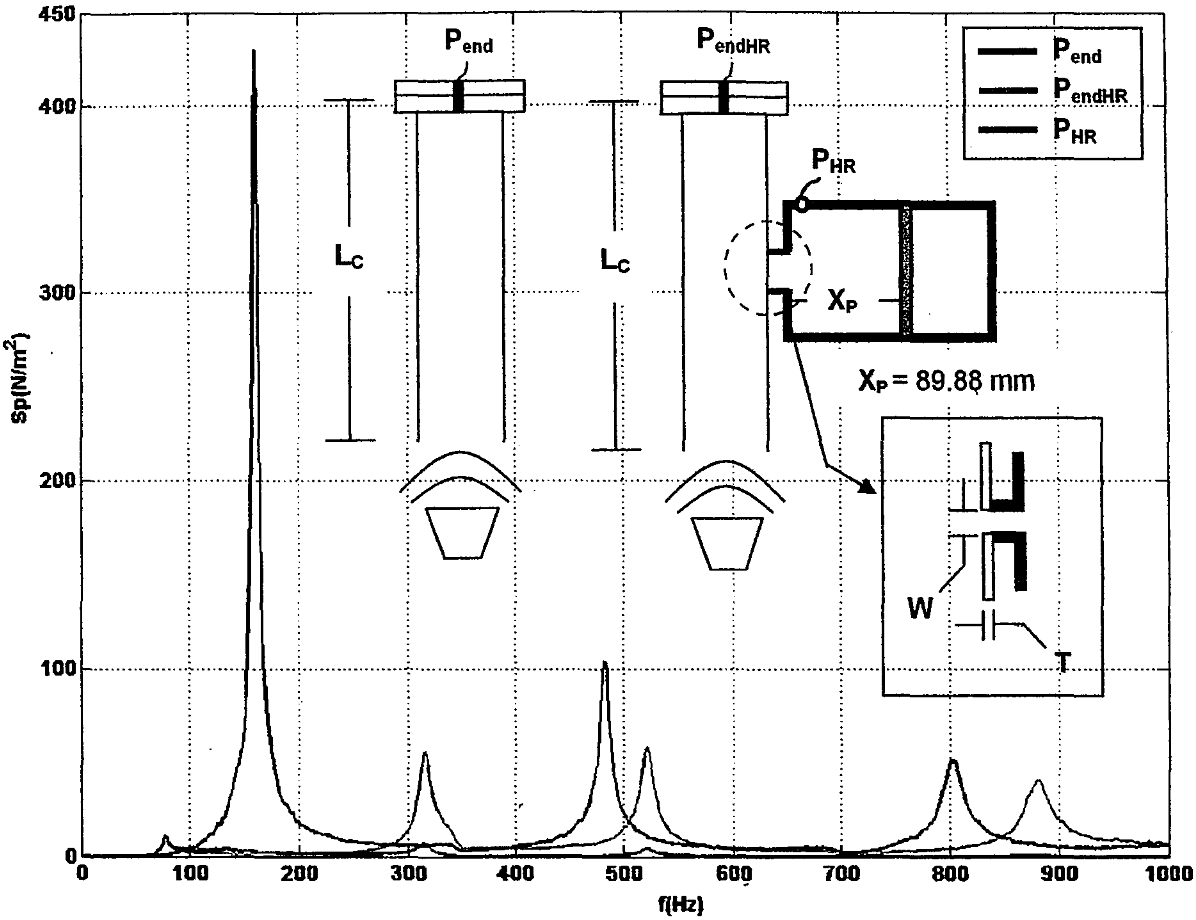

Figure 5.2g: Spectra of pressure fluctuations inside duct with and without the Helmholtz resonator due to pure tone excitation as a function of length X_P. The mouth area of Helmholtz resonator on duct is A = 242 mm^2 and the thickness T of cavity wall is 3.18 mm. The length of volume is X_P = 89.88 mm and the volume of the resonator is 1,657,923 mm^3.

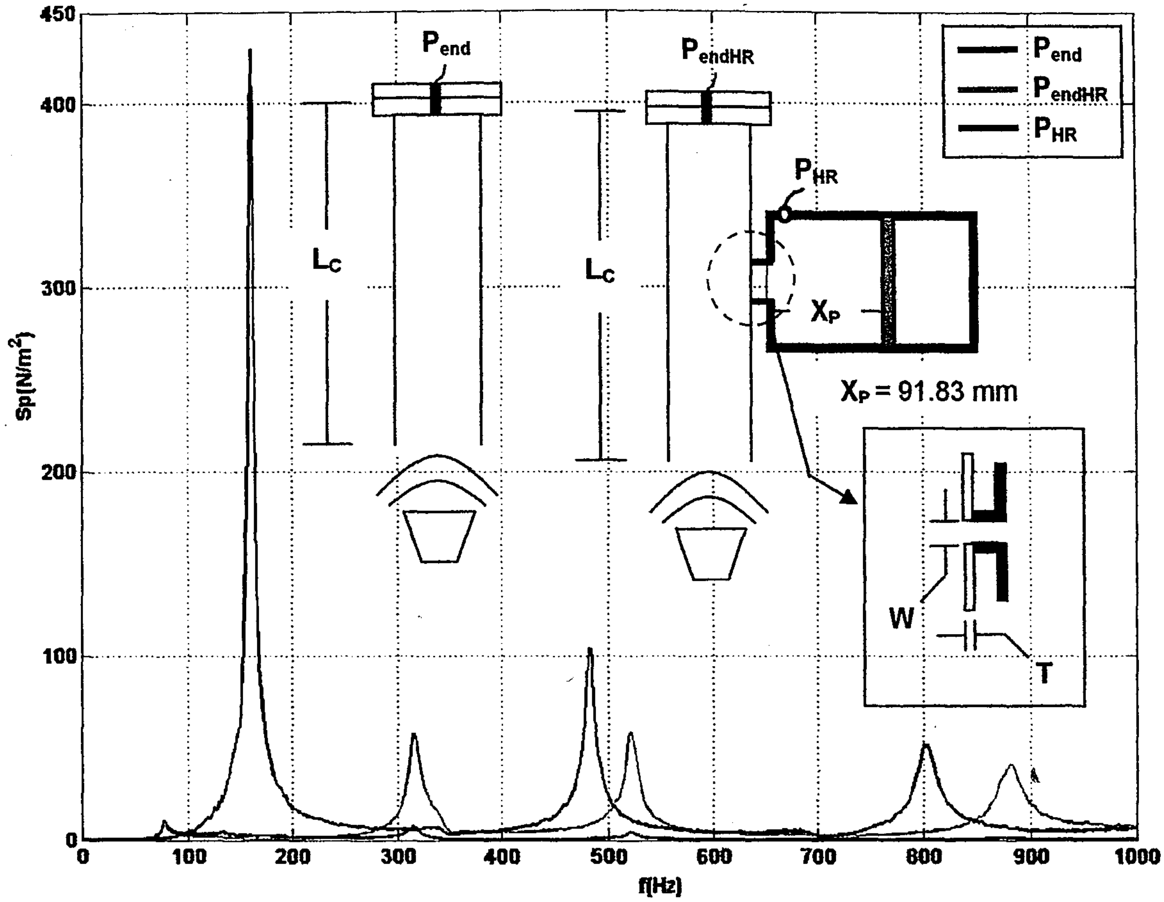

Figure 5.2h: Spectra of pressure fluctuations inside duct with and without the Helmholtz resonator due to pure tone excitation as a function of length X_P. The mouth area of Helmholtz resonator on duct is A = 242 mm^2 and the thickness T of cavity wall is 3.18 mm. The length of volume is X_P = 91.83 mm and the volume of the resonator is 1,693,564 mm^3.

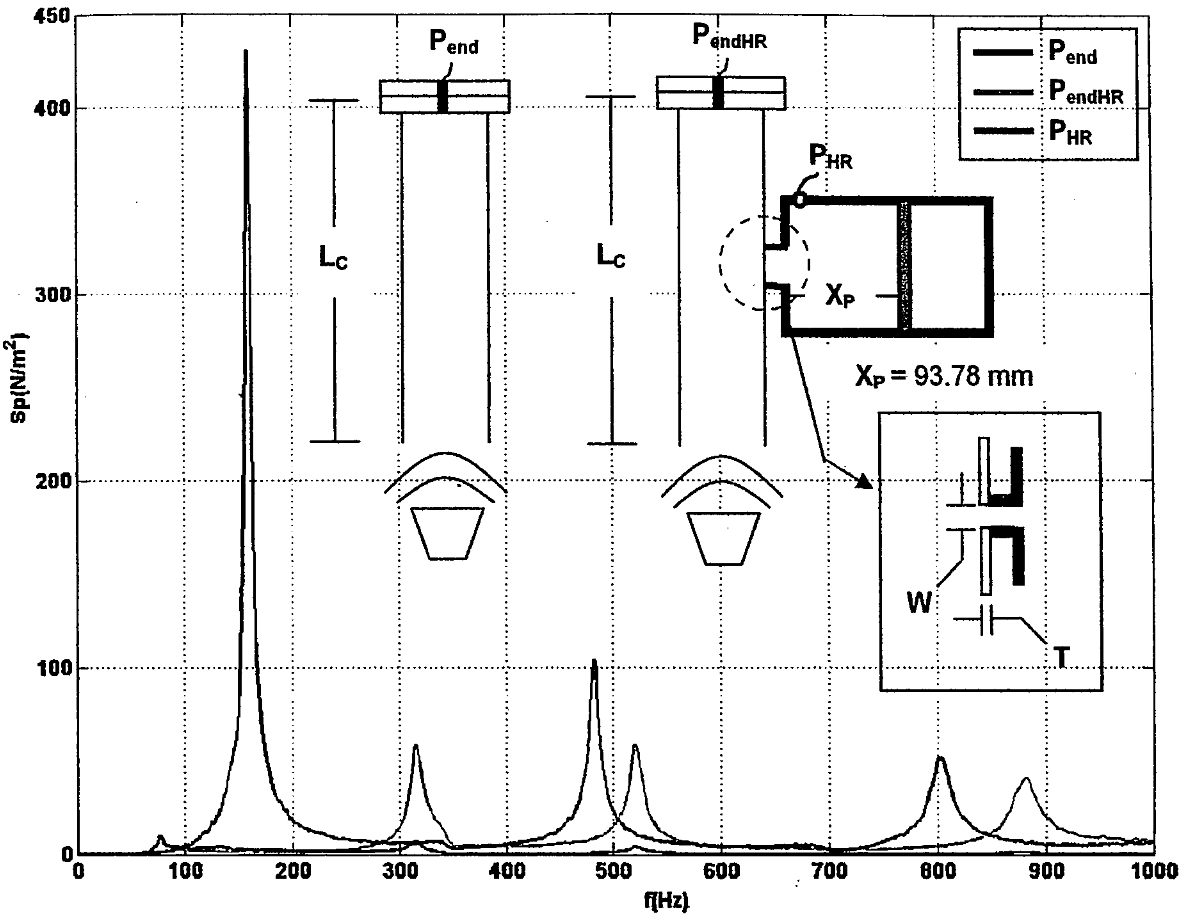

Figure 5.2i: Spectra of pressure fluctuations inside duct with and without the Helmholtz resonator due to pure tone excitation as a function of length X_P. The mouth area of Helmholtz resonator on duct is A = 242 mm^2 and the thickness T of cavity wall is 3.18 mm. The length of volume is X_P = 93.78 mm and the volume of the resonator is 1,729,205 mm^3.

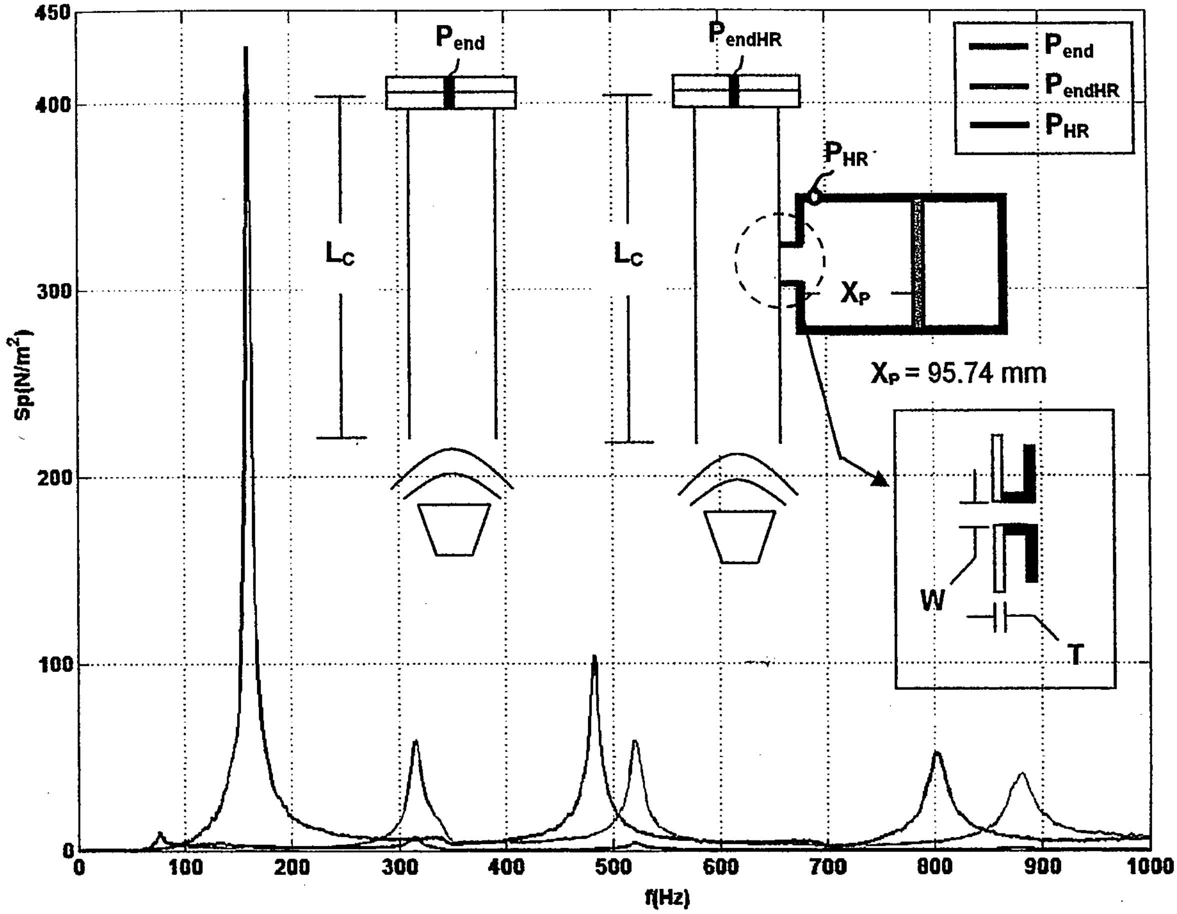

Figure 5.2j: Spectra of pressure fluctuations inside duct with and without the Helmholtz resonator due to pure tone excitation as a function of length X_P. The mouth area of Helmholtz resonator on duct is A = 242 mm^2 and the thickness T of cavity wall is 3.18 mm. The length of volume is X_P = 95.74 mm and the volume of the resonator is 1,764,846 mm^3.

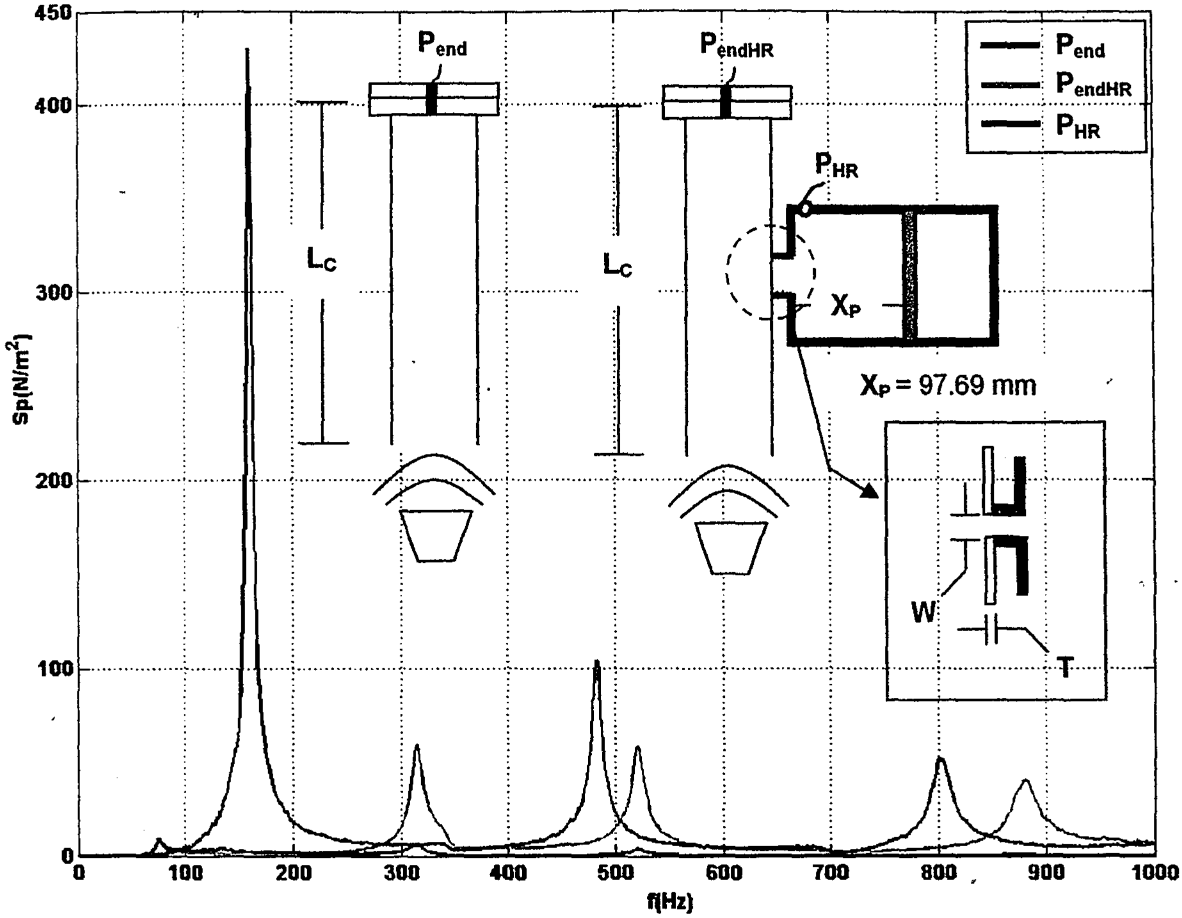

Figure 5.2k: Spectra of pressure fluctuations inside duct with and without the Helmholtz resonator due to pure tone excitation as a function of length X_P. The mouth area of Helmholtz resonator on duct is A = 242 mm^2 and the thickness T of cavity wall is 3.18 mm. The length of volume is X_P = 97.69 mm and the volume of the resonator is 1,800,487 mm^3.

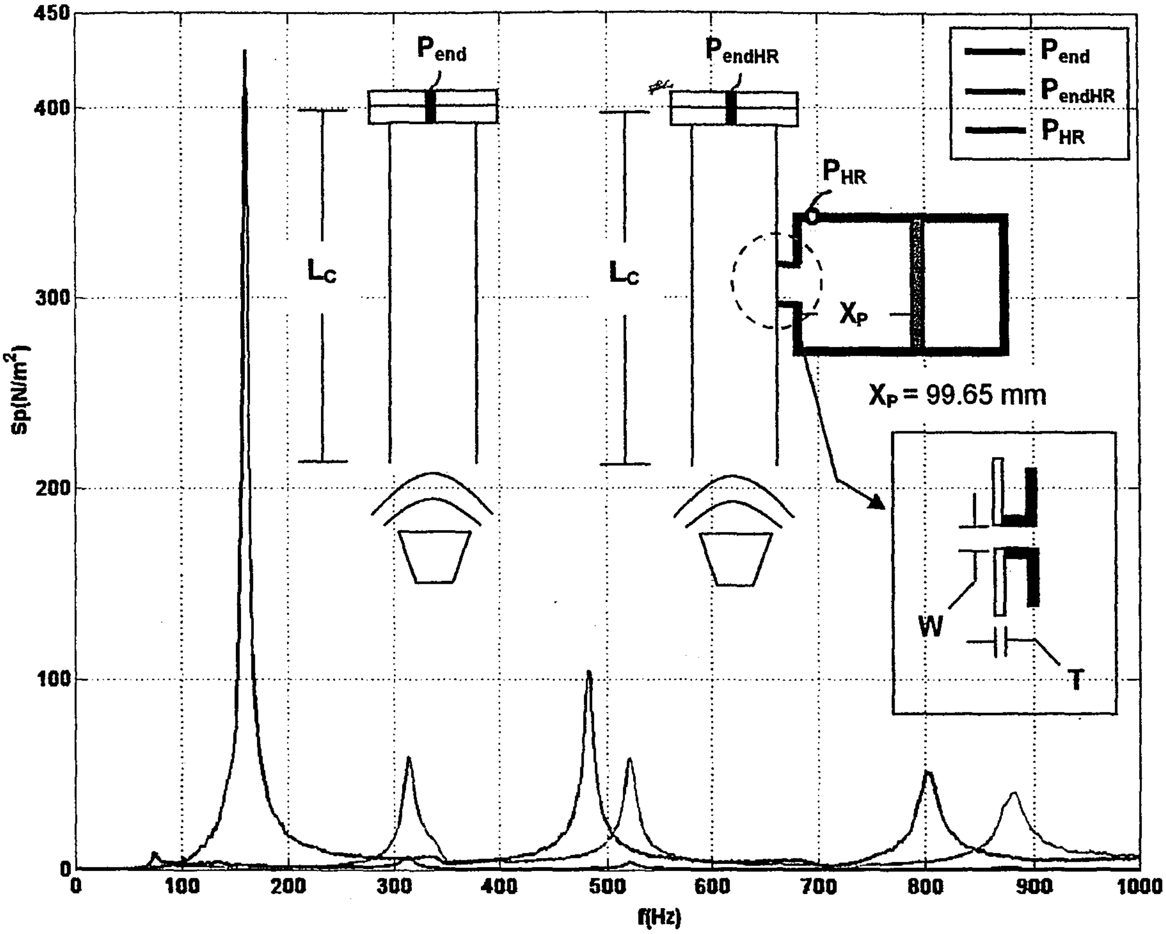

Figure 5.2l: Spectra of pressure fluctuations inside duct with and without the Helmholtz resonator due to pure tone excitation as a function of length X_P. The mouth area of Helmholtz resonator on duct is A = 242 mm^2 and the thickness T of cavity wall is 3.18 mm. The length of volume is X_P = 99.65 mm and the volume of the resonator is 1,836,127 mm^3.

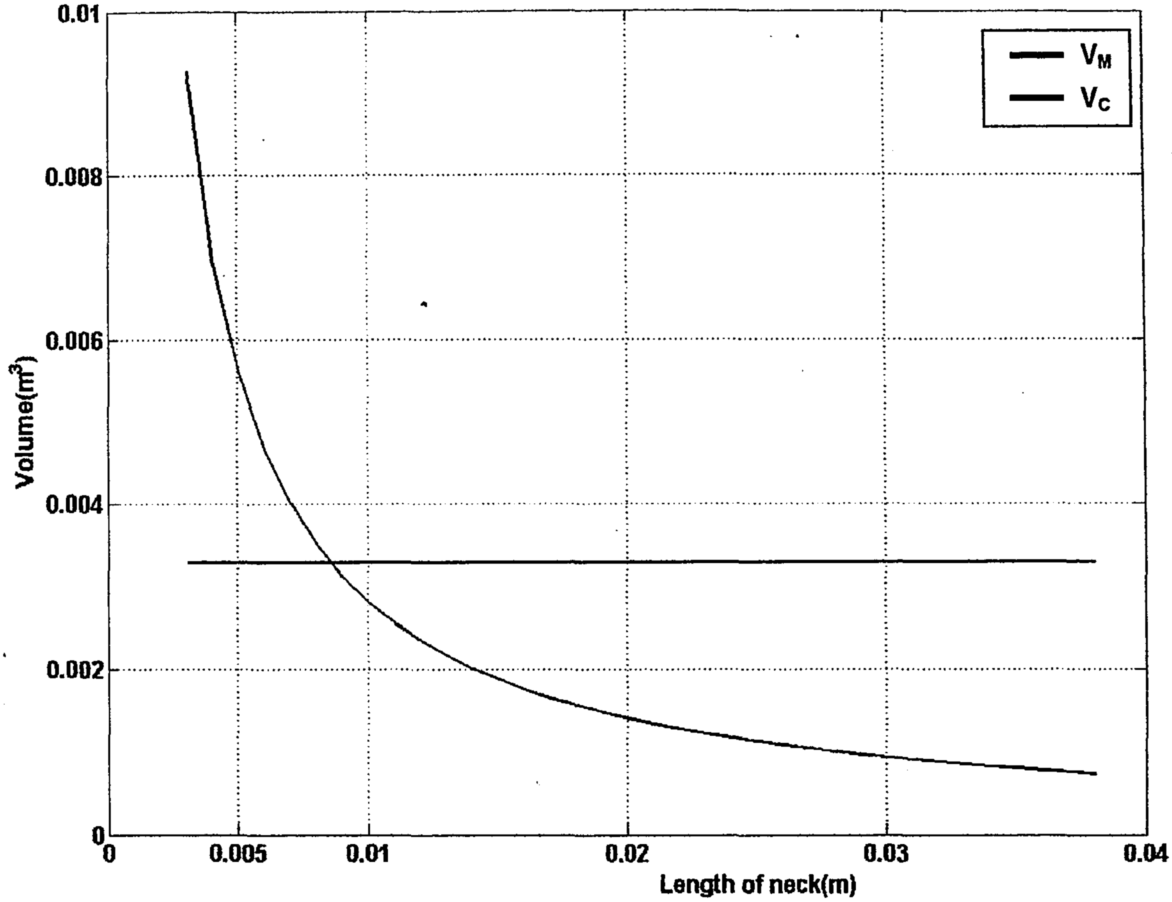

Figure 5.3: The calculated volume of Helmholtz resonator expressed as a function of the actual length of neck under the condition of constant cross-sectional area. V_M is the maximum volume of Helmholtz resonator, and V_C is the calculated volume of Helmholtz resonator.

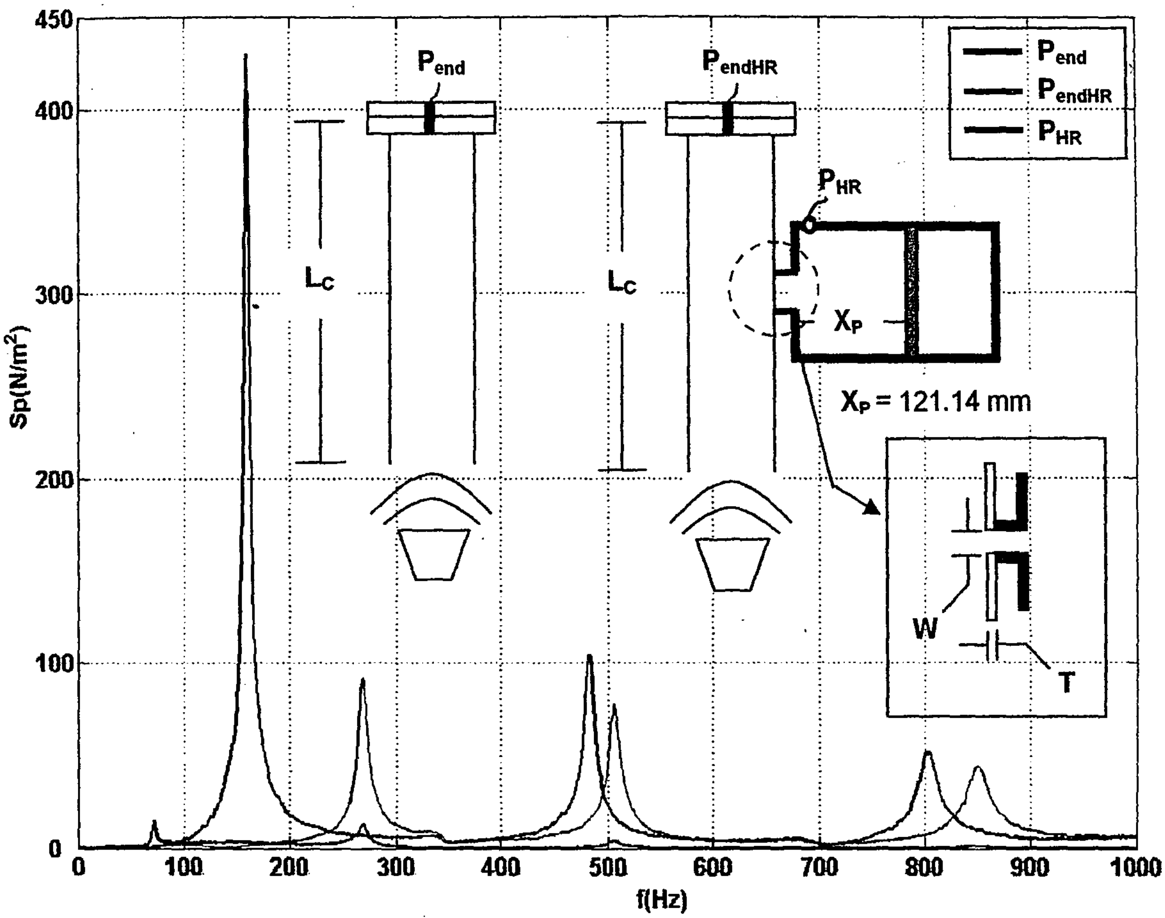

Figure 5.4: Spectra of pressure fluctuations inside duct with and without the Helmholtz resonator due to pure tone excitation as a function of length X_P. The mouth area of Helmholtz resonator on duct is A = 242 mm^2 and the actual length of neck of Helmholtz resonator is 12.7 mm. The length of volume is X_P = 121.14 mm and the volume of the resonator is 2,224,072 mm^3.

LIST OF REFERENCES

De Bedout, J.M., Francheck, M.A., Bernhard R. J. and Mongeau, L. "Adaptive-Passive Noise Control with Self-Tuning Helmholtz Resonators", *Journal of Sound and Vibration*, (1997) **202**(1), 109-123.

Tang, S.K. "On Helmholtz Resonators with Tapered Necks", *Journal of Sound and Vibration*, **279** (2005) 1085-1096.

Dickey, N.S. and Selamet, A. "Helmholtz Resonators: One Dimensional Limit for Small Cavity Length-to-Diameter Ratios", *Journal of Sound and Vibration*, (1996) **195**(3), 512-517.

Selamet, A., Dickey, N.S. and Novak, J.M. "Theoretical, Computational and Experimental Investigation of Helmholtz Resonators with Fixed Volume: Lumped Versus Distributed Analysis", *Journal of Sound and Vibration*, (1995) **187**(2), 358-367.

Ji, Z.L, "Acoustic Length Correction of Closed Cylindrical Side-branched Tube", *Journal of Sound and Vibration*, **283** (2005) 1180-1186.

Selamet, A. and Ji, Z.L. "Circular asymmetric Helmholtz Resonators", J. Acoust. Soc. Am. **107**(5), Pt. 1, May 2000.

Yang, Yingchen. Ph.D. Dissertation, Lehigh University, 2005.

Naudascher, Eduard and Rockwell, Donald. "Flow-Induced Vibration", pp.72-73.

McLennan, J.E. (2003) "A0 and A1 studies on the violin using CO_2, He, and air/helium mixtures." *Acustica,* **89**, 176-180.

Website:"http://www.diracdelta.co.uk/science/source/h/e/helmholtz%20resonator/source.html", Science & Engineering Encyclopedia.

Appendix A: Resonant Frequency of Helmholtz Resonator

Consider a basic force balance $F = ma$, where m is mass and a is acceleration,

$a = \frac{d^2x}{dt^2}$. One can therefore write

$$\frac{d^2x}{dt^2} = \frac{F}{m} \tag{1}$$

Consider

$$\frac{P}{P_0} = \gamma\frac{\Delta V}{V}, \tag{2}$$

$$\Delta V = -Sx, \tag{3}$$

where P_0 is atmospheric pressure, S is cross-sectional area, and x is displacement. We have:

$$\mathrm{P} = \gamma\frac{SxP_0}{V} \tag{4}$$

where $\mathrm{x(t)} = e^{i\omega t}$, and ω is angular frequency, $\omega = 2\pi f$.

Force F can also be expressed in term of pressure:

$$F = PS = \gamma\frac{SxP_0}{V}S = \gamma\frac{S^2xP_0}{V} \tag{5}$$

$$m = \rho v = \rho SL, \text{ where } L \text{ is length of neck} \tag{6}$$

Equation (1) becomes, by substitution of equations (4), (5) and (6)

$$\frac{d^2x}{dt^2} = (i\omega)^2e^{i\omega t} = \frac{\gamma\frac{S^2xP_0}{V}}{\rho SL} = -\frac{\gamma SP_0}{\rho VL}e^{i\omega t} \tag{7}$$

$$-\omega^2 = -\frac{\gamma SP_0}{\rho VL} \tag{8}$$

$$2\pi f = \sqrt{\frac{\gamma S P_0}{\rho V L}} \Rightarrow f = \frac{1}{2\pi} \cdot \sqrt{\frac{\gamma S P_0}{\rho V L}} \tag{9}$$

The sound of speed c is $c = \sqrt{\gamma \frac{P_0}{\rho}}$.

Then,

$$f = \frac{1}{2\pi} \cdot \sqrt{\frac{\gamma S P_0}{\rho V L}} = f = \frac{1}{2\pi} \cdot \sqrt{\gamma \frac{P_0}{\rho}} \cdot \sqrt{\frac{S}{VL}} = \frac{c}{2\pi} \cdot \sqrt{\frac{S}{VL}} \tag{10}$$

Therefore, the resonant frequency is defined as

$$f = \frac{c}{2\pi} \sqrt{\frac{S}{VL}} \tag{11}$$

Appendix B: Code for Spectral Analysis

```
close all;
clear all;
clc;

% 1. Setting experiment condition

% Frequency
f=4096;                          % Hz
pt=1;                            % Period time

% Range of puretone frequency
pfs=1;                           % Starting frequency
pfe=500;                         % Ending frequency
pfr=pfe-pfs+1;                   % Time difference

% The number of pure tone
ne=pfr;

% The Number of FFT ( Fast Fourier Transform )
n1= 2^9;                         % 2^9 = 512
n2= 2^10;                        % 2^10 = 1024
n3= 2^11;                        % 2^11 = 2048
n4= 2^12;                        % 2^12 = 4096
n5= 2^13;                        % 2^13 = 8192
%n0= fix(log10(r)/log10(2));     Equation for deciding the number of FFT
nf=n4;                           % The number of FFT for present analysis

% pa/psi=6.89627379*1000
pa_psi=6.89627379*1000

% Sensitivity and Gain of Piezotronics multi-channel sensor signal condition
% Sensitivity
s_val70594=1;                    % unit          Ch0= Validyne
s_cavityend=1593.3;              % unit=mV/psi   Ch1= Cavity End
s_cavitydn1=188.5;               % unit=mV/kpa   Ch2= Cavity Duct Down
s_cavitymid2=1396.2;             % unit=mV/psi   Ch3= Cavity Duct Middle
s_cavityup3=194.6;               % unit=mV/kpa   Ch4= Cavity Duct Up
s_helmholtz=1313.3;              % unit=mV/psi   Ch5=Helmholtz Resonator
s_ref=518.3;                     % unit=mV/psi   Ch6=Reference
s_hotwire=1                      % unit          Ch7=Hot Wire

% Gain
ch_g=20;
ch0_g=1;                         % Ch0= Validyne1
```

```
ch1_g=20;                           % Ch1= Cavity End
ch2_g=20;                           % Ch2= Cavity Duct Down
ch3_g=20;                           % Ch3= Cavity Duct Middle
ch4_g=20;                           % Ch4= Cavity Duct Up
ch5_g=20;                           % Ch5= Helmholtz Resonator
ch6_g=20;                           % Ch6= Input Reference
ch7_g=1;                            % Ch7= Hot Wire

% Making matrix name and filename
for i=1:ne
  Filename(i,:) = {sprintf('HE%d.txt',pfe+1-i)};
end

for(i=1:1:ne/2)
  Temp=Filename(i,:);
  Filename(i,:)=Filename(ne+1-i);
  Filename(ne+1-i)=Temp;
end

% Loading Date and making matrix
for i = 1:ne
[data,ErrorMessage]=fopen(char(Filename(i)),'rt');
[Matrix(:,:,i), count]=fscanf(data,'%f',[9,inf]);  %file name, format, size(M*N)
end
fclose('all');


% Size of Matrix= [m,n] & Length
Size=size(Matrix);
c=Size(1,1);  % Column
r=Size(1,2);  % Row
d=Size(1,3);  % Dimension


% Distribution of All Data and Making each matrix

% Row: Time
% Column: Experiment Number

for(i=1:1:ne)                             %where ne is the number of experiment
  M_Time(:,i)=transpose(Matrix(1,:,i));
  M_Va70954(:,i)=transpose(Matrix(2,:,i));      %A/D conv.= #0
  M_CavityEnd(:,i)=transpose(Matrix(3,:,i));    %A/D conv.= #1
  M_DuctDn1(:,i)=transpose(Matrix(4,:,i));      %A/D conv.= #2
  M_DuctMid2(:,i)=transpose(Matrix(5,:,i));     %A/D conv.= #3
  M_DuctUp3(:,i)=transpose(Matrix(6,:,i));      %A/D conv.= #4
```

```
  M_Helmholtz(:,i)=transpose(Matrix(7,:,i));      %A/D conv.= #5
  M_Reference(:,i)=transpose(Matrix(8,:,i));      %A/D conv.= #6
  M_HotWire(:,i)=transpose(Matrix(9,:,i));        %A/D conv.= #7
end

% Calculation of sound pressure
M_Pressure_CavityEnd=M_CavityEnd*(pa_psi)*(10^3)/(ch1_g*s_cavityend);
M_Pressure_DuctDn1=M_DuctDn1*(10^3)*(10^3)/(ch2_g*s_cavitydn1M_Pressure_Du
ctMid2=M_DuctMid2*(pa_psi)*(10^3)/(ch3_g*s_cavitymid2);
M_Pressure_DuctUp3=M_DuctUp3*(10^3)*(10^3)/(ch4_g*s_cavityup3);
M_Pressure_Helmholtz=M_Helmholtz*(pa_psi)*(10^3)/(ch5_g*s_helmholtz);
M_Pressure_Reference=M_Reference*(pa_psi)*(10^3)/(ch6_g*s_ref);
M_Pressure_HotWire=M_HotWire*(pa_psi)*(10^3)/(ch7_g*s_hotwire

% Window Function, Hann
Winfunc_Hann=hann(r);

for(j=1:1:ne) %ne: the number of experiment
  for(i=1:1:r)
    W_Pressure_CavityEnd(i,j)=M_Pressure_CavityEnd(i,j)*Winfunc_Hann(i);
    W_Pressure_DuctDn1(i,j)= M_Pressure_DuctDn1(i,j)*Winfunc_Hann(i);
    W_Pressure_DuctMid2(i,j)= M_Pressure_DuctMid2(i,j)*Winfunc_Hann(i);
    W_Pressure_DuctUp3(i,j)= M_Pressure_DuctUp3(i,j)*Winfunc_Hann(i);
    W_Pressure_Helmholtz(i,j)=M_Pressure_Helmholtz(i,j)*Winfunc_Hann(i);
    W_Pressure_Reference(i,j)=M_Pressure_Reference(i,j)*Winfunc_Hann(i);
    W_Pressure_HotWire(i,j)= M_Pressure_HotWire(i,j)*Winfunc_Hann(i);
  end
end

% Fast Fourier Transform
FFT_CavityEnd=abs(2*fft(W_Pressure_CavityEnd,nf))/(nf/2);
FFT_DuctDn1= abs(2*fft(W_Pressure_DuctDn1,nf))/(nf/2);
FFT_DuctMid2= abs(2*fft(W_Pressure_DuctMid2,nf))/(nf/2);
FFT_DuctUp3= abs(2*fft(W_Pressure_DuctUp3,nf))/(nf/2);
FFT_Helmholtz=abs(2*fft(W_Pressure_Helmholtz,nf))/(nf/2);
FFT_Reference=abs(2*fft(W_Pressure_Reference,nf))/(nf/2);
FFT_HotWire= abs(2*fft(W_Pressure_HotWire,nf))/(nf/2);


% Frequency Domain for pure tone
% Frequency Domain for Puretone
for(i=1:1:pfr)                          % pfr= Range of puretone frequency
  Freq_Puretone(i)=pfs+i-1;
end
```

```
% Result of FFT
for(i=1:1:ne)                                %ne: the number of experiment
   R_FFT_CavityEnd(i)=FFT_CavityEnd(Freq_Puretone(i)+1,i);
   R_FFT_DuctDn1(i)= FFT_DuctDn1(Freq_Puretone(i)+1,i);
   R_FFT_DuctMid2(i)= FFT_DuctMid2(Freq_Puretone(i)+1,i);
   R_FFT_DuctUp3(i)= FFT_DuctUp3(Freq_Puretone(i)+1,i);
   R_FFT_Helmholtz(i)=FFT_Helmholtz(Freq_Puretone(i)+1,i);
   R_FFT_Reference(i)=FFT_Reference(Freq_Puretone(i)+1,i);
   R_FFT_HotWire(i)= FFT_HotWire(Freq_Puretone(i)+1,i);
end

% Data Table of FFT
Datatable(:,1)=Freq_Puretone;
Datatable(:,2)=R_FFT_CavityEnd;
Datatable(:,3)=R_FFT_DuctDn1;
Datatable(:,4)=R_FFT_DuctMid2;
Datatable(:,5)=R_FFT_DuctUp3;
Datatable(:,6)=R_FFT_Helmholtz;
Datatable(:,7)=R_FFT_Reference;
Datatable(:,8)=R_FFT_HotWire

% Save result into text File
save PS1.txt Datatable -ascii;

 % Figures
figure(1)
plot(Datatable(:,1),Datatable(:,2),'c-');
xlabel('Hz');
ylabel('P_Amplitude');
title ('Puretone Spectrum');
grid on
hold on
plot(Datatable(:,1),Datatable(:,3),'g-');
hold on
plot(Datatable(:,1),Datatable(:,4),'r-');
hold on
plot(Datatable(:,1),Datatable(:,5),'b-');
hold on
plot(Datatable(:,1),Datatable(:,6),'m-');
legend('PEnd','PDn1','PMid2','PUp3','PHelm');
hold off

figure(2)
subplot(5,1,1);
plot(Datatable(:,1),Datatable(:,2),'c-');
legend('PEnd');
```

```
subplot(5,1,2);
plot(Datatable(:,1),Datatable(:,3),'g-');
legend('PDn1');

subplot(5,1,3);
plot(Datatable(:,1),Datatable(:,4),'r-');
legend('PMid2');

subplot(5,1,4);
plot(Datatable(:,1),Datatable(:,5),'b-');
legend('PUp3');

subplot(5,1,5);
plot(Datatable(:,1),Datatable(:,5),'m-');
legend('PHelm');
```

VITA

The author was born in South Korea on July 21, 1979. He received his Bachelor degree in Electronical Engineering from Korea Military Academy in March 2002. During his graduate study at Lehigh University, he worked under the supervision of Professor Donald Rockwell. He is currently enrolled in the Master of Science in Mechanical Engineering program in the P. C. Rossin College of Engineering at Lehigh University and will work for Korean army.

END OF TITLE